Assessment of lake-groundwater interactions

Turawa case, Poland

AMR EL ZEHAIRY

February, 2014

SUPERVISOR:
Dr. Ir. Maciek W. Lubczynski

CO-SUPERVISORS:
Dr. Zoltan Vekerdy
Dr. Jacek Gurwin

ADVISOR:
S.M. Tanvir Hassan

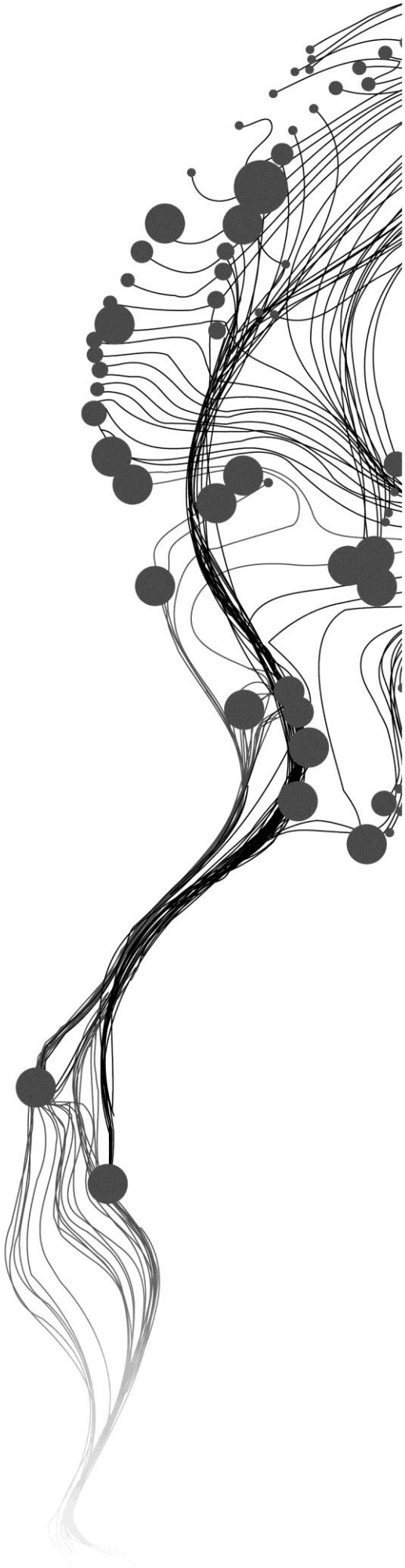

Assessment of lake-groundwater interactions

Turawa case, Poland

AMR EL ZEHAIRY
Enschede, The Netherlands, February, 2014

Thesis submitted to the Faculty of Geo-Information Science and Earth Observation of the University of Twente in partial fulfilment of the requirements for the degree of Master of Science in Geo-information Science and Earth Observation.
Specialization: Water Resources and Environmental Management

SUPERVISOR:
Dr. Ir. Maciek W. Lubczynski

CO-SUPERVISORS:
Dr. Zoltan Vekerdy
Dr. Jacek Gurwin

ADVISOR:
S.M. Tanvir Hassan

THESIS ASSESSMENT BOARD:
Prof. Dr. Ing. Wouter Verhoef (Chair)
Dr. Ir. Martijn Booij (External Examiner, Universiteit Twente)

This work is dedicated to my beloved parents, my brothers, my future wife, and the whole family.

ABSTRACT

The Turawa Lake is an artificial lake located in the South of Poland within the Mala Panew catchment. The lake is heavily contaminated, and the main contamination source of the lake is the industrial sediment from the steel-works factory in Ozimek located upstream of the lake. Besides there are some other sources of pollution such as agriculture activities, and urban and domestic sewage. Recently in Turawa Lake, excessive algae growth and eutrophication due to phosphorous compounds have been observed. Therefore, there is an urgent need for a better understanding of the dynamic interaction between surface water and groundwater in this area, especially the water balance between the groundwater and the lake. Furthermore, as the Turawa Lake is an artificial lake, it is necessary to understand how the construction of this lake affects the hydrology of the adjacent area.

The interaction of Lake Turawa with the groundwater was numerically simulated using three-dimensional steady state and transient state models. The Lake Package (LAK7) with MODFLOW-NWT under ModelMuse environment was used. The steady state and transient models were calibrated manually due to the long time needed for automatic calibration using ModelMate. All data, including time series of piezometric head observations, rainfall, lake stages, rivers discharges for a five-year period (including one year warming up), were analysed on a daily basis. For that purpose daily infiltration rates, potential evapotranspiration and lake evaporation were calculated. The advantage of the applied method was that the groundwater recharge was not assigned arbitrarily but internally simulated using the recently developed Unsaturated Zone Flow (UZF1) Package, and also the Stream Flow Routing (SFR7) Package controlling groundwater interactions with rivers and drains.

The study area of the Turawa Catchment (South Poland) has an area of ~100 km^2, with ~11.5 km length and ~9 km width. The Lake Turawa is centrally located and occupies an area of ~16.3 km^2. Its bathymetry was measured with a sonar and represented by 5 m resolution digital elevation model [DEM]. The 3D numerical model of the study area was discretized horizontally by 200x200 m grid and vertically by four layers, including one inactive upper layer to simulate the lake. The steady-state model was based on the mean of the four-year simulation fluxes and heads. The transient model time span was five years (from 1st Nov. 2003 to 31st Oct. 2008) including the first year as a warming up period. The whole simulation period was discretized into daily time steps and daily stress periods.

The manual calibration progress was evaluated by the error between observed and simulated heads, and between observed and simulated lake stages. In the steady state model, the simulated piezometric heads matched the observations with a squared correlation coefficient equal to 0.96, while the simulated lake stage was nearly equal to the 4 years average daily lake stage with accuracy less than 1 cm. In the transient model, the squared correlation coefficients between the daily observed and the simulated time series piezometric heads and lake stages were equal to 0.99 and 0.93, respectively.

The steady state model sensitivity was tested by changing some parameters and stresses. The analysis of model parameters showed that the model is sensitive to the horizontal hydraulic conductivity [K_h], while the stream beds hydraulic conductivity and the lake bed leakance seem to be non-sensitive with respect to the simulated groundwater heads. While, the analysis showed that the model is sensitive only to the horizontal hydraulic conductivity [K_h] and low values of lake bed leakance with respect to the simulated lake stages. Regarding the hydrologic stresses, the river inflows show very high sensitivity to the simulated groundwater heads and lake stages, and the lake evaporation and precipitation show relatively lower sensitivity to the simulated lake stages. The transient state sensitivity analysis showed that most of the

tested parameters are not sensitive except the horizontal hydraulic conductivity with respect to both the simulated groundwater heads and lake stages. While, lower specific yield values seemed to be sensitive with respect to groundwater heads only. The river inflows showed high sensitivity to both of the simulated groundwater heads and lake stages.

The steady state model results showed that the lake seepage to groundwater is slightly higher than groundwater inflow to the lake. The four years transient state simulation showed that the seepage from the lake to groundwater is dominant during high and average lake water levels, and vice versa during low lake water levels.

The lake level variations may have large influence on groundwater heads in one location and relatively low effects for another location, depending whether groundwater seepage occurs from lake to groundwater or vice versa and on the type of the boundary conditions and their distance from the lake. The seepage from lake to groundwater occurs mainly in the western deep part of the lake near the earthen dam, while in the middle and in the eastern part of the lake groundwater inflow to the lake is dominant.

Key words: Lake Turawa; Groundwater modelling; Lake-groundwater interaction.

ACKNOWLEDGEMENTS

First and foremost, praise and thanks to Allah (God) almighty who gave me the knowledge and power to finish this work.

I would like to express my gratitude to the Netherland's Government that gave me the opportunity to do my Master of Science degree course at the ITC through the Netherlands Fellowship Program (NFP) that provides me with the scholarship. Also, it was my great pleasure to be granted an academic leave of absence from my employer, the Dean of the Faculty of Engineering, Mansoura University, Egypt.

I am immensely indebted to my first supervisor, Dr. Maciek Lubczynski, for his proper guidance and support during the fieldwork and throughout the whole study period. Also, I would like to acknowledge my second supervisor, Dr. Zoltan Vekerdy, for his encouragement and care during this study.

I would like to register special thanks to Dr. Jacek Gurwin for his help and hospitality during field work.

I would like to thank my advisor, S.M. Tanvir Hassan, for his support and help during this study.

I am very thankful to Dr. Christiaan van der Tol , Ms. Lichun Wang, Drs. Richard Knippers and Mr. Bas Retsios for their valuable advices and help during this study.

I am grateful to the help and care of Mr. Arno van Lieshout, during the whole study period in the ITC.

I would like to thank Ms. Erna Leurink and Ms. Ceciel Wolters for providing me with all the facilities needed to conduct my study.

I am very grateful to Dr. Richard Niswonger and Mr. Richard Winston for their help and support with the USGS software (UZF Package, MODFLOW, and ModelMuse) during the whole study period.

My thanks to all the staff members of the Water Recourses Department in the ITC for all the support and guidance given. I do acknowledge all the help of all other ITC academic and support staff.

Last but not least, I would like to thank my parents, brothers, sisters, the whole family, and all my colleagues for all their support and encouragement which have led me through the difficult times.

Contents

LIST OF FIGURES

LIST OF TABLES

LIST OF ABBREVIATIONS:

AQUIFEM-1	AQUIfer Finite-Element Model
ArcGIS	Arc Geographic Information System
FORTRAN	FORmula TRANslating System
GHB	General Head Boundary Package of MODFLOW
GMS	Groundwater Modeling System
GSFLOW	Groundwater and Surface-Water FLOW model
HBV	"Hydrologiska Byråns Vattenbalansavdelning" model
HFB	Horizontal Flow Barrier Package of MODFLOW
HOB	Head Observation Package of MODFLOW
ILWIS	Integrated Land and Water Information System
LAI	Leaf Area Index
LAK7	Lake Package of MODFLOW
MODFLOW	MODular three-dimentional finite difference groundwater FLOW model
NWT	Newtonian
PRMS	Precipitation-Runoff Modeling System
SFR7	Streamflow Routing Package 7
SWAT	Soil and Water Assessment Tool
SRTM	Shuttle Radar Topography Mission
UCODE	A Computer Code for Universal Modeling Optimization
UTM	Universal Transverse Mercator coordinate system
UZF	Unsaturated-Zone Flow Package of MODFLOW
ZONBUDGET	Zone Budget program

1. INTRODUCTION

1.1. Introduction

Groundwater and surface water are in a continuous dynamic interaction. Water resources management and policy rely on understanding the behaviour of each component of the hydrological cycle and the interaction between these components. Thus, development or contamination of one of them commonly affects the other (Sophocleous, 2002). For instance, groundwater pumping can affect the quantity of water in streams, lakes or wetlands. While withdrawal from surface water bodies can deplete groundwater. Furthermore, contamination can spread out from surface water to groundwater and vice versa (Yimam, 2010).

Processes of interaction between surface water and groundwater are very complex. In the past, hydrological models were developed taking into consideration either surface water or ground water alone. Such hydrological models can be referred as standalone models. Surface models such as HBV, PRMS or SWAT are used to simulate surface runoff processes simplifying interactions with groundwater. Other models, such as MODFLOW and AQUIFEM-1, focus on groundwater arbitrary simplifying surface processes. Therefore, the most recent research focuses on development and application of models internally handling surface-groundwater interactions, so called integrated models.

Lake-groundwater interactions require codes dynamically integrating groundwater, unsaturated zone and lake fluxes such as MODFLOW-2005 or MODFLOW-NWT extended with Lake Package, Unsaturated Zone Flow (UZF) Package and Stream Flow Routing Package (SFR). In this study, the Lake Turawa - groundwater interaction is simulated by building steady state and transient state models using MODFLOW-NWT under ModelMuse environment, taking into consideration the interaction between surface water and ground water by activating the Lake Package (LAK7), the Stream Flow Routing Package (SFR7), and the Unsaturated Zone Flow (UZF1) Package.

1.2. Location of the study area

The Turawa Lake is an artificial lake located in the south of Poland within Mala Panew River (MPR) catchment. The MPR is the right tributary of the Odra River [Figure 1-1]. The earthen dam of the Turawa Lake (TL), located at its western edge [Figure 1-2], was constructed in 1938. The TL is supplied with water not only by MPR but also by two other small rivers Libawa and Rosa. The TL is used for standard flow regulation, flood prevention and for touristic purposes (Simeonov et al., 2007).

As this study was focussed on surface–groundwater interaction, the area of investigation of ~100 km^2 (~11.5 km length and 9 km width) was delimited by MPR watershed boundaries from the north, topographic divide from the south and by artificial boundaries from the east and west. The TL is centrally located and occupies an area ~16.3 km^2 between latitudes 50° 45` 29`` N and 50° 40` 33`` N, and longitudes 18° 03` 16`` E and 18° 13` 05`` E. In this study all the coordinates were adjusted to the Polish coordinate system PUWG_92. The bounding coordinates of the study area in that system were: X= 433,250.64 m from the west, X= 444,820.35 m from the east, Y= 312,441.23 m from the south, and Y= 321,608.06 m from the north.

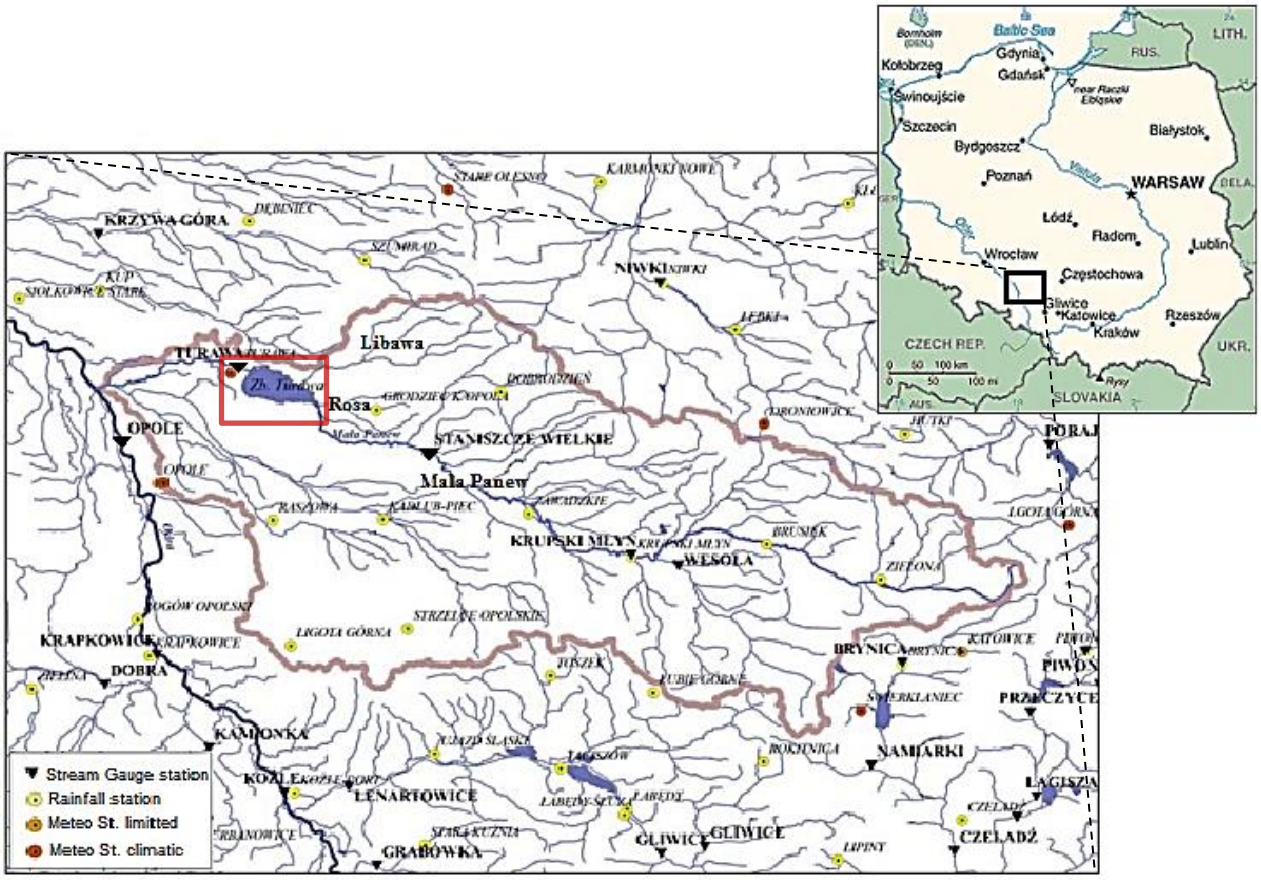

Figure 1-1 Location of the Mala Panew watershed and artificial Lake Turawa.

1.3. Problem definition

The Lake Turawa is a heavily contaminated lake therefore its impact on groundwater is of critical importance. The main contamination source of the lake is the industrial sediment from the steel-works factory in Ozimek (upstream of the lake), moving along the Mala Panew River and entering the lake at its SE section. Besides there are some other sources of pollution such as agriculture activities, and urban and domestic sewage. As a result an excessive algae growth and eutrophication due to phosphorous compounds have been observed (Gurwin et al., 2004).

Considering the lake contamination and its interaction with the surrounding environment, particularly with groundwater, there is an urgent need for a better understanding of that interaction including quantitative assessment of the water balance exchange between groundwater and the lake. The Lake Turawa and the adjacent area have an extraordinary data base acquired within EU regional cooperation project (Gurwin et al., 2004) in which ITC was a partner. That project was led by Wroclaw University and headed by ITC collaborator Dr. Jacek Gurwin who is in charge of that data base.

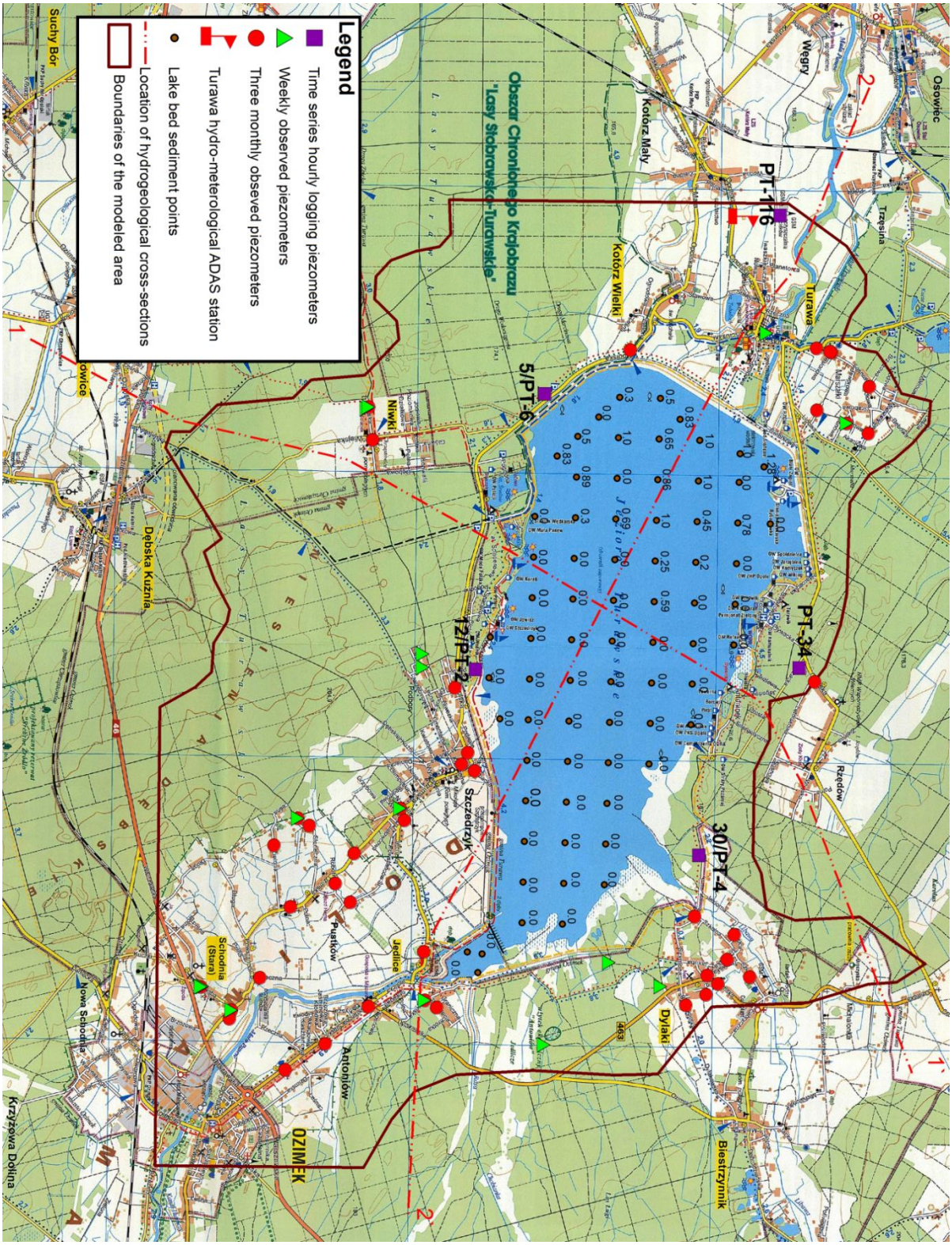

Figure 1-2 Monitoring network of Turawa area, lake bed deposit thickness in meters, and location of hydrogeological cross-sections 1-1` and 2-2`.

1.4. Previous work in the Turawa catchment

Gurwin (2008) performed a study, at nearly the same study area [Figure 1-3], using a simple, standalone, [GMS 6.0], groundwater model setup. He built two steady-state models; one representing high flow condition (lake stage=176 m a.m.s.l.) and the other low flow condition (lake stage =170 m a.m.s.l.). That model consisted of three model layers; surficial unconfined and deep confined aquifers, and aquitard in between. The western model boundary was assigned arbitrarily as head constant boundary (H = constant) downstream of the dam, whereas all other boundaries were assigned as general head boundaries (GHB) [Figure 1-3]. Approximately, similar area as used in the previous study is kept in my study, but with different boundaries. Gurwin (2008) used General Head Boundary Package (GHB) to simulate the lake, River and Drain Packages to simulate rivers and drains, Horizontal Flow Barrier Package (HFB) for simulating the dam, besides the Recharge Package. In this study, all the boundaries were carefully revised attempting to assign physically based boundaries.

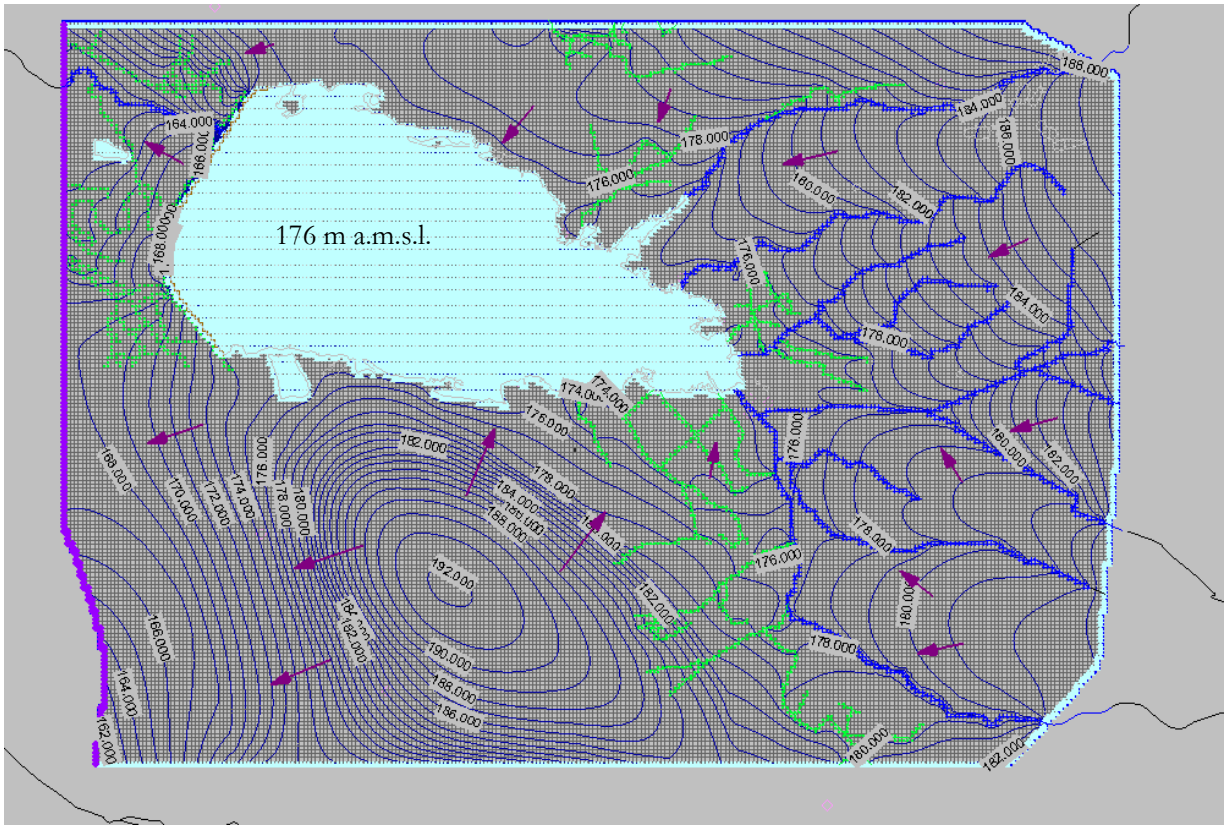

Figure 1-3 Potentiometric map at the maximum lake water level 176 m a.m.s.l. (Gurwin, 2008) .

1.5. Topography and DEM

The Mala Panew catchment has a slightly rolling topography with local gentle hills. A digital elevation model [DEM] [Figure 1-4] including the lake bathymetry [Figure 1-5] at 5x5 m pixel size, was obtained from Wroclaw University in ILWIS format. However, the obtained DEM did not cover the whole study area, so some small parts at the north and the west had to be adjusted.

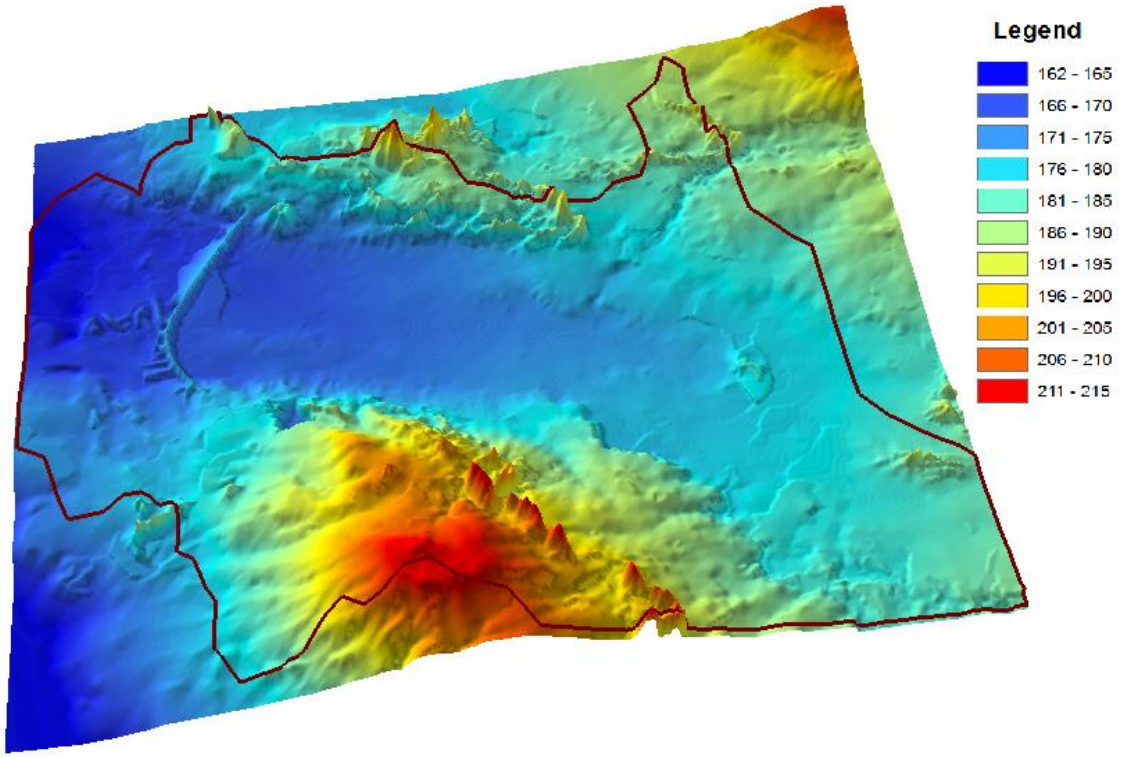

Figure 1-4 Digital Elevation Model [DEM] of the study area (brown line represents study area boundary) with 5 m pixel size.

1.6. Lake characteristics

1.6.1. Lake bathymetry

Figure 1-5 shows the lake bathymetry map obtained from Wroclaw University which was measured with sonar and represented by 5 m resolution digital elevation model. The lake is quite shallow in the eastern part, and its depth increases gradually to the west. The lake has its deepest point at the western outlet next to the earthen dam.

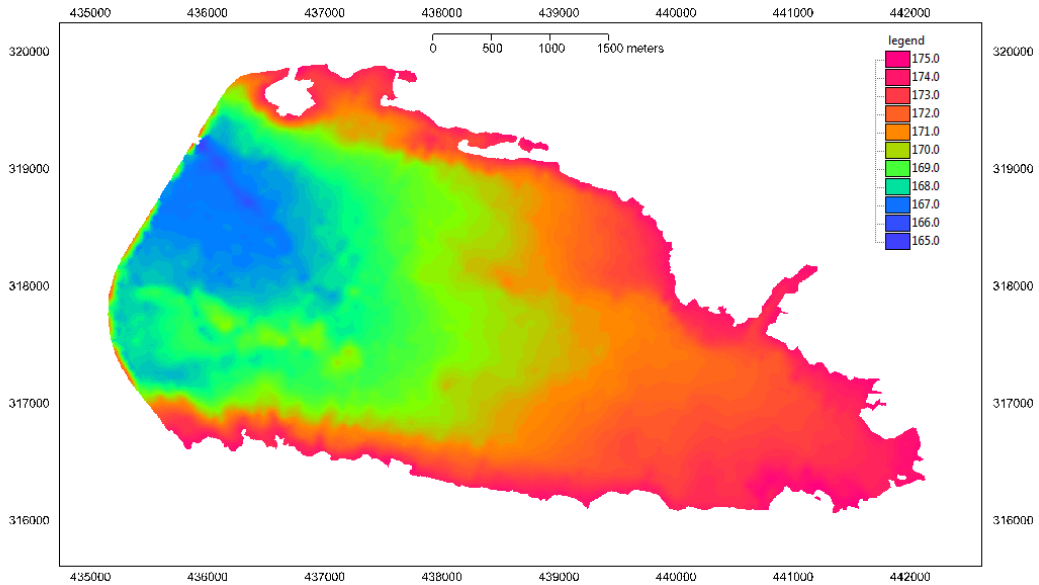

Figure 1-5 Bathymetric map of the Turawa Lake (May 2004).

1.6.2. Lake bed deposit

The steel-works factory in Ozimek, upstream of the Turawa Lake, contaminates the MPR with industrial sediment so consequently also the lake. This industrial sediment is cumulated over years and formed what is called "sapropel", which is dark-coloured sediment with low permeability. In 2004, Wroclaw University did investigations to determine the thickness of this deposit [Figure 1-2] and its chemical content (Gurwin et al., 2004).

1.6.3. Lake water fluctuation

Lake Turawa has relatively large water table fluctuation ranging from ~171.0 m to 176 m a.m.s.l. [Figure 1-6]. The daily lake stages obtained from Wroclaw University are available for the period from 1st November 2003 to 31st October 2009, with data gap from 16th June 2007 to 31st December 2007.

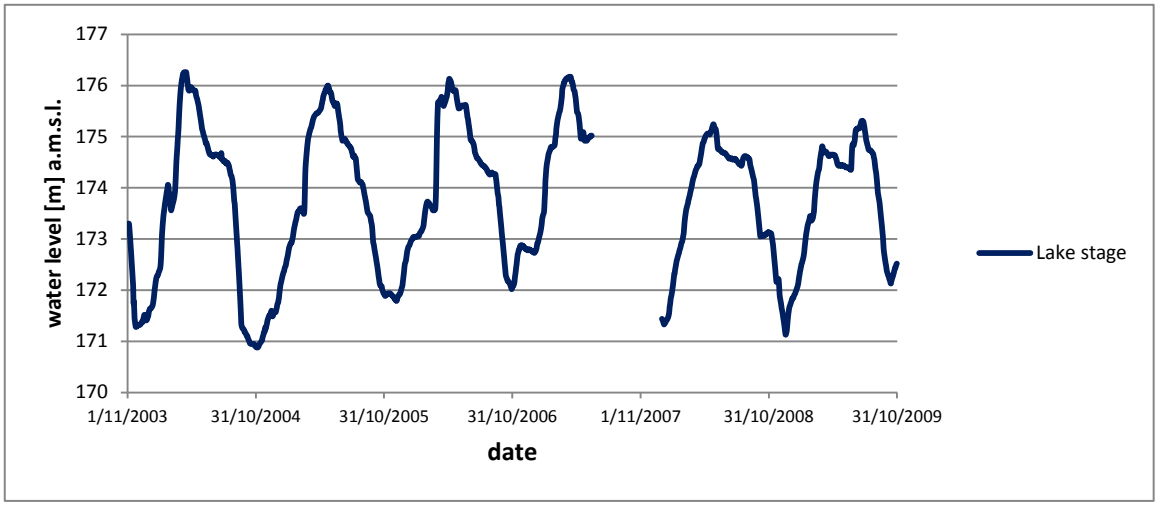

Figure 1-6 The available daily records of Turawa Lake stages [m a.m.s.l.].

1.7. Climate and meteorological data

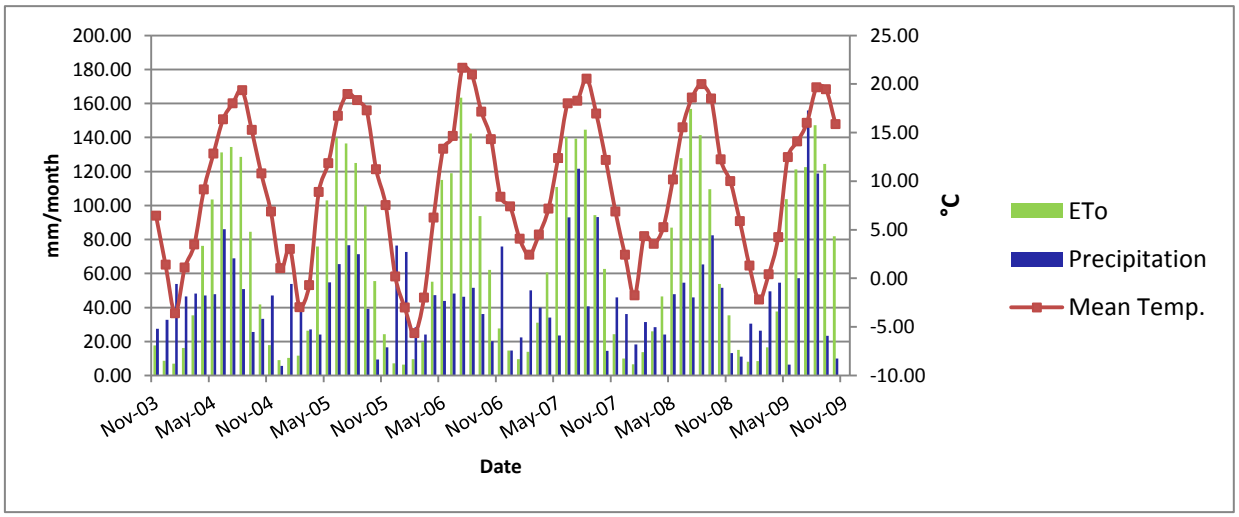

Figure 1-7 Monthly precipitation, reference evapotranspiration and mean temperature at Opole station.

Figure 1-7 gives a general idea about the climate in the south of Poland (at Opole station, Figure 1-1); the figure contains monthly mean temperature and precipitation retrieved from NNDC climate online data "CLIMVIS database" (http://www7.ncdc.noaa.gov/CDO/cdo#TOP), it contains also the reference

evapotranspiration calculated from the obtained data according to Hargreaves Equation [Equations 2.18 to 2.22, section 2.5.2.].

The figure shows that the higher ET_o and rainfall values are corresponding to higher temperatures.

In the study area, there was hydro-meteorological automated data acquisition system (ADAS) (Figure 1-2), capable of providing measurements of precipitation, incoming solar radiation, relative humidity, wind speed, and air temperature at heights 2 m and 6 m above the ground level. Besides, the ADAS provided subsurface measurements of soil heat flux and soil temperatures at depths 5 cm and 15 cm. All these data were recorded hourly in the period from 15th November 2003 to 14th March 2010 with some gaps. The methods used for filtering these data and filling the gaps are described in chapter 2.

1.8. Hydrology

Figure 1-1 shows the topographic boundaries of Mala Panew River (MPR) catchment and the hydrometerological ADAS stations within the catchment and the surrounding area. The Turawa Lake is supplied mainly by the MPR entering at the south east and leaving at the west of the lake. Rosa, the smallest river, enters the lake from the east and Libawa from the north east. The lake has only one outlet, through sluice gates within the earthen dam, to the MPR in the downstream. The MPR inflow and outflow measurements were available for this study only at "Staniszcze Wielkie" (upstream of the lake) and "Turawa" (downstream of the lake) stations [see Figure 1-1]. The river discharges and their corresponding river stages were obtained from the Hydro-meteorological Institute in Poland for the period from 1st November 2003 to 31st October 2009. The study area also contains some artificial drains "diches" ending up in the lake, all are shown, in green, in Figure 1-3.

1.9. Hydrogeology

1.9.1. Lithology and soil

The lithology map of the study area, obtained from Wroclaw University, is shown in Figure 1-8. The dominant soil types are sand and sand with gravels surrounding the Mala Panew stream at the inlet and the outlet of the lake, and also limited occurances of clay and peats.

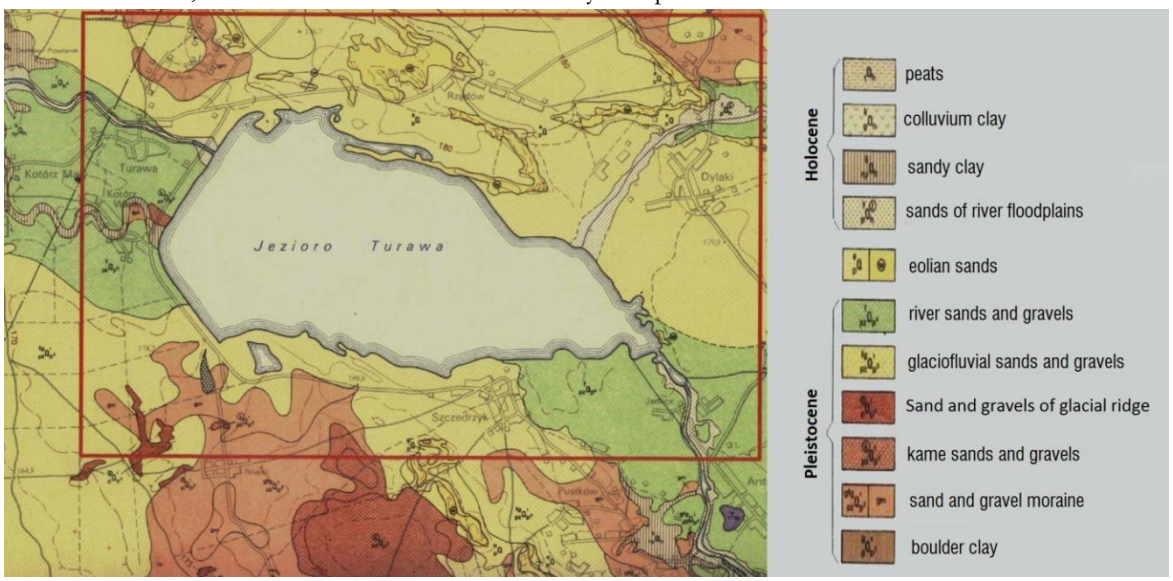

Figure 1-8 The lithology map of the study area.

1.9.2. Hydrostratigraphy, pumping tests, and hydraulic conductivities

The hydrogeological investigations done in the study area (Gurwin et al., 2004) showed that the groundwater flow system is composed of three layers; the upper unconfined aquifer, the middle sandy-loam aquitard, and the bottom confined aquifer underlain by an impermeable clayey layer as presented in two hydrogeological cross sections in Figures 1-10 and 1-11. The location of these two cross sections (cross section 1-1` and 2-2`) is shown in Figure 1-2.

The pumping test data for the study area are shown in Appendix 1. That table contains the coordinates in the Polish Coordinate System PUWG_92, the hydraulic conductivity, and the transmissivity of each borehole. In addition, a number of boreholes were drilled to determine the top and the bottom of each of the three layers [Appendix 2]. All these borehole data were used in this study and also to construct the hydrogeological cross-sections. Based on the available geological studies and the pumping test information, hydraulic conductivity, transmissivity, specific yield, and specific storage parameters were estimated.

1.9.3. Piezometric heads

The available piezometric heads obtained from Wroclaw University within the study area comprise hourly logging data and weekly as well as three-monthly direct observations. The time series of head data logged hourly are presented in Figure 1-9, while the logged piezometers' location in Figure 1-2. Besides there are 17 piezometers, shown in green in Figure 1-2, that have weekly direct instantaneous measurement of water table in the period from 28th March 2004 to 14th March 2005. Finally there are 42 piezometers and dug wells, shown as red circles in Figure 1-2, with 5 sets of direct measurements in three months interval on the following dates: 15th November 2003, 27th February 2004, 2nd May 2007, 29th July 2004, and 2nd October 2004.

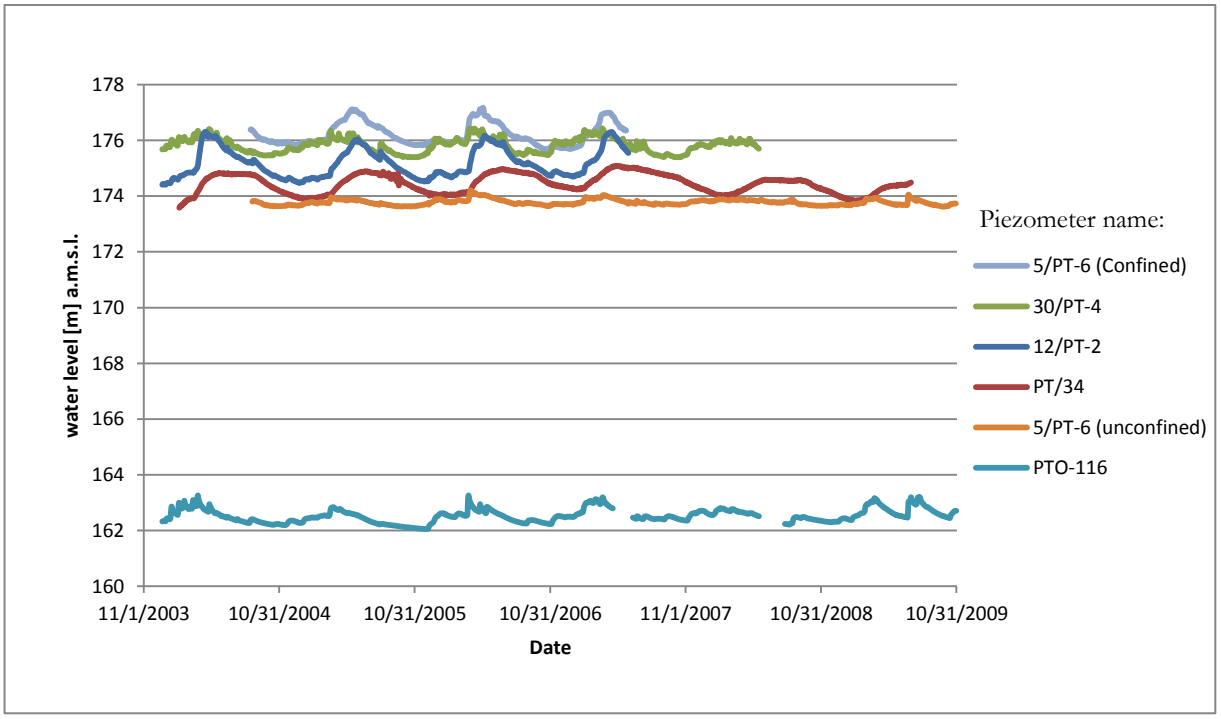

Figure 1-9 Daily time series heads obtained from the hourly logging piezometers (Figure 1-6 shows the location of these piezometers).

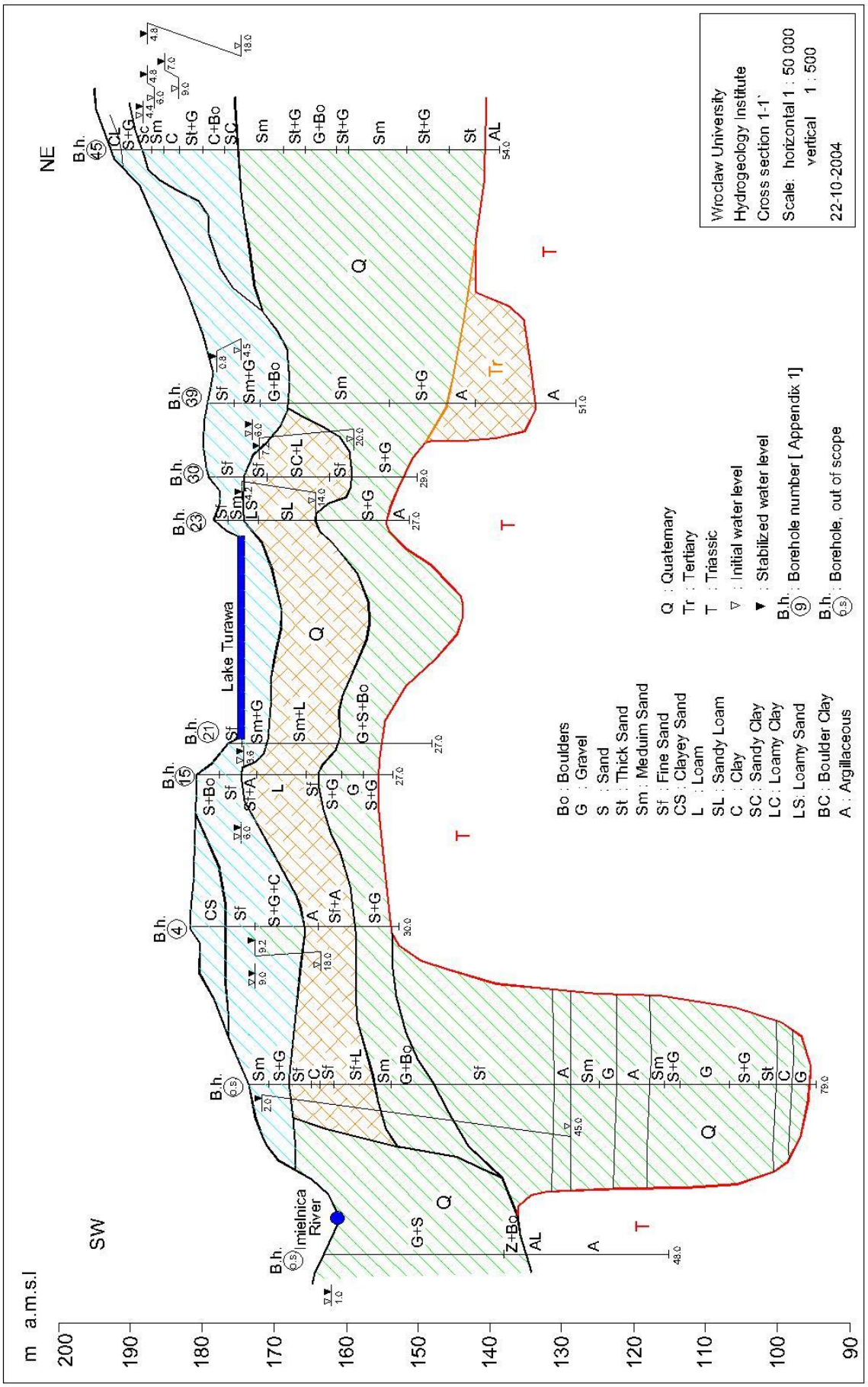

Figure 1-10 Hydrogeological cross-section 1-1`.

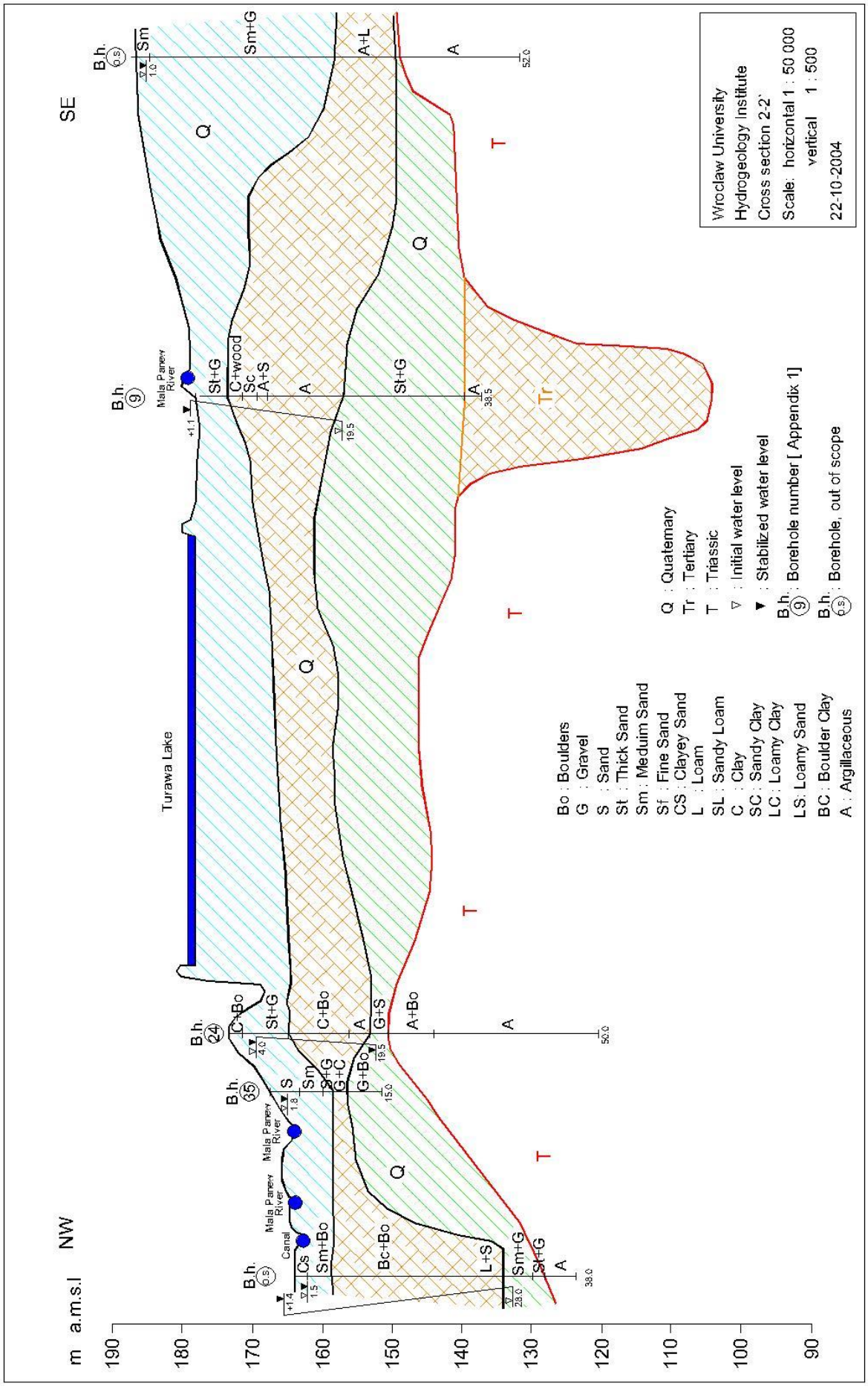

Figure 1-11 Hydrogeological cross section 2-2`.

1.10. Objectives and research questions

The main and specific objective of the study can be outlined as follows:

1.10.1. Main objective

- To evaluate lake-groundwater interactions in the area adjacent to the Lake Turawa.

1.10.2. Specific objectives

- To develop and calibrate a steady state and transient state model of the Lake Turawa and its adjacent area;
- To characterize inter-relationship between lake water levels and groundwater levels in the area adjacent to the lake;
- To analyze exchange of water fluxes between the lake and aquifers.

1.10.3. Main research question

- What is the impact of artificial Lake Turawa on the hydrologic system adjacent to the lake area?

1.10.4. Specific research questions

- What is the impact of the lake level variations on the temporal variability of groundwater heads and on the spatial extent of that influence?
- How does the lake affect water balance of the study area?

2. METHODOLOGY

2.1. Review of modelling lake-groundwater interactions

Furman (2008), in his review, discussed different approaches used to couple surface–subsurface flow processes. These approaches differ between physical models that conserve mass and momentum and numerical models. Regarding the physical models, he mentioned five different categories depending on how the boundary conditions are defined at the interface between surface and subsurface systems. The first category implies the continuity of velocity and its gradient along the interface, the second, implies also velocity continuation but by weighting the velocity gradient with the kinematic viscosity, the third, assumes continuous velocity along the interface but includes a jump condition within the gradient, the fourth is a special case of the third category where the jump has a different representation form, and the fifth takes into consideration only the derivative form of the velocity from the free side of the fluid. Regarding numerical models, Furman (2008) described three different categories: no-coupling, iterative coupling, and full coupling. In the simplest, no-coupling approach, the surface water system is solved first, then the boundary condition is defined and the subsurface system is solved later. The second approach is similar to the first but the solution of the subsurface system is used to update the boundary condition in the same time step. The third, most sophisticated approach solves the two systems with the internal boundary condition simultaneously. In this study, MODFLOW numerical model approach is used with the Unsaturated Zone Flow Package (UZF), Lake Package (LAK7), and Stream Flow Routing Package (SFR7). Using MODFLOW with the three previously mentioned packages provides fully coupled modelling approach.

The modelling of surface-groundwater interactions in areas adjacent to lakes was a topic of many studies, applying many different approaches. One of these approaches is to simulate lakes using MODFLOW River Package developed by Harbaugh (2005). River Package could represent a lake as a constant head sink or source extending over the aquifer. One of the disadvantages of this approach is that the river stage is constant during each stress period and not changing due to the interaction between the river (the lake) and the groundwater system.

Another approach is to simulate lakes using MODFLOW Reservoir Package (Fenske et al., 1996). This approach does not differ much from the first approach except that the Reservoir Package allows the lake stage to vary according to the user specified limits and this requires a previous knowledge of the amount of seepage through the lake bed (Merritt & Konikow, 2000).

Gurwin (2008) used the General Head Boundary Package (GHB) for lake simulation. In his study, the lake bed sediment was simulated by adjusting the conductance of each cell simulated as a GHB. This approach is very similar to the River Package approach with all its disadvantages.

Yihdego and Becht (2013) used a "High-K" method to simulate the lake-aquifer interaction at Lake Naivasha, Kenya. In that approach, a high hydraulic conductivity values were used to simulate the lake cells. Yihdego and Becht (2013) concluded that this approach is limited only to seepage lakes, which do not have outlet and lose water mainly by seepage through bottom and sides, such as Lake Naivasha and it could cause instability problems with groundwater heads solution. The main disadvantage of using the "High-K" approach is that it is difficult in simulating accurately the connection between streams and the lake (Merritt & Konikow, 2000). The same approach was used by Lee (1996) to simulate the transient

groundwater interactions and lake stage for Lake Barco, an acidic seepage lake in the mantled karst of north central Florida. Lee found that the model underestimated the groundwater inflow compared to the inflow calculated from the lake hydrologic budget computed from the energy budget method.

Cheng and Anderson (1993) developed a numerical code that could be used with MODFLOW to simulate groundwater interaction with lakes and streams for steady and transient states. That code can be considered as the basics of the Lake Package, later developed by Merritt and Konikow (2000), except that it did not take into account that some of the lake bed cells could become dry due to low lake water levels. Also it did not consider the flow resistance within the aquifer which might be quite important and larger than lake bed resistance in case of thin lake beds (Merritt & Konikow, 2000).

Kidmose et al. (2011) conducted a study to ivestigate the spatial distribution of seepage at Lake Hampen, Western Denmark. They built a 3-D MODFLOW steady state model including LAK3 Package to simulate lake-groundwater interaction. They compared the seepage meter measurements with the steady state model results and concluded that the two results compared well if direct seepage measurements from near shore were combined with measurements from deeper parts of the lake.

Anderson et al. (2002) used both, the "High-K" approach and the Lake Package to simulate lake levels in Pretty Lake, Wisconsin. They concluded that the "High-K" method simulates the lake more accurately than other methods, but in the same time it needs more post processing and longer run time. In contrast, Hunt (2003) in his review paper stated that the LAK3 Package is superior to all other lake simulation approaches because any change in the lake stage, due to interaction with groundwater system and/or streams is appropriately simulated by the Lake Package and not taken into account when using any other approaches. Besides, the LAK3 Package has been proved to be more stable in simulating lake-groundwater interaction than other techniques. It has also the capability of simulating multiple lakes within one model, and simulates better the lake–stream connections. The software used in this study (ModelMuse) [see section 2.2.] is integrated with the most recent version of the Lake Package (LAK7) which, according to my knowledge, was not used before for any similar studies.

2.2. Software selection

In order to achieve the objectives of this study, a steady state and a transient state groundwater model was built using MODFLOW-2005 (Harbaugh, 2005) applying ModelMuse software environment (Winston, 2009) that includes the Lake Package (Merritt & Konikow, 2000). ModelMuse is the graphical user interface which is selected because: (i) it supports making input files for MODFLOW-2005 or later versions such as MODFLOW-NWT (Niswonger et al., 2011). (ii) according to my knowledge, it is the first and the only software that is integrated with Lake (LAK7) Package which is particularly suitable for this study area; (iii) it serves as pre-processor and post-processor for MODFLOW-2005 as well as for GSFLOW. In addition, it has some additional options such as the Unsaturated Zone Flow (UZF1) Package integrating surface and groundwater through flow in the unsaturated zone, and Stream-Flow Routing (SFR7) Package integrating interactions between streams and groundwater.

At the beginning of this study, MODFLOW-2005 was selected, then due to some circumstances that will be discussed later, that software was changed to MODFLOW-NWT.

2.3. Work plan

The schematic representation of the work plan is shown in Figure 2-1.

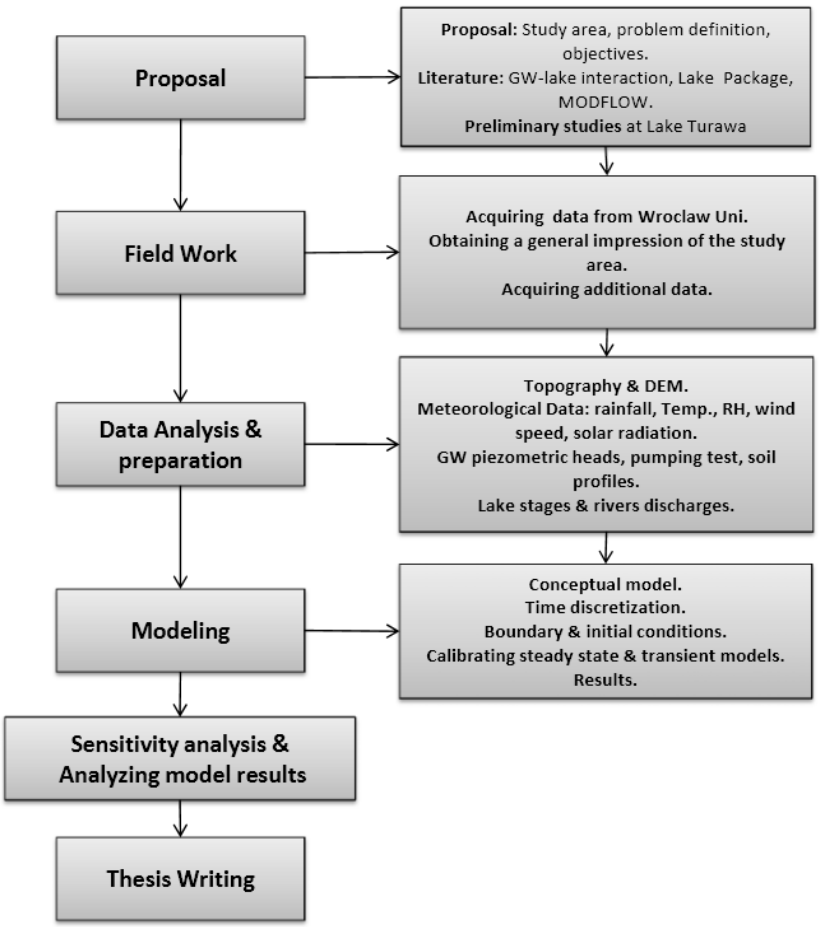

Figure 2-1 Schematic representation of the work plan.

2.4. DEM adjustment

As the available digital elevation model [DEM] obtained from Wroclaw University does not cover the total study area, in order to extent the available 5 m resolution DEM obtained from Wroclaw University to cover the whole study area, at the beginning, a 90 meter resolution DEM was obtained from SRTM database (http://srtm.csi.cgiar.org/), then after comparing the two DEMs a vertical shift was found between the two maps, probably due to different resolution, different datum used, and different sources of data, so it could not be used properly. Finally, instead of using the 90 m resolution DEM, the contour lines of the topographic map at the scale 1:10000 [Figure 1-2] were digitized in ILWIS software and interpolated to form the final DEM raster map.

2.5. Hydro-meteorological calculations

Precipitation and evapotranspiration are the main driving forces of any hydrological model. The Turawa study area has a hydro-meteorological ADAS station (shown in Figure 1-2) capable of recording all the meteorological data on hourly basis. The data of this station were mainly used for all the hydro-meteorological calculations in this study. The time step for this study was selected to be daily in order to match with the UZF Package input data requirements [section 2.8.3.3.] of daily precipitation and daily potential evapotranspiration. After investigating the available time series data, the study period was selected to start at the beginning of the hydrological year, on 1st November 2003 until the end of the hydrological year on 31st October 2009.

2.5.1. Precipitation

In order to fill in the rainfall record gaps in the Turawa ADAS station, a new rainfall data from a nearby station were required to setup correlation between the two. At the beginning, rainfall data from "Opole" ADAS station [see Figure 1-1] were downloaded from online NNDC climate database "CLIMVIS". These data however, did not give a good correlation. Surprisingly, rainfall data from the same station (Opole), but acquired from hydro-meteorological Institute in Poland gave better correlation results.

2.5.2. Potential evapotranspiration

This section aims at calculating the daily potential evapotranspiration , according to "FAO Penman Monteith" method, from the available meteorological data. Due to some gaps within the data obtained from Turawa ADAS station, Hargreaves equation was used to calculate the daily reference evapotranspiration in order to be correlated with the calculated FAO reference evapotranspiration values to fill in the gaps. Finally, the continuous calculated values of the daily FAO reference evapotranspiration were converted to daily potential evapotranspiration using the single crop coefficient method.

The available hourly incoming solar radiation, relative humidity, wind speed, air temperature, and soil heat flux available from the Turawa hydro-meteorological ADAS tower were used to calculate the daily potential evapotranspiration using "FAO Penman Monteith" method (Allen et al., 1998). According to Wang et al. (2012); the international scientific community has accepted the FAO Penman-Monteith (P-M) method as the most accurate approach for calculating evapotranspiration compared to other approaches. The summary of the method below follows Allen et al. (1998).

FAO Penman-Monteith method uses the original P-M equation [Equation 2.1] after some simplification to calculate reference evapotranspiration. Reference evapotranspiration is the evapotranspiration from the reference surface represented by a hypothetical grass reference crop with an assumed crop height of 0.12 m, a fixed surface resistance of 70 s m^{-1} and an albedo of 0.23.

$$\lambda ET = \frac{\Delta(Rn-G)+\rho_a \cdot C_p \cdot \frac{(e_s-e_a)}{r_a}}{\Delta+\gamma\cdot\left(1+\frac{r_s}{r_a}\right)} \qquad (2.1)$$

where λET is the latent heat flux representing the evapotranspiration, Rn is the net radiation, G is the soil heat flux, (e_s - e_a) represents the vapour pressure deficit of the air, ρ_a is the mean air density at constant pressure, C_p is the specific heat of the air, Δ represents the slope of the saturation vapour pressure temperature relationship, γ is the psychrometric constant, and r_s and r_a are the (bulk) surface and aerodynamic resistances. r_a can be calculated according to Equation 2.2.

$$r_a = \frac{ln\left[\frac{z_m-d}{z_{om}}\right]\cdot ln\left[\frac{z_h-d}{z_{oh}}\right]}{k^2\cdot u_z} \qquad (2.2)$$

where z_m is the height of wind measurements [m], z_h is the height of humidity measurements [m], d is the zero plane displacement height [m], z_{om} is the roughness length governing momentum transfer [m], z_{oh} is the roughness length governing transfer of heat and vapour [m], k is the von Karman's constant and equal to 0.41 [-], and u_z is the wind speed at height z [m s^{-1}].

According to FAO Penman-Monteith, the aerodynamic resistance can be calculated using the following equations:

$$d = 2/3\ h \qquad (2.3)$$

$$z_{om} = 0.123\ h \tag{2.4}$$

$$z_{oh} = 0.1\ z_{om} \tag{2.5}$$

Where h is the crop height [m]. Substituting from Equations 2.3, 2.4, and 2.5 into Equation 2.2, and assuming that $z_m = z_h = 2$ m, then r_a can be calculated from Equation 2.6.

$$r_a = \frac{208}{u_2} \tag{2.6}$$

And regarding r_s, it can be calculated from Equation 2.7.

$$r_s = \frac{r_l}{LAI_{active}} \tag{2.7}$$

Where r_s is the (bulk) surface resistance [s m^{-1}], r_l is the bulk stomatal resistance of the well-illuminated leaf [s m^{-1}], LAI_{active} is the active (sunlit) leaf area index [m^2 (leaf area) m^{-2} (soil surface)]. The LAI for grass can be assumed equal to 24*h, and the $LAI_{active} = 0.5$ LAI.

The following equations (Equation 2.8 to Equation 2.14) can also be used to calculate the atmospheric pressure P_{atm} [K.Pa], γ [K.Pa.°C^{-1}], RH [-], e_s [K.Pa], Δ [K.Pa.°C^{-1}], R_n net radiation [MJ.m^{-2}.day^{-1}], the net solar or shortwave radiation R_{ns} [MJ.m^{-2}.day^{-1}], and the net longwave radiation R_{nl} [MJ.m^{-2}.day^{-1}].

$$P_{atm} = 101.3\left(\frac{293-0.0065\,Z}{293}\right)^{5.26} \tag{2.8}$$

$$\gamma = \frac{c_p \cdot P_{atm}}{\varepsilon \cdot \lambda} = 0.665 * 10^{-3}\ P_{atm} \tag{2.9}$$

$$RH = \frac{e_a}{e_s} * 100 \tag{2.10}$$

$$e_s = 0.6108 * e^{\left[\frac{17.27*T}{T+237.3}\right]} \tag{2.11}$$

$$\Delta = \frac{4098\left[0.6108\, e^{\left(\frac{17.27\,T}{T+237.3}\right)}\right]}{(T+237.3)^2} \tag{2.12}$$

$$R_n = R_{ns} - R_{nl} = (1-\alpha)R_s - R_{nl} \tag{2.13}$$

$$R_{nl} = \sigma\left[\frac{T_{max,K}^4 + T_{min,K}^4}{2}\right] \cdot \left(0.34 - 0.14\sqrt{e_a}\right) \cdot \left(1.35\frac{R_s}{R_{So}} - 0.35\right) \tag{2.14}$$

$$ET_o = \frac{0.408\,\Delta \cdot (Rn-G) + \gamma \cdot \frac{900}{T+273} \cdot u_2 \cdot (e_s - e_a)}{\Delta + \gamma(1+0.34\,u_2)} \tag{2.15}$$

Where T is the air temperature at elevation z [°C], α is the albedo [-], $T_{max,K}$ is the daily maximum air temperature [°K], $T_{min,K}$ is the daily minimum air temperature [°K], e_s is the saturation vapour pressure for a given time period [k.Pa], e_a is the actual vapour pressure [k.Pa], R_s is the solar or shortwave radiation [MJ.m^{-2}.day^{-1}], and R_{so} is the clear-sky solar or clear-sky shortwave radiation [MJ.m^{-2}.day^{-1}]. R_{so} and the extra-terrestrial radiation R_a [MJ.m^{-2}.day^{-1}] can be calculated from Equations 2.16 and 2.19.

$$R_{so} = (0.75 + 2 * 10^{-5} * z)\ R_a \tag{2.16}$$

The computed reference evapotranspiration [ET_o] should be converted later to potential evapotranspiration [PET] as required by the used modelling software [ModelMuse]. McMahon et al. (2013) adapted Dingman's definition for potential evapotranspiration and recommended following final definition "is the rate at which evapotranspiration would occur from a large area completely and uniformly covered with growing vegetation which has access to an unlimited supply of soil water, and without advection or heating effects".

According to FAO-56 (Allen et al., 1998) there are two methods that could be used to convert ET_o to PET for different crop types, the single and the dual crop coefficient approaches. In the single crop coefficient method, PET can be calculated by multiplying ET_o by a single crop factor [K_c] which depends on the crop type and its growing stage [Equation 2.17]. Regarding the dual crop coefficient approach, the crop coefficient is divided into two other factors; the first factor characterizes the evaporation differences and the second factor characterizes the transpiration differences between the crop and the reference surface. The dual crop coefficient approach required more sophisticated data about the crops and the soil which were not available for this study so only the single crop factor [K_c] was used.

$$PET = ET_c = K_c * ET_o \quad (2.17)$$

The study area in the surrounding of Turawa Lake is covered mainly with "Pinus sylvestris L" trees besides grasses and very few buildings. The crop coefficient for these land covers are not mentioned exactly in the FAO-56 book. For grass areas; K_c was assumed as having the same properties as the reference surface or the reference grass. Regarding the "Pinus sylvestris L" trees; the most similar type of trees mention in the FAO-56 book is "Conifer Trees" which has a K_c value equal to 1.0 during any growing stage. The building areas were neglected and assumed to have the same evapotranspiration values as grass covered areas.

In order to fill in the missing data in the Turawa ADAS database used for calculating the potential evapotranspiration; first of all the daily minimum, average, and maximum temperatures during the study period were retrieved from the online "CLIMVIS database" and correlated with the available temperatures to fill in the missing temperature values. After that, the available temperatures after filling the gaps were used to calculate the Hargreaves reference evapotranspiration (Equation 2.18 to 2.22). Finally, the calculated reference evapotranspiration values were correlated with the FAO Penman-Monteith reference evapotranspiration values to fill in the reference evapotranspiration gaps.

$$ET_o = 0.0023 \cdot (T_{mean} + 17.8) \cdot (T_{max} - T_{min})^{0.5} \cdot R_a \quad (2.18)$$

$$R_a = \frac{24*60}{\pi} G_{sc} \cdot d_r \cdot [\omega_s \cdot sin(\emptyset) \cdot sin(\delta) + cos(\emptyset) \cdot cos(\delta) \cdot sin(\omega_s)] \quad (2.19)$$

$$d_r = 1 + 0.033\, cos\left[\frac{2\pi}{365} \cdot J\right] \quad (2.20)$$

$$\delta = 0.409\, sin\left[\frac{2\pi}{365} \cdot J - 1.39\right] \quad (2.21)$$

$$\omega_s = arccos[-tan(\emptyset) \cdot tan(\delta)] \quad (2.22)$$

Where T_{mean} is the daily mean air temperature [°C], $T_{max,}$ is the daily maximum air temperature [°C], $T_{min,}$ is the daily minimum air temperature [°C], G_{sc} is the solar constant=0.0820 [MJ.m^{-2}.min^{-1}], d_r is the inverse relative distance Earth-Sun [-], ω_s is the sunset hour angle [rad], ϕ is the latitude [rad] +ve for the northern hemisphere and –ve for the southern hemisphere, δ is the solar declination [rad], J is the Julian number of the day in the year [-], and the remaining parameters have been previously defined.

2.5.3. Lake evaporation

In this study, Penman equation was used to calculate open-surface water evaporation. According to (McMahon et al., 2013), daily open water evaporation using Penman approach can be calculated from Equation (2.23).

$$E_{openW} = \frac{\Delta}{\Delta+\gamma} \cdot \frac{R_n}{\lambda} + \frac{\gamma}{\Delta+\gamma} \cdot E_a \qquad (2.23)$$

Where E_{OpenW} is the daily open-surface water evaporation (mm day^{-1} = kgm^{-2} day^{-1}), R_n is the net daily radiation at the water surface (MJ.m^{-2}.day^{-1}), λ latent heat of vaporization [MJ.kg^{-1}], E_a is a function of the average daily wind speed and can be calculated from Equations 2.24 and 2.25, and other terms have been previously defined. In this study, the water albedo was assumed to be fixed and equal to 0.1 as recommended by Govaerts (2013), and R_n was calculated from Equations 2.13 and 2.14.

$$E_a = f(u) \cdot (e_s - e_a) \qquad (2.24)$$
$$f(u) = a + b \cdot u_2 \qquad (2.25)$$

Where f(u) is the wind function, (e_s-e_a) is the vapour pressure deficit (k.Pa), a and b are the wind speed function constants and values of a=1.313 and b=1.381 are recommended by McMahon et al. (2013), and u is the daily average wind speed (m s^{-1}).

In order to fill in the gaps for the lake evaporation, the calculated daily lake evaporation resulting from Penman equation were directly correlated with the daily reference evapotranspiration from Hargreaves equation.

2.5.4. Infiltration rates

The infiltration rates are required as input to the Unsaturated Zone Flow Package "UZF" that was used in this study in order to calculate both, the groundwater recharge and the ground water evapotranspiration. The infiltration rate according to the UZF concept (Niswonger et al., 2006) is equal to the rainfall values minus the interception loss, or in other words it is the amount of rainfall water that reaches the land surface. The infiltrated water is further percolated within the unsaturated zone soil voids according to the vertical hydraulic conductivity of the soil and the degree of saturation of the unsaturated zone. The UZF Package further divides the percolated water into unsaturated zone evapotranspiration, groundwater evapotranspiration, unsaturated zone storage, and groundwater recharge. If the applied infiltration rate is higher than the vertical hydraulic conductivity of the soil in the unsaturated zone, the percolation rate will be limited by the vertical hydraulic conductivity of the soil and the excess infiltration will be routed as surface runoff either to streams or to the lake.

Wang et al. (2007) published in their literature some field measurements of interception loss for different land covers and different locations over the globe. One of these measurements was carried out in the United Kingdom (at 52° 20` N and 0° 42` W) where the vegetation type was *Pinus silvestris* and the interception value was found to be 27.3 % of the rainfall. As the climate in the United Kingdom is

comparable to the study area in Poland, that interception value was used in this study in order to evaluate infiltration rates.

2.5.5. Rivers discharge estimation

The Turawa Lake is supplied with water by three rivers: Mala Panew, Libawa, and Rosa. However, the lake inflow data were only available for the Mala Panew River at "Staniszcze Wielkie" gauging station [Figure 2-2]. In order to estimate the total amount of inflow to the lake, ArcGIS software was used to geo-reference an image containing the three catchments [Figure 2-2], and the catchment area for each river was estimated. Next, the MPR discharge at the "Staniszcze Wielkie" gauging station was divided by the MPR catchment area upstream of the gauging station, hatched in blue in Figure 2-2, to obtain discharge contributing factor. That factor was then used to multiply the catchment areas of Libawa, Rosa and the remaining MPR catchment area downstream of the "Staniszcze Wielkie" gauging station to estimate all the contributing inflows to the Turawa Lake. This method might subject to some uncertainties due to different discharge properties of each catchment; therefore these discharges were later in the model calibration considered as uncertain and adjusted accordingly during model calibration process.

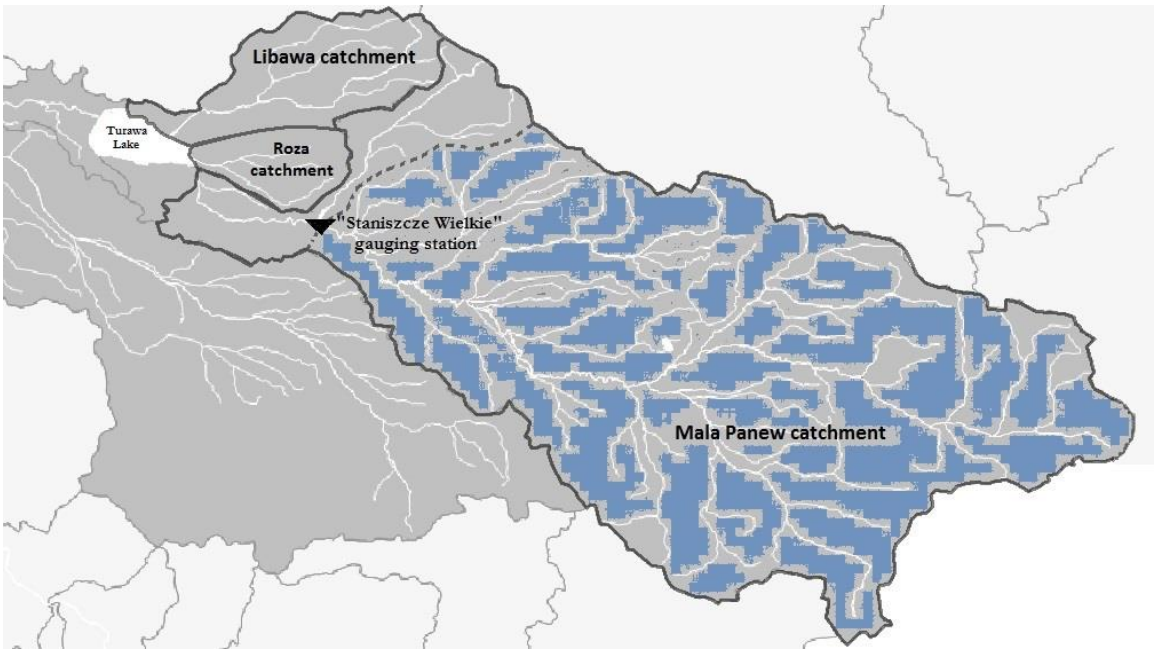

Figure 2-2 The catchment area for Mala Panew, Libawa, and Roza Rivers.

2.6. Software description

MODFLOW–2005 is a 3-D finite-difference groundwater model developed by USGS. It can be used to model steady and transient flow in any system of aquifer layers; confined, unconfined, a combination of confined and unconfined, regularly or irregularly shaped. MODFLOW was firstly developed by McDonald and Harbaugh (1988), who used Equation 2.23 to describe the three dimensional incompressible groundwater flow through porous material.

$$\frac{\partial}{\partial x}\left(K_x \cdot \frac{\partial h}{\partial x}\right) + \frac{\partial}{\partial y}\left(K_y \cdot \frac{\partial h}{\partial y}\right) + \frac{\partial}{\partial z}\left(K_z \cdot \frac{\partial h}{\partial z}\right) + W = S_S \cdot \frac{\partial h}{\partial t} \qquad (2.23)$$

Where K_x, K_y, and K_z are values of hydraulic conductivity along the x, y, and z coordinate axes, which are assumed to be parallel to the major axes of hydraulic conductivity (L/T), h is the potentiometric head (L), W is a volumetric flux per unit volume representing sources and/or sinks of water, with $W < 0.0$ for flow

out of the ground-water system, and W > 0.0 for flow into the system (T^{-1}); S_S is the specific storage of the porous material (L^{-1}); and t is time (T).

Equation 2.23 together with the initial and boundary conditions form a mathematical representation of the groundwater flow system. MODFLOW uses a finite difference approach in which a discretized linear algebraic difference form of Equation 2.23 is used for solving the potentiometric head for each cell, every time step, during the simulated period of time (Harbaugh, 2005). Figure 2-3 shows MODFLOW-2005 methodology under ModelMuse environment. In Model Muse, there is an option for the user to choose either MODFLOW-2005 or MODFLOW-NWT for running the same model with the same packages and boundary conditions used.

MODFLOW-NWT is Newton formulation of MODFLOW-2005. MODFLOW-NWT was developed mainly to solve problems caused by drying and rewetting nonlinearities of the unconfined groundwater-flow equation (Niswonger et al., 2011). This problem was met at the beginning of this study, with MODFLOW-2005, due to some dry cells located over the mountainous part south west of the study area [Figure 1-4] and it was overcome by using MODFLOW-NWT. Another important difference is that groundwater heads in MODFLOW-NWT are calculated for dry cells, even if they are below the cell's bottom, whereas in the standard MODFLOW-2005 they are excluded.

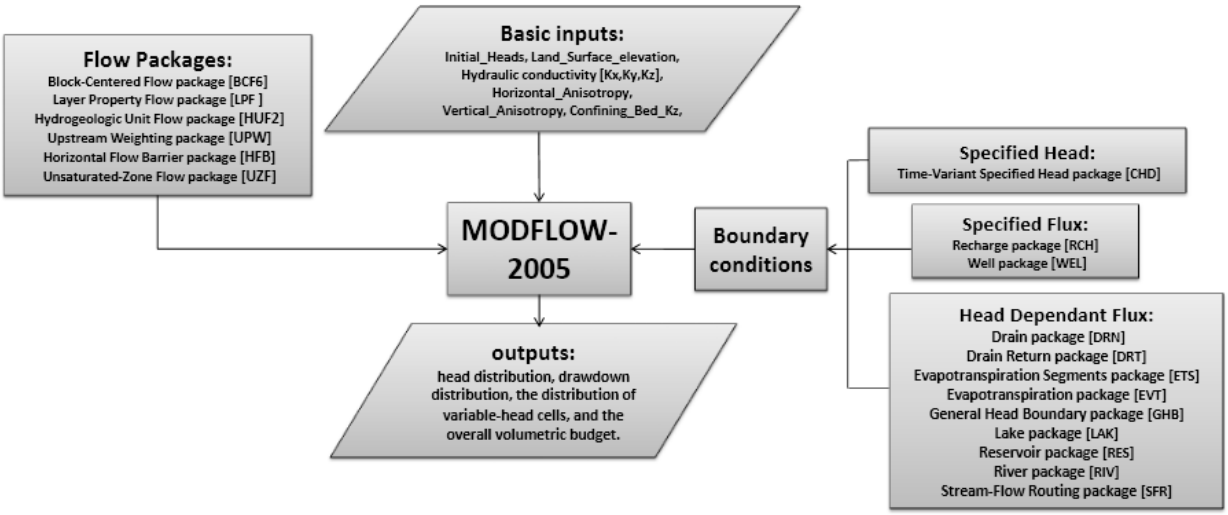

Figure 2-3 MODFLOW-2005 methodology under ModelMuse environment.

In addition, many recently developed packages for MODFLOW-2005, such as UZF and SFR packages, apply nonlinear boundary conditions to the groundwater-flow equation. Using these packages under MODFLOW-NWT improves convergence and computational efficiency (Niswonger et al., 2011).

ModelMuse gives the user the capability of defining the spatial and temporal inputs of MODFLOW-2005 and MODFLOW-NWT, by drawing points, lines, or polygons on top, front, and side views of the model domain. These objects can have 3-D extend by associating one or two formulas to it. These formulas define the extent of the objects perpendicular to its plane of view. Formulas can be used also to specify the spatial data (data sets) values. The values of data sets can be defined using objects, regardless of the spatial and temporal discretization of the model. Therefore, the grid and stress periods for the model can be adjusted automatically without re-specifying the model spatial data and boundary conditions (Winston, 2009).

2.7. Conceptual Model

This study focuses on the area adjacent to the Lake Turawa (Figure 1-2). According to the cross sections in Figures 1-10 and 1-11, and the borehole data (Appendix 1), the groundwater flow system is composed of three hydro-stratigraphic units forming three layers (Figure 2-5). The upper aquifer layer is an unconfined aquifer which has a thickness ranging between 1.5 meters and 35.0 meters; it is composed mainly of boulders, gravel, fine, medium, and coarse sand besides a little bit of clay and loam. The middle aquitard layer has relatively low permeability, its thickness is relatively small and ranges between 1.0 to 15.5 meters; it is composed mainly of loam with addition of sandy clay, clay, and argillaceous material. The lower layer is a confined aquifer which has thickness ranging between 0.7 and 36.6 m; it is composed mainly of gravel and sand. The three layers were assumed to be internally homogenous anisotropic with Kx = Ky and Kz = Kx/10.

According to the available piezometric heads, the general groundwater flow direction is from the east to the west. That flow is restricted at the north and south by no-flow boundaries [see section 2.8.2.1.]. The sources of groundwater inflow into the system are: recharge by rainfall, lake seepage, streams seepage, and lateral groundwater inflow across the eastern boundary of the area. The groundwater outflows from the study area by groundwater evaporation, lateral groundwater outflow across the western boundary, and groundwater contribution to the lake and the streams.

The Turawa Lake is supplied with water by Malwa Panew, Libawa and Rosa Rivers, rainfall, groundwater inflow to the lake and surface runoff from the area surrounding the lake. Water flows out from the lake through Mala Panew River downstream of the lake, by evaporation, and by seepage.

2.8. Numerical model

2.8.1. General modelling setup

Three layers were used to simulate flow through the upper unconfined and the lower confined aquifers, with a second aquitard layer in between. A grid consistent with the PUWG_92 Polish coordinate system and having a rectangular cell size 200 meters by 200 meters was used. The overall model grid was designed with 46 rows and 58 columns, giving a total number of cells equal to 2668 cells.

2.8.2. External boundary conditions

In this study, the same external boundary conditions were used for all the model layers, i.e. either no-flow boundaries or general head boundaries (GHB). These boundaries were defined based on topography and subsurface hydro-geological assessment. The no-flow boundaries are represented by groundwater divides and the general head boundaries are where groundwater flows in or out across the boundaries.

2.8.2.1. No-flow boundaries

Figure 2-2 shows the topographic divides for each sub-catchment within the Mala Panew catchment. From the figure, there is a topographic divide at the north of the lake and at the south of the lake as well. Using the 90 meter resolution DEM obtained from SRTM database (http://srtm.csi.cgiar.org/), the topographic boundaries were investigated again with the help of watershed tool in ArcGIS, and it was matching with the available topographic divides shown in Figure 2-2.

2.8.2.2. General head boundaries

Along the boundaries of the area under concern, cells which were not simulated as a no-flow boundary, were simulated as a general head boundary (GHB) in order to account for the groundwater inflow and outflow from the system. Figure 2-4 shows the final external boundary conditions used in this study where

the GHB are shown in red, these boundaries are assigned where either groundwater inflow or outflow is expected according to the arrows in the figure.

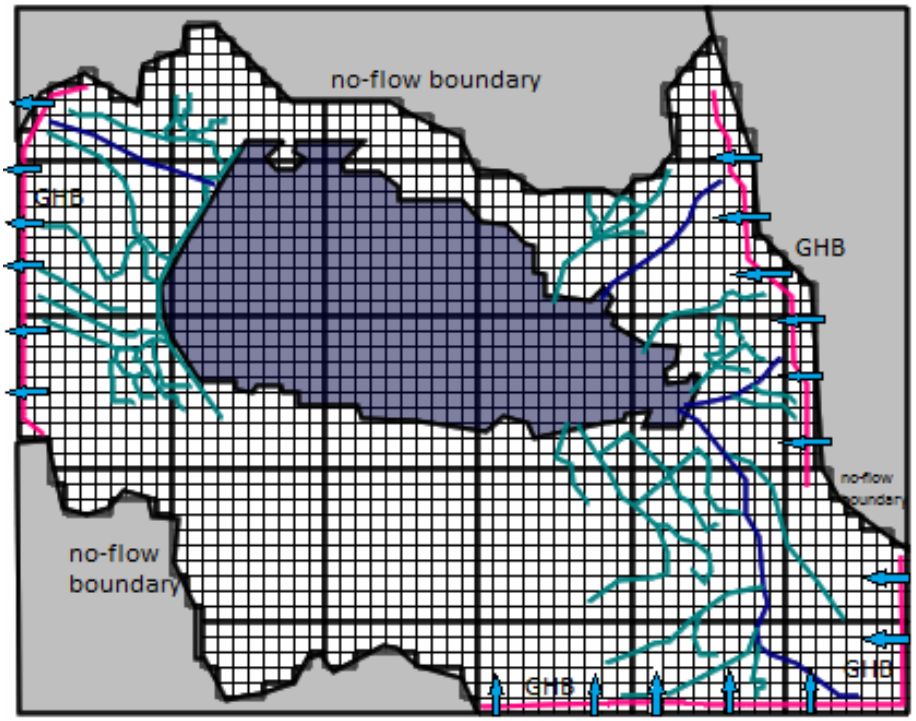

Figure 2-4 External boundary conditions; in black no-flow boundaries and in red, inflow and outflow boundaries.

2.8.3. Internal boundary conditions

2.8.3.1. Lake simulation

One of the advantages of MODFLOW-NWT under ModelMuse is the possibility of using the Lake Package to simulate lake-groundwater interaction. Unlike the Reservoir package, the head in the lakes can rise and fall due to interaction with groundwater and/or with streams simulated with the stream flow routing package [SFR]. The Lake Package is integrated into MODFLOW-NWT by specifying lake nodes in the model finite-difference grid, then, the lake stage is calculated relying on the computed fluxes into and out of the lake and the overall lake water balance (Hunt, 2003). Seepage between the lake and the adjacent aquifer system relies on the lake stage, the hydraulic head in the groundwater system, and the conductance between lake and aquifer, and it is quantified using Darcy's Law [Equation 2.24] (Reta, 2011) and (Merritt & Konikow, 2000).

$$q = K\frac{h_l - h_a}{\Delta l} \qquad (2.24)$$

Where q is the specific discharge (seepage rate) (L/T); K is the hydraulic conductivity (L/T) of materials between the lake and a location within the aquifer below the water table; h_l is the stage of the lake (L); h_a is the aquifer head (L); Δl is the distance (L) between the points at which h_l and h_a are measured.

In order to quantify the volumetric flux (L^3/T), Equation 2.24 can be written in the following form:

$$Q = q\,A = \frac{K\,A}{\Delta l}(h_l - h_a) = c\,(h_l - h_a) \qquad (2.25)$$

Where $c = KA/\Delta l$ is the conductance (L^2/T), $K/\Delta l$ is the leakance (T^{-1}).

Regarding the lake water budget calculation, the lake head is updated at the end of each time step independent of the ground-water budget according to the shown explicit form of Equation 2.26. Updating a lake water budget requires estimation of gains and losses of water from the lake, such as gains from rainfall, overland runoff, and inflowing streams, and losses due to evaporation and outflowing streams, in addition to any other kinds of gains and losses.

$$h_l^n = h_l^{n-1} + \Delta t \frac{P - E + SRO - W - SP + Q_{SI} - Q_{SO}}{A} \qquad (2.26)$$

Where h_l^n and h_l^{n-1} are the lake stage (L) during the current and previous time step, Δt is the time step length (T), P is the precipitation rate (L^3/T) on the lake, E is the evaporation rate (L^3/T) from the lake, SRO is the surface runoff rate (L^3/T) to the lake, W is the withdrawal rate (L^3/T) from the lake, SP is the net rate of seepage (L^3/T) between the lake and the aquifer, Q_{SI} and Q_{SO} are the rate of inflow and outflow (L^3/T) to streams during the time step, and A is the surface area of the lake (L^2) at the beginning of the time step.

There are a number of inputs required to activate the Lake Package in ModelMuse, such as: Time-weighting factor (Theta), maximum number of iterations (NSSITR), convergence criterion (SSCNCR), height of lake bottom undulations (SURFDEPTH), print lake output (LWRT), and lake bathymetry (TABLEINPUT). Theta determines either the lake package solution is explicit (THETA = 0.0), semi-implicit (0.0 < THETA < 1.0), or implicit (THETA = 1.0) for the lake stages (Merritt & Konikow, 2000). For all steady-state stress periods the default value of Theta is adjusted automatically as 1.0, however, for transient simulations Theta has a limited range from 0.5 to 1.0. If Theta has a value of 0.5 this would represent a lake stage midway between the current and the previous time step. If Theta has a value of 1.0 (fully implicit) this would represent a lake stage at the end of the current time step. ModelMuse generally recommends a value of 0.5 as slight errors may result in the solution of lake stage and seepage when Theta is greater than 0.5. A value greater than 0.5 is also recommended for damping oscillations in streamflow-routing equations.

NSSITR and SSCNCR are not needed for a transient solution and should be omitted when the solution is transient. For steady-state aquifer head solution, (NSSITR) is the maximum number of iterations for Newton's method solution for equilibrium lake stages in each MODFLOW iteration. (SSCNCR) is the convergence criterion for equilibrium lake stage solution by Newton's method (Merritt & Konikow, 2000). If SSCNCR is equal to 0.0, a value of 0.0001 is recommended to be used instead. Newton's method is used to achieve equilibrium between all the lake inflows and out flows in steady state models, however, this is not a necessary condition for transient models. SURFDEPTH represents the height of lake bottom undulations, and it has been added recently to the lake package in order to reduce the numerical oscillations. Values from 0.01 to 0.5 are generally recommended and have been used successfully. Checking the Print lake output (LWRT) check box in ModelMuse will cause LWRT to be set to 0 which allows Lake Package data to be printed.

Lake Bathymetry (TABLEINPUT) is also one of the recently added options to the Lake Package. As indicated in the online help of ModelMuse; "if the optional key word (TABLEINPUT) is specified on the first line of the Lake package input file then the program reads values of lake stage, volume, and area from external lake bathymetry text files". Each lake bathymetry input file must contain exactly 151 lines [150 intervals] with values of lake stage and the corresponding lake volume, and surface area in each line. Water exchange between lakes and groundwater is based on cell-by-cell calculation using the area of cells, not the lake surface area from the external lake bathymetry file.

In this study, THETA was set to 1.0 during steady state and 0.5 during transient state, and the default values of NSSITR, SSCNCR, and SURFDEPTH which are equal to 1000, 0.001 and 0.2 were used. The Lake Bathymetry (TABLEINPUT) was defined manually from the available data according to appendix 3. As the lake is simulated by a group of inactive cells (Merritt & Konikow, 2000), at the beginning of this study the lake itself was simulated by dividing the top layer into two equal horizontal layers; within the lake area, the lower layer had its top equal to the lake bottom and outside the lake area it had a thickness equal to half of the original top layer, the upper layer within the lake area had its top equal to the maximum lake level and outside the lake its top was equal to the top of the model (DEM level). Such conceptualization of the system was tested by a preliminary model run and resulted in cell drying process, enhanced by the division of the upper layer into two layers. The final lake simulation was done by adding an inactive layer at the top of the model having 1 meter thickness outside the lake, and within the lake area; the top is equal to the maximum lake water level and the bottom is equal to the lake bottom elevation [Figure 2-5]. This solution was kept during the whole study.

The presence of the sapropel layer at the bottom of the lake [see section 1.6.2.] may cause the lake bed to have different laekance values. Two zones were assigned for the lake bed leakance for the steady state and transient state models; one zone for the bed covered with sapropel, and another zone for the remaining lake bed area. The lake bed leackance for each zone was kept constant for each model alone and adjusted during the calibration process.

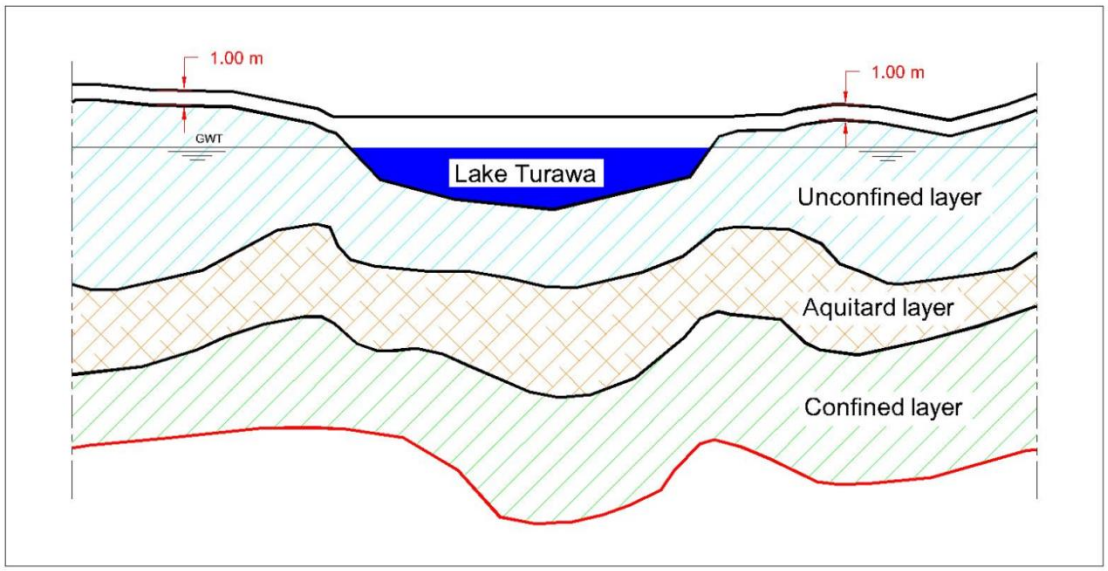

Figure 2-5 Cross section showing the lake conceptualization.

2.8.3.2. Rivers and drains simulation

In this study the Stream Flow Routing Package was used to simulate both; rivers and drains. One of the advantages of the SFR package is that it is linked to the Lake Package, and it was developed to accommodate streams that discharge water into and from lakes (Prudic et al., 2004). Also, the SFR Package has the ability of simulating volumetric surface water discharges not only head driven flow as in the River Package or Drain Package. The SFR Package allows several options for calculating the stream water depth; it can be calculated either by a user specified stream depth, using Manning's equation for wide rectangular channels, using Manning's equation with a channel cross section defined by eight points, using depth-discharge and width-discharge relations, or by specifying the values of stream depth and width at each observation point and the values between the observation points will be interpolated automatically. The SFR Package also allows the user to add or subtract water from streams due to runoff, precipitation,

and evapotranspiration (Prudic et al., 2004). In the SFR Package, each stream or segment is composed of number of reaches and all segments must have a sequential order (number) from the upstream to the downstream.

The interaction between streams and aquifer is computed according to Equation 2.27 and it is similar to the method used in the River Package.

$$Q = \frac{K\,w\,L}{m} \cdot (h_s - h_a) \qquad (2.27)$$

Where Q is a volumetric flow between a given section of stream and volume of aquifer (L^3/T), K is the hydraulic conductivity of streambed sediments (L/T), w is a representative width of stream (L), L is the length of stream corresponding to a volume of aquifer (L), m is the thickness of the streambed deposits extending from the top to the bottom of the streambed (L), h_s is the head in the stream determined by adding stream depth to the elevation of the streambed (L), and h_a is the head in the aquifer beneath the streambed (L).

An advantage of the SFR Package is that it allows four options for simulating diverting flow and that it allows the simulation of connections between streams and each other's and between streams and lakes. The connection between streams and each other's is adjusted mainly by the number of each segment, and the connection between streams and the lake is adjusted by giving the lake a number equal to -1.

In this study, for the sake of simplicity, all the rivers and drains were simulated by rectangular sections, the stream bed thickness for all streams was assumed equal to 1.0 meter, the hydraulic conductivities for the stream beds were adjusted during the calibration process, Manning coefficient for all streams was assumed equal to 0.035, the Mala Panew River width upstream of the lake was set equal to 20 meters and 30 meters downstream of the lake, and the width of Libawa and Rosa Rivers and all the drains was set equal to 10 meters, 10 meters and 5 meters respectively. As MODFLOW under ModelMuse environment does not allow the lake outlet of the MPR to have a stream bed elevation lower than the lake bed elevation (the free overfall case), the MPR downstream of the lake was disconnected from the lake and the lake outflow values, measured at Turawa gauging station downstream of the lake [see Figure 1-1], were assigned as both; withdrawal from the lake and inputs to the MPR in order to satisfy the measured outflows from the lake, and to adjust the groundwater heads downstream of the lake.

2.8.3.3. Recharge and ground water ET (UZF Package)

One of the most recently developed packages in MODFLOW is the Unsaturated Zone Flow "UZF" Package. It was developed mainly to simulate the unsaturated zone flow between the land surface and the groundwater table. The UZF Package provides relatively accurate approach for recharge estimation substituting both; the Recharge Package and the Evapotranspiration Package (Niswonger et al., 2006).

The main input to the UZF Package is called "the infiltration rate" [P_e] at land surface which is equal to precipitation minus interception loss. The UZF Package simulates the flow through the unsaturated zone vertically, in one dimension only. The applied infiltration rate is limited according to the saturated vertical hydraulic conductivity. Another required input to the UZF Package is the evapotranspiration demand or potential evapotranspiration and the evapotranspiration extinction depth below which no more water will be removed by evapotranspiration. The way in which UZF Package works may differ from the Evapotranspiration Package; at the beginning the evapotranspirated water is removed from the unsaturated zone (ET_u), then if the evapotranspiration demand is not met, water is extracted further from the saturated zone (ET_g) as far as the groundwater table is above the evapotranspiration extinction depth [see Figure 2-6]. In the UZF Package there is also an option to route water to streams or lakes, if either of

these packages is active, in case the groundwater table is higher than the land surface or in case the applied infiltration rate is higher than the soil saturated vertical hydraulic conductivity (Niswonger et al., 2006). The UZF Package requires as inputs the soil residual water content, the soil saturated water content, and the extinction water content, while the initial soil water content is an optional input.

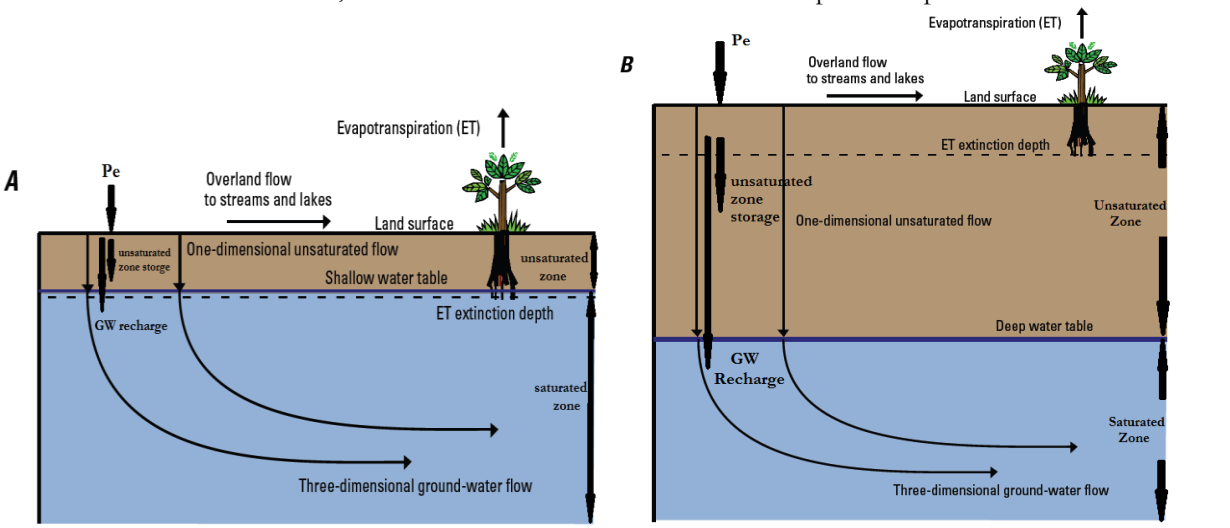

Figure 2-6 Flow through the unsaturated Zone: A) groundwater table is higher than ET extinction depth, B) groundwater table is lower than ET extinction depth.

In this study, the infiltration rates and the potential evapotranspiration were calculated daily according to sections number 2.5.4 and 2.5.2, respectively. The excess infiltration rate was selected to be routed to the lake, the evapotranspiration extinction depth was assumed equal to 2.0 meters according to the root depth of the dominant trees species, the evapotranspiration extinction water content was assumed equal to 0.05 (m^3/m^3) and equal to the soil residual water content, and the soil saturated water content was assumed equal to 0.30 (m^3/m^3). In the steady state model, the initial soil water content was not specified, but in the transient model it was specified equal to 0.05 (m^3/m^3) in order to give an average recharge rate during the first time step equal to the recharge rate in the steady state model. The UZF Package was activated for the land area only and it did not include the lake area.

2.8.3.4. Dam simulation (including HFB Package)

The diaphragm wall under the earthen dam, shown in Figure 1-2 and in the cross section in Figure 2-7, was simulated in the model using the Horizontal Flow Barrier "HFB" Package (Hsieh & Freckleton, 1993). Both, the barrier thickness and the barrier hydraulic conductivity were adjusted during the calibration process.

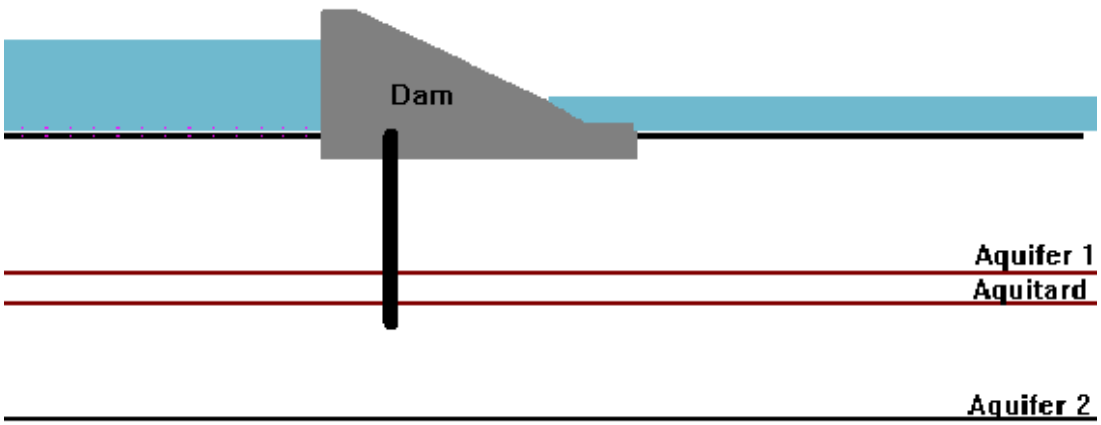

Figure 2-7 Cross section through the earthen dam downstream of the lake.

2.8.4. ZONEBUDGET

ModelMuse can produce the overall volumetric groundwater balance, but it doesn't provide the water balance for each simulated layer alone or for a specific area in the model. Harbaugh (1990) developed the ZONEBUDGET; which is a FORTRAN code capable of using MODFLOW results for calculating any sub-regional water budgets. In order to calculate the water budget for any zone, ZONEBUDGET uses cell-by-cell flow data saved by the model. The ZONEBUDGET is available also under ModelMuse environment. It allows creating the water budget for any single zone by specifying a different number for each single zone and it can also create the water budget for composite zones as well in order to reduce the calculations that may be done by the user.

2.8.5. Initial potentiometric map

The initial heads required for both; the steady state and the transient state model were assigned using one of the available potentiometric maps [Figure 2-8 and 2-9] retrieved from Wroclaw University. These potentiometric maps were created by using simultaneous water table measurements converted to hydraulic heads from all available piezometers. The potentiometric map was imported to ModelMuse as a shape file and assigned as initial heads. For the cells which were not covered by the shape file, the initial heads were assigned by extrapolating the available initial head values.

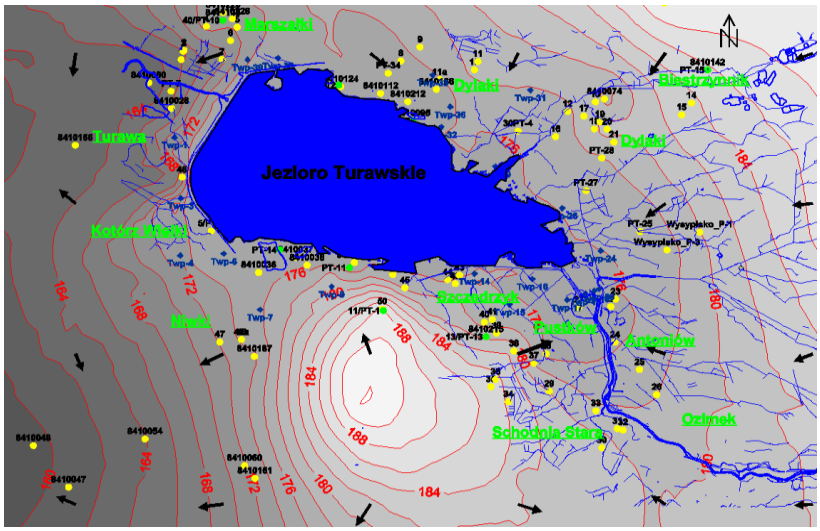

Figure 2-8 High water level potentiometric map (lake stage= 175.94 m a.m.s.l., 3rd May 2004).

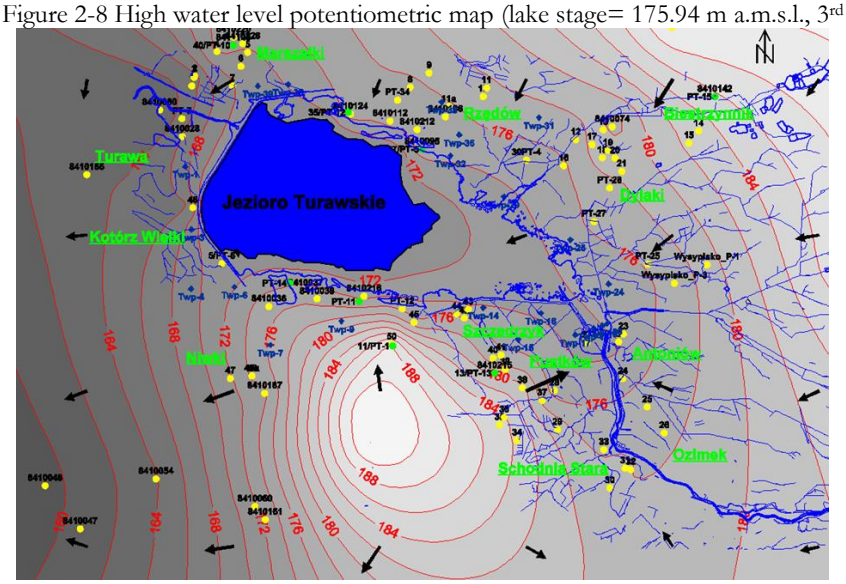

Figure 2-9 Low water lever potentiometric map (lake stage= 171.16 m a.m.s.l., 2nd October 2004).

2.8.6. Instantaneous and time series head observations

The Head Observation (HOB) Package was used to simulate both the instantaneous and the time series head records. For each piezometer, the data required are the piezometer name, time step and the observed head. After activating the HOB Package, all the piezometer's coordinates [see Table 1] were imported as points to ModelMuse, and then the data were assigned to each point individually. The observation layer, confined or unconfined, is defined in ModelMuse by assigning the higher Z-coordinate and lower Z-coordinate to the top and bottom elevation of each layer. The HOB Package can also be used to simulate multilayer observations using a weighted average of the heads in the entire layer, but this is out of scope of this study.

2.9. Steady state model

For the steady state model, the long-term average stresses (precipitation, potential evapotranspiration, lake evaporation, streams inflows and outflows) during the whole study period [from 1st Nov. 2004 to 31st Oct. 2008] were calculated and imposed on the model. The total inflows for Mala Panew, Libawa, and Rosa rivers were estimated and adjusted during model calibration to close the water balance (see section 2.5.5). The steady state lake stage was calculated as an average for the whole lake stages during the study period (173.77 m a.m.s.l.), and the model parameters were adjusted during the calibration process in order to obtain a simulated lake stage matching with this average lake stage. All the units used in the steady state model (and in transient state model) were meters and days.

MODFLOW-NWT with the Newtonian (NWT) solver was used to run the steady state model. The solver head tolerance was adjusted to 0.001 meter and the flux tolerance was 500 m^3/day as recommended by Niswonger et al. (2011). The model complexity was set as moderate, and all the remaining solver criteria were accepted by default. In the upstream weighting package which is used by default with the Newtonian solver, the IPHDRY option was deselected in order to print the final calculated heads for dry cells even if these heads were below the cell bottom.

At the beginning of the study the model cell size was adjusted to 50 x 50 m, but this was causing a convergence problems. Then later, the final cell size was adjusted to 200 x 200 m. 100 x 100 m cell size was also tested, but the model runs were too time consuming; each lasting for more than 15 minutes.

2.9.1. Steady state model calibration

Model calibration is the process of establishing a set of parameters, boundary conditions, and stresses that produce simulated heads and fluxes that match with the field measured values within a range of an acceptable error (Anderson & Woessner, 1991). The mean error, mean absolute error, and root mean square error [see Equations 2.28, 2.29, and 2.30] is used as a measure for groundwater heads and lake stages calibration, while the discrepancy value is used for the water balance. The discrepancy value is known as the difference between the total inflow and outflow divided by either inflow or outflow. A discrepancy value for the water balance around 1% or less is usually accepted (Anderson & Woessner, 1991).

There are usually two types of model calibration procedures; inverse and forward calibration. In the inverse procedure, the objective is to determine parameters and hydrologic stresses from known heads. In the forward procedure parameters (hydraulic conductivity, specific yield, and specific storage) and hydrologic stresses (recharge) are specified and then the model calculates heads, the parameters and hydrologic stresses should be adjusted until the difference between the observed and the simulated heads is within an acceptable range of error. There are also two ways for forward estimating calibrated model

parameters; by trial and error adjustment or automatic calibration using optimisation software (Anderson & Woessner, 1991).

Banta (2011) developed ModelMate, which is a graphical user interface that can be used with ModelMuse to prepare input files for optimisation software, UCODE_2005. ModelMate can also be used to run UCODE_2005 and display the analysis results. "UCODE can perform the following analyses: sensitivity analysis, parameter estimation, tests of model linearity, prediction sensitivity, nonlinear uncertainty, and investigation of an objective function" (Banta, 2011). At the beginning of this study while using MODFLOW-2005 under ModelMuse, due to the presence of some dry cells and consequently their conflict with MODFLOW-2005 and ModelMate, the MODFLOW-2005 had to be replaced with MODFLOW-NWT. However, ModelMate is not adapted to work with relatively new MODFLOW-NWT yet. An attempt was made to adapt ModelMate with MODFLOW-NWT through personal contact with USGS software developer Mr. Richard Winston who suggested a "work-around" solution for automated optimisation. After some trials this ModelMate solution was abandoned because each ModelMate run was taking a very long time. Finally, all the calibration processes were done manually, by trial and error, for both steady and transient states models. The steady state calibration process was challenging due to the presence of many unknowns such as rivers inflows, rivers and drains cross sections, rivers and drains stages, bed thickness and bed hydraulic conductivity, lake bed conductance, GHB heads and conductance, and the hydraulic conductivities for the three model layers. Part of the previous mentioned unknowns was assumed based on the field experience and archive literature data. The remaining part was adjusted to achieve a final accepted discrepancy values for the groundwater budget and the lake budget with a good match between observed and simulated heads within an acceptable error criteria. All the streams were assumed to have rectangular cross sections and 1 meter bed thickness, the GHB head was assigned based on the available piezometric heads and the GHB conductance was assumed 1.5 [m^2/day] per unit length base on an average value of the available hydraulic conductivities. The main calibration parameters that needed a lot of trials to be adjusted were the aquifers horizontal hydraulic conductivity, lake bed leakance, rivers inflow, stream stages and stream bed hydraulic conductivities.

2.9.2. Error assessment and sensitivity analysis

The errors' criteria in each case were calculated according to Equations 2.28, 2.29 and 2.30.

Mean error $$ME = \frac{\sum(H_{obs.} - H_{calc.})}{N} \quad (2.28)$$

Mean absolute error $$MAE = \frac{\sum|H_{obs.} - H_{calc.}|}{N} \quad (2.29)$$

Root mean square error $$RMSE = \sqrt{\frac{\sum(H_{obs.} - H_{calc.})^2}{N}} \quad (2.30)$$

Where N is the number of observations.

The main aim of doing sensitivity analysis is to determine the uncertainties in the calibrated model due to the use of uncertain parameters, stresses, and boundary conditions. The magnitude of change in groundwater head or lake stage from the calibrated parameters is an indicator to the sensitivity of the solution to this specific parameter. The sensitivity analysis results are usually expressed in terms of error criteria due to the change in a selected parameter value (Anderson & Woessner, 1991).

In this study, the sensitivity of steady state model was tested by investigating the effect of changing selected model parameters [the hydraulic conductivity of the top unconfined aquifer, streams bed

hydraulic conductivity, lake bed leakance, and rivers inflow] and hydrologic stresses on the piezometric heads shown in Table 1. Also, the effect of lake bed leakance, rivers inflow, and lake evaporation on the lake stage was investigated.

2.10. Transient model

Steady state solution represents an average solution for the analysed problem, while transient state solution produces a set of solutions corresponding to time steps of a specific stress period (Shakya, 2001). The no-flow boundary conditions in the steady state were kept in the transient state solution. There were six hourly time series piezometric records [Figure 1-2]; one of them at the western edge was used for assigning the head at the general head boundary. The remaining piezometric time series were quite far from the eastern and the southern general head boundaries. At the beginning the daily lake stages were correlated with one of the time series piezometers to find if there was a correlation factor that could be assigned between the lake stage and the general head boundaries, but the correlation coefficient was very bad. Finally, the instantaneous records at the remaining general head boundaries were used to assign an average ratio between these instantaneous records and the nearest time series piezometer, and the nearest time series piezometric records were used to assign the GHB head after multiplying all the records with the calculated ratio.

The same hydraulic conductivity zones and values as in the steady state model were used in the transient model, and they were subjected to modification later during the calibration process. All the units were fixed to meters and days. Due to the large difference between the average river inflows and outflows in the steady state model and the daily discharge values at the beginning of the transient model, it was difficult to start the initial conditions for the transient model assuming the steady state model condition. This was causing large water balance discrepancy values. To handle this problem, initially, the transient model started with a short warming up period of 70 days, followed by the normal simulation period.

2.10.1. Time discretisation

During this study, all the daily data were entered to the transient model in ModelMuse year by year. Due to some uncertainties in the last year data, the final simulation period for the transient model was fixed to five years [from 1st Nov. 2003 to 31st Oct. 2008], including the first year as warming up year [see section 2.10.3.].

Before the development of the UZF Package, normally the Recharge and the Evapotranspiration Packages were used to arbitrary assign the groundwater recharge and evapotranspiration values. Most of the previous studies were assigning the stress periods based on the change in the recharge, evapotranspiration or the response of the aquifers to water level changes. In MODFLOW, a stress period is a block of time that might have different lengths and represents an individual simulation period with hydrological stresses different from the other stress periods. These stress periods are usually further divided into time steps which may be one day, days, weeks, or months depending on the frequency of the available data.

After the development of the UZF Package, in which recharge and evapotranspiration are calculated internally not assigned as before in the Recharge and Evapotranspiration Packages, and because all the data used in this study are daily data, the UZF Package automatically assigned daily stress periods whatever else was assigned by the user in this study, resulting in daily stress period with one day time step.

2.10.2. Specific yield and specific storage

Specific yield which is known as the drainable porosity is a ratio, less than or equal to the effective porosity, indicating the volume of water per aquifer volume that a given aquifer will yield in response to

water table declination when the water is allowed to drain out of it under the forces of gravity. The specific storage is the amount of water that a portion of an aquifer releases from storage, per unit volume of aquifer, per unit change in hydraulic head, while remaining fully saturated (Anderson & Woessner, 1991). The specific yield and the specific storage are known as the storage coefficients, but specific yield is important for the unconfined aquifers and specific storage for confined aquifers. The specific yield value can range from 0.01 in case of clay and up to 0.40 in case of gravel or coarse sand. According to Anderson and Woessner (1991) the specific storage can have a value of 0.000003 [m^{-1}] in rocky soil or gravel and up to 0.02 [m^{-1}] in some kinds of clay. Based on the available boreholes and lithology data, an average specific yield (0.15) and specific storage (0.00001) values were assumed for the whole model at the beginning, and in selected zones these values were adjusted during the calibration process.

2.10.3. Transient model calibration

The initialization of the transient model is more important than in the steady state model. In the steady state model, the initial conditions are required only to speed up the model convergence as the time variable in the steady state model is set to infinite. In transient state models, assigning inaccurate or wrong initial conditions (heads, hydrologic stresses, or lake stage) may give wrong solution during the calculation process, and this wrong initial conditions may cause a cumulative error spreading over the total running time (Rientjes, 2012).

One of the well-known approaches used for model initialization is to assign arbitrary stresses and then run the model for a specific period, known as the warming up period, until the model results match the measured observations (Rientjes, 2012). This approach was followed during the calibration of the transient model; at the beginning a short warming up period, 70 days, was used to achieve the initial aquifer heads and lake stage at the first time step of the simulation period. After achieving these initial conditions, and in the following up time steps, a systematic error was found especially for the simulated lake stages; the simulated lake stages were diverting from the observed values and the error between the simulated and the observed lake stages was increasing with time. Firstly, there was a doubt about the uncertainties that may occur during the calculation of the rivers inflow, lake evaporation, the assigned hydraulic conductivity, specific yield, specific storage, or lake bed conductance. All the previous mentioned variables and parameters were revised and modified in order to reduce the error, but finally the main cause of the error was found to be too short warming up period. The model needed to be run with longer warming up period, for example one year, to adjust the trend of the model simulated values at the beginning of the simulation period.

Due to the complexity of the model and because it would be difficult to assign arbitrary data on daily basis for rivers inflows and out flows, rainfall, evapotranspiration, lake evaporation, and GHB heads, the first year of data, from 1st November 2003 until 31st October 2004, was 'sacrificed' as a warming up period in which the inflow was reduced by a specific factor 0.86, adjusted during the calibration process. In the follow up, 'valid' years simulation was carried out without any adjustment factor.

The main calibration parameters in the transient state model were the lake bed conductance, and the horizontal hydraulic conductivity of the three active layers. Besides, some changes to the assigned specific yield, specific storage, streams stages, and the thickness and hydraulic conductivity of the earthen dam were made.

2.10.4. Error assessment and sensitivity analysis

The error of the transient models simulation was assessed in similar way as in the steady state model, i.e. by applying Equations 2.28, 2.29 and 2.30.

The main aim of the sensitivity analyse is to find out the most sensitive parameter or hydrologic stress in order to give it special attention during the calibration process or in model prediction scenarios. During the sensitivity analysis of the transient model, the magnitude of groundwater heads' (for the logged time series piezometers) and lake stages' excursion from the corresponding calibrated values were investigated by changing the upper aquifer horizontal hydraulic conductivity (K_h), upper aquifer specific yield (S_y), lower aquifer specific storage (Ss), lake bed leakance, and rivers inflow to the lake by certain factors. Due to the large number of runs required for such sensitivity analysis, and because each model run in the transient state lasted long time (~45 minutes), the model used to perform the sensitivity analysis was run for three year period only (one year warming up and two years simulation) but only the results of the last two years were used for the sensitivity analysis.

2.10.5. Spatial and temporal effect of the lake on groundwater

In order to characterize spatio-temporal impact of the lake on groundwater heads in the area surrounding the lake, two transects of fictitious piezometers where assigned in the model, Northern Transect shown in red and Southern Transect shown in blue (Figure 2-10). The location of these two series of piezometers was selected to be far away from any groundwater divides or streams that might have additional effect on the groundwater heads. The first piezometer in each series was located 100 m away from the lake shoreline, and this distance increased sequentially by 200 m for each following piezometer.

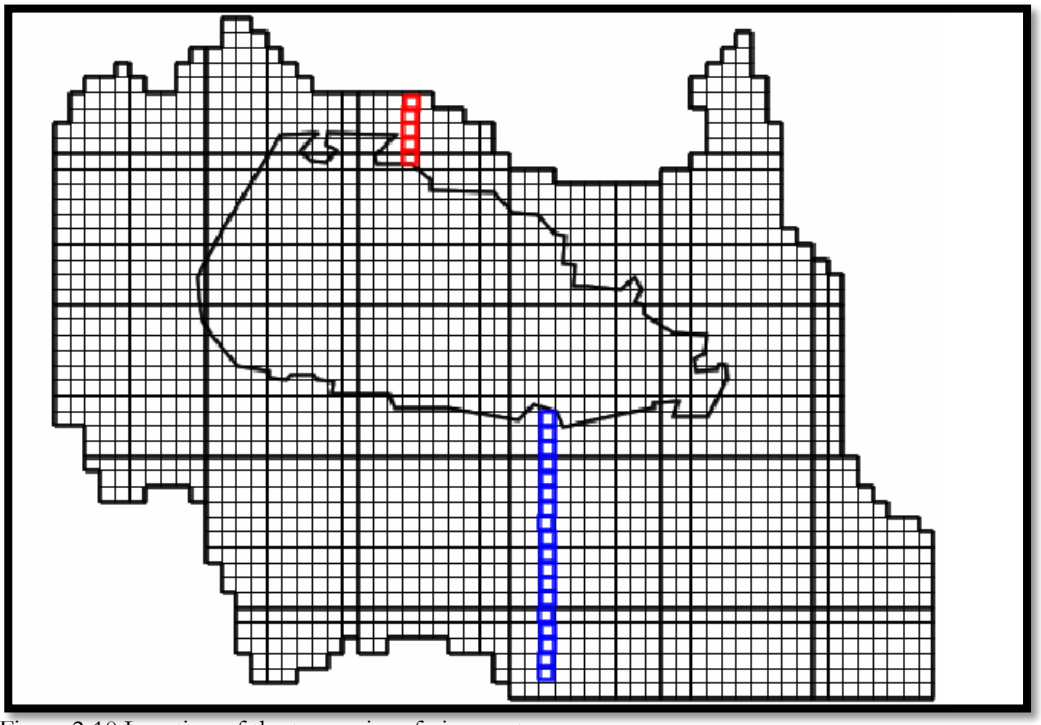

Figure 2-10 Location of the two series of piezometers.

3. RESULTS AND DISCUSSION

3.1. Hydro-Meteorological calculations

3.1.1. Precipitation

Figure 3-1 and 3-2 show that the correlation between the rainfall data available in Turawa area and the data obtained from CLIMVIS website is lower than the correlation between the rainfall data available in Turawa area and the data obtained from Hydro-meteorological Institute in Poland at Opole station. The final equation shown in Figure 3-2 was used to fill in the available rainfall data gaps in order to give the final daily continuous rainfall records [Figure 3-3].

Although the correlation coefficient 0.39 was not spectacular (Figure 3-2), the amount of necessary data gap infillings was also quite limited (Figure 3-3), so eventual error related to relatively low rainfall correlation can be considered as negligible.

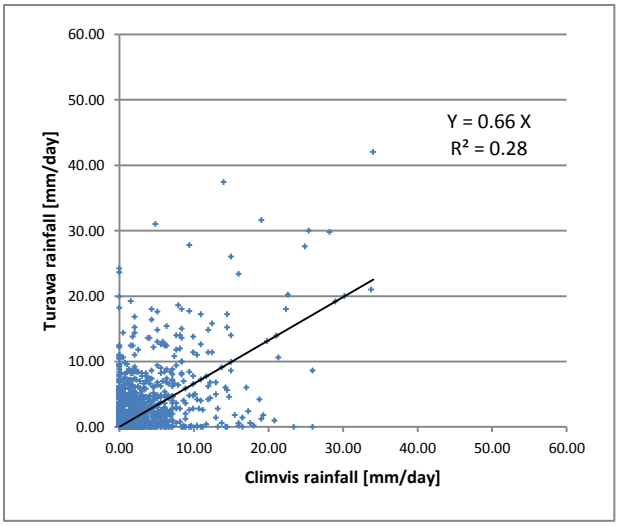

Figure 3-1 Correlation between Turawa and CLIMVIS rainfall data.

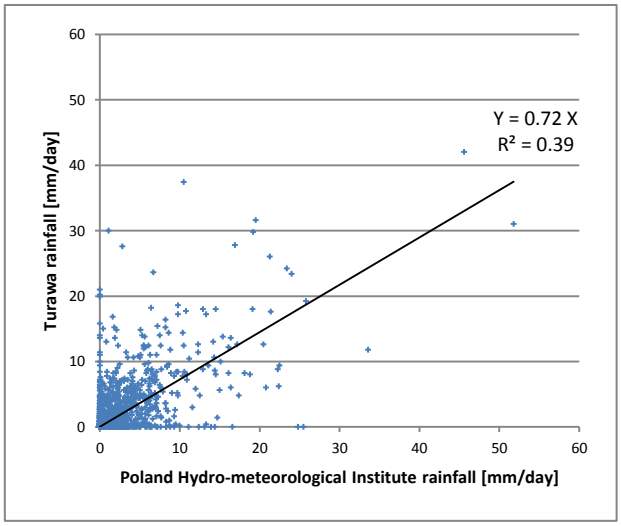

Figure 3-2 Correlation between Turawa and Opole rainfall data.

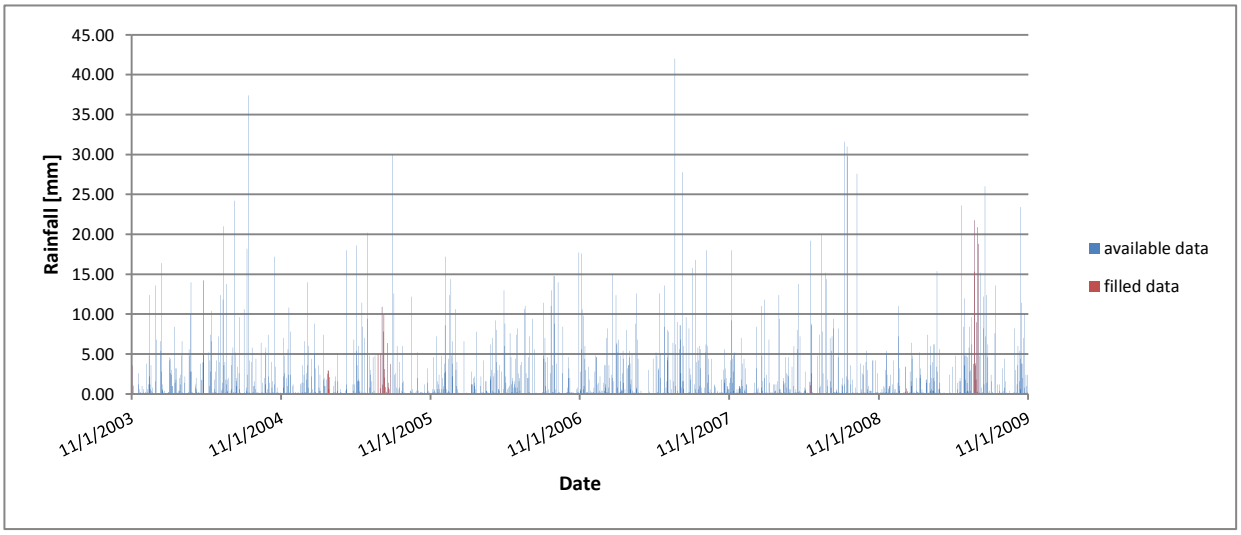

Figure 3-3 Daily rainfall after filling gaps [from 1 Nov.2003 to 31 Oct. 2009]

3.1.2. Evapotranspiration

A good correlation was found between the minimum, average, and maximum temperatures available in Turawa area and those obtained from CLIMVIS database (Figure 3-4). The three regression equations shown in Figure 3-4 were used to fill in the temperature gaps for the available data. Then the continuous daily records of temperatures were used to calculate the daily Hargreaves reference evapotranspiration further used for its correlation with the FAO-Penman-Monteith reference evapotranspiration for data gap filling of the latter (Figure 3-5). The final FAO-Penman-Monteith potential evapotranspiration values obtained after filling in the ET_o gaps and multiplying each value by the crop coefficient (Equation 2.17) are shown in Figure 3-6. The final PET values are ranging from -0.06 to 6.9 mm/day with very few, small negative values. These negative values might exist when the term (R_n-G) in Equation 2.15 or R_n has a negative value during very cold periods and might be considered as condensation. As they were very few and very small, they were neglected and substituted with zero.

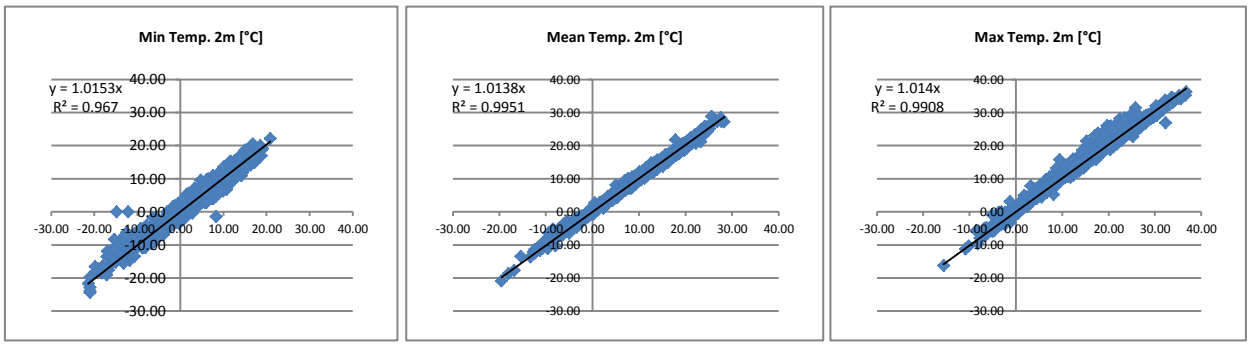

Figure 3-4 The correlation between the available minimum, average, and maximum temperatures from the meteorological tower and those obtained from CLIMVIS database at Opole station.

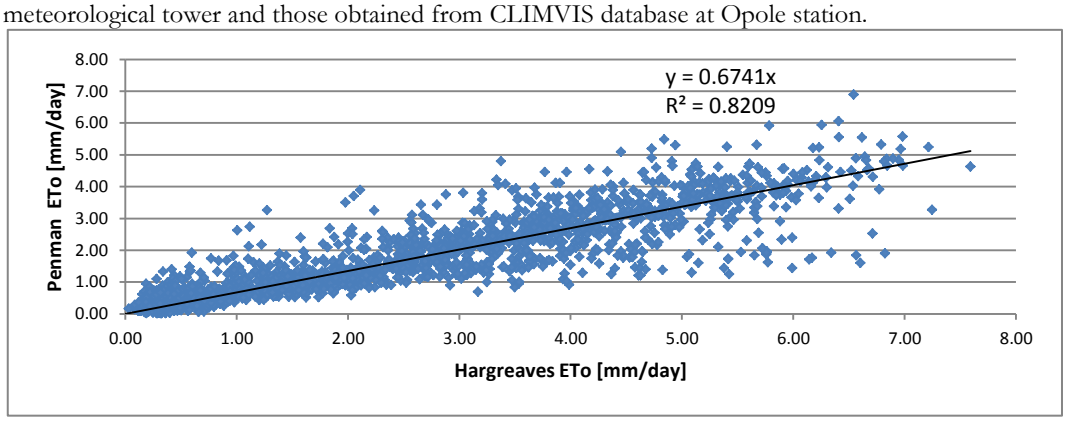

Figure 3-5 The correlation between reference evapotranspiration values obtained from FAO-Penman-Monteith and Hargreaves equation.

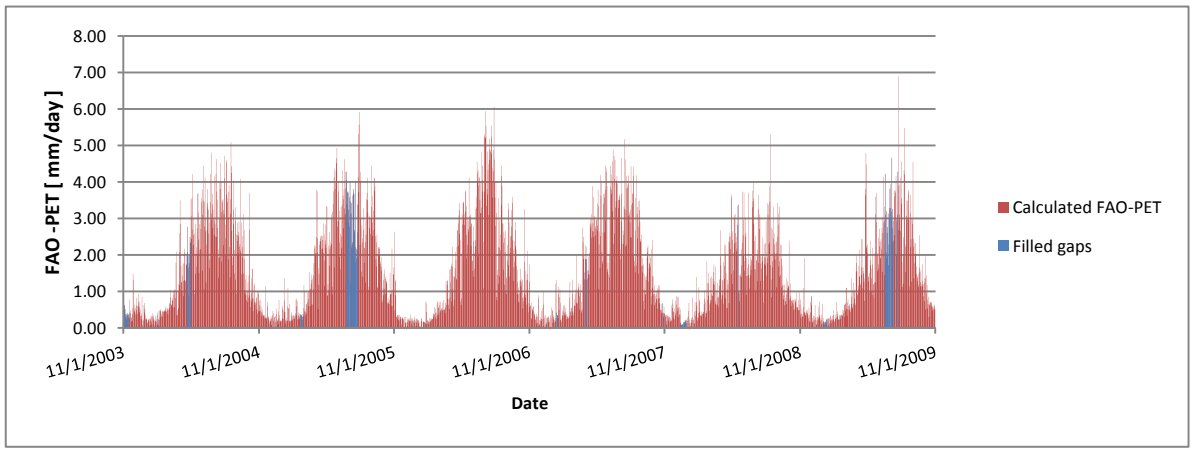

Figure 3-6 The final continuous values of PET calculated according to FAO-Penman Monteith.

3.1.3. Penman Lake Evaporation

Figure 3-7 shows the correlation between the lake evaporation calculated from Penman equation (Equation 2.23) and the evapotranspiration values obtained from Hargreaves equation (Equation 2.18). The final lake evaporation values after filling in the E_{lake} data gaps is shown in Figure 3-8. The E_{lake} values range between -0.17 to 8.25 mm/day also with very few and small negative values. In general, the evapotranspiration and the lake evaporation values are high during summer periods and low during winter due to low temperature and because of the presence of clouds.

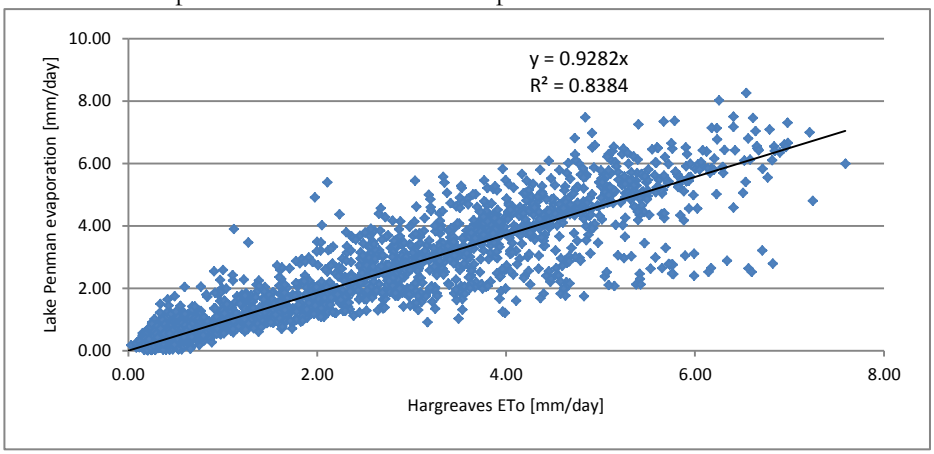

Figure 3-7 The correlation between Hargreaves ET and lake Penman Evaporation (E_{lake}).

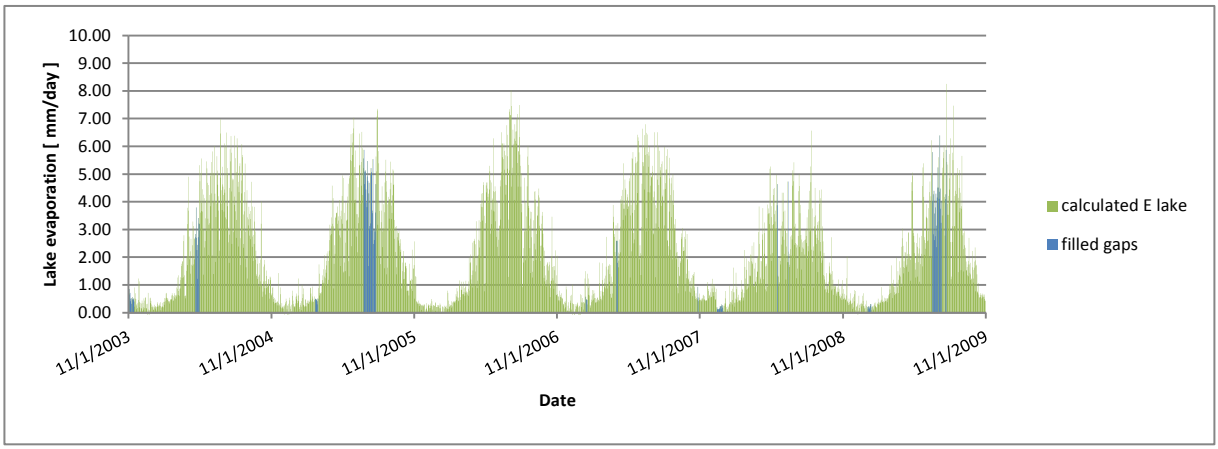

Figure 3-8 The final continuous values of lake evaporation calculated according to Penman Equation.

3.1.4. River discharges

According to Figure 2-2 and the calculations done in ArcGIS, the total area of the Mala Panew, Libawa, and Rosa Rivers catchments are 1191.5, 114.6, 46.2 km^2 respectively, and the area of the Mala Panew catchment upstream of "Staniszcze Wielkie" station is equal to 1078.8 km^2 . Using the gauged station area, an area ratio of discharge versus upstream contributing area was used to estimate the total final inflow for each river. Figure 3-9 and 3-10 show the inflow for the three rivers and the outflow from Turawa Lake, respectively. The very large inflow peaks in Figure 3-9, are likely due to snow melting, not due to rainfall events. As the method used to estimate the river discharges may have uncertainties due to the different properties of each river catchment, and the different rates of water use, the final Mala Panew River inflow was adjusted during the calibration of the steady state model. That adjustment involved multiplication of all the records by factor 1.021. Libawa and Rosa River inflows were kept the same as originally estimated. The pattern of lake outflow, which is generally < 20 [m^3.sec^{-1}] (Figure 3-10), points out at the dumping role of the reservoir.

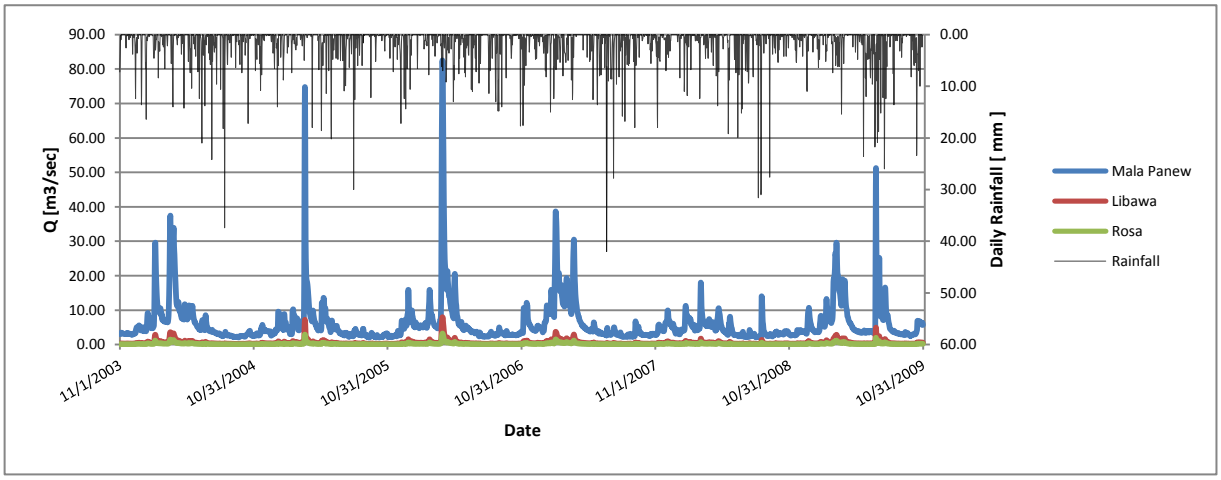

Figure 3-9 Mala Panew, Libawa, and Rosa Rivers inflow and rainfall.

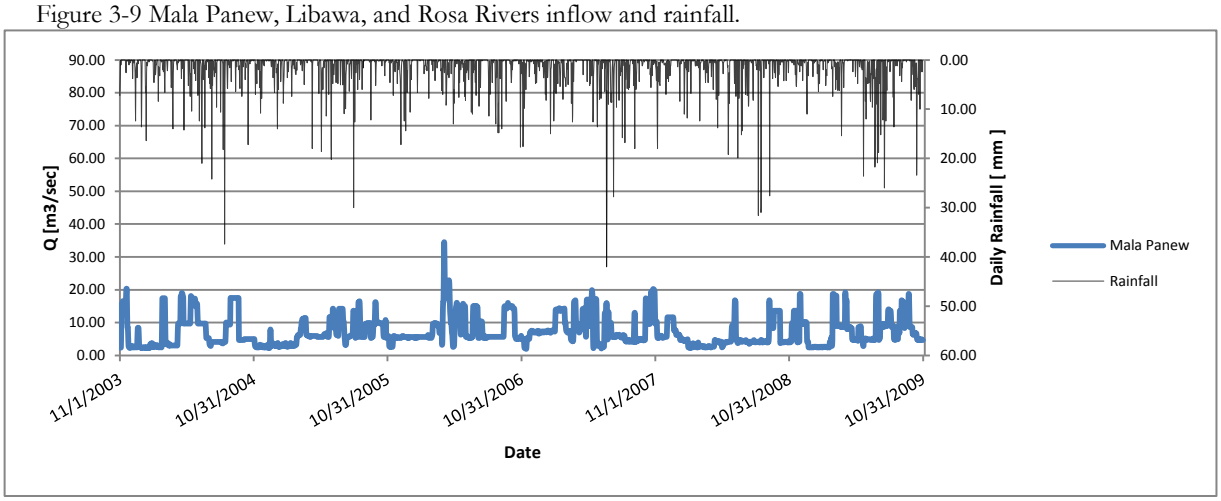

Figure 3-10 Mala Panew River outflow and rainfall.

3.2. Steady state model results

3.2.1. Head calibration

Table 1 shows the coordinates, the average observed heads, the steady state simulated heads, and the calculated errors of each observation point. According to Equations 2.28, 2.29, and 2.30; the mean error, mean absolute error, and the root mean square error are equal to -0.49, 0.89, and 1.16 [m] respectively. The largest absolute error is equal to -2.97 m. Figure 3-11 shows a scatter plot of the measured versus the simulated heads for 49 points where the deviation of points from the straight line is randomly distributed on both sides. All these observation points are located in the upper unconfined aquifer except one available point, which is located in the lower confined aquifer (named "P_5_PT_6_con"). Figure 3-12 shows a histogram showing the frequency of each of the following residual classes [<-3, -3:-2.5, -2.5:-2.0, -2.0:-1.5, -1.5:-1.0, -1.0:-0.5, -0.5:0.0, 0.0:0.5, 0.5:1, 1.0:1.5, 1.5:2.0, 2.0:2.5, 2.5:3.0, >3.0]. It can be concluded from that histogram that small errors have larger frequency which points at correctness of the calibration.

3.2.2. Hydraulic conductivities

The final calibrated horizontal hydraulic conductivity (K_h) of the upper unconfined layer ranges between 0.1 m/day and 60 m/day. According to Figure 3-13, the low K_h values are located in the southern part of the area, in the north-eastern and north-western parts of the study area. In the rest of the modeled area, the K_h has values between 10 and 60 m/day.

Table 1: The coordinates of the observation points, observed heads, simulated heads, and the calculated errors.

Observation point	Coordinate		$H_{observed}$	$H_{simulated}$	$H_{observed} - H_{simulated}$	$\lvert H_{observed} - H_{simulated} \rvert$	$(H_{observed} - H_{simulated})^2$
	X [m]	Y [m]	[m] a.m.s.l.	[m] a.m.s.l.			
Report_3	442804.40	318165.30	177.38	178.33	-0.95	0.95	0.89
Report_4	442510.00	317530.00	176.83	175.98	0.85	0.85	0.72
Report_5	443520.00	316730.00	176.37	176.62	-0.25	0.25	0.06
Report_8	442972.16	315266.14	173.90	174.92	-1.02	1.02	1.05
Report_9	442804.00	312531.00	181.00	180.49	0.51	0.51	0.26
Report_10	440733.78	313703.76	185.07	185.40	-0.33	0.33	0.11
Report_11	440613.40	314963.18	177.04	177.57	-0.53	0.53	0.28
Report_12	438714.00	315240.00	188.65	189.90	-1.25	1.25	1.56
Report_14	435700.00	314550.00	174.00	176.72	-2.72	2.72	7.37
Report_17	434770.80	319468.70	161.43	162.66	-1.23	1.23	1.50
Report_18	435878.68	320455.93	171.00	171.71	-0.71	0.71	0.50
P_12_PT_2	438903.26	315889.25	175.07	176.90	-1.83	1.83	3.36
P_30_PT_4	441240.00	318690.00	175.80	175.63	0.17	0.17	0.03
P_5_PT_6_unc	435519.70	316740.20	173.74	173.57	0.17	0.17	0.03
P_1	434957.93	320084.20	165.72	165.77	-0.05	0.05	0.00
P_2	435010.85	320269.41	166.34	166.91	-0.57	0.57	0.33
P_4	435427.57	320733.75	172.82	172.52	0.30	0.30	0.09
P_5	436005.68	320719.20	172.00	173.67	-1.67	1.67	2.79
P_6	435878.68	320455.93	170.76	171.71	-0.95	0.95	0.90
P_7	435719.93	320086.84	169.05	168.26	0.79	0.79	0.63
P_12	442166.51	319072.17	177.02	175.67	1.35	1.35	1.83
P_13	442685.09	319260.01	179.05	179.59	-0.54	0.54	0.29
P_16	441940.28	318581.37	176.00	176.16	-0.16	0.16	0.03
P_17	442470.78	318983.53	178.74	180.07	-1.33	1.33	1.76
P_18	442665.25	318734.82	179.33	179.83	-0.50	0.50	0.25
P_19	442771.07	318871.08	179.57	179.55	0.02	0.02	0.00
P_27	442375.52	315252.90	173.86	174.50	-0.64	0.64	0.41
P_28	441766.98	314349.35	175.28	176.13	-0.85	0.85	0.73
P_29	441823.87	313613.81	179.64	178.70	0.94	0.94	0.89
P_30	442806.79	312511.82	180.37	180.68	-0.31	0.31	0.09
P_31	443095.19	312886.20	179.25	178.15	1.10	1.10	1.20
P_32	443199.71	312861.07	178.13	178.10	0.03	0.03	0.00
P_33	442694.35	313236.78	177.85	177.38	0.47	0.47	0.22
P_34	441063.19	313411.40	183.66	183.32	0.34	0.34	0.11
P_35	440733.78	313703.76	184.97	185.40	-0.43	0.43	0.18
P_36	440822.42	313846.64	184.47	183.36	1.11	1.11	1.22
P_37	441536.79	314165.47	177.66	176.73	0.93	0.93	0.87
P_38	441165.05	314399.62	181.34	180.72	0.62	0.62	0.38
P_40	440613.40	314963.18	176.78	177.57	-0.79	0.79	0.62
P_41	440760.24	315016.09	176.47	176.75	-0.28	0.28	0.08
P_42	440071.00	315714.60	176.88	177.95	-1.07	1.07	1.14
P_43	440149.06	315878.64	174.74	175.81	-1.07	1.07	1.15
P_44	439926.81	315793.97	175.40	177.76	-2.36	2.36	5.56
P_45	439129.09	315633.90	176.55	179.40	-2.85	2.85	8.12
P_46	436083.60	314624.76	174.10	177.07	**-2.97**	2.97	8.84
P_48	434975.13	317791.58	165.96	166.74	-0.78	0.78	0.60
PT_34	438820.00	319820.00	174.40	177.01	-2.61	2.61	6.79
PT_116	433322.08	319635.24	162.40	162.21	0.19	0.19	0.04
P_5_PT_6_con	435519.70	316740.20	176.27	176.60	-0.33	0.33	0.11
Sum					**-24.02**	**43.78**	**65.97**

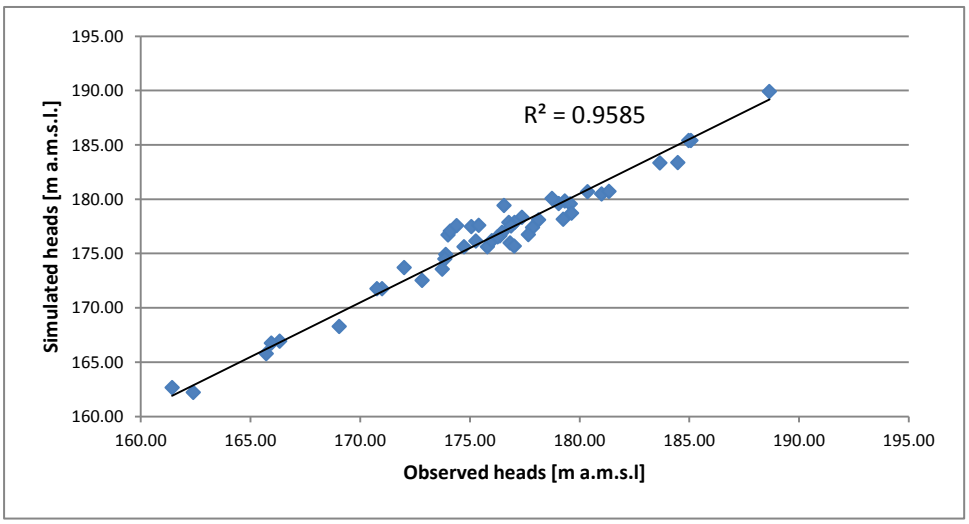

Figure 3-11 Steady state calculated versus observed heads.

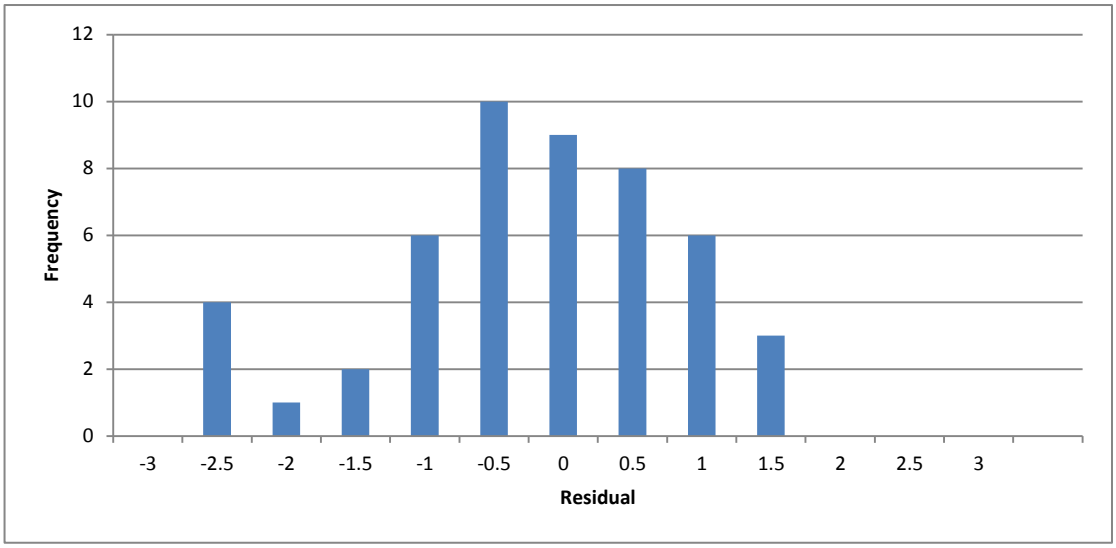

Figure 3-12 The residuals histogram.

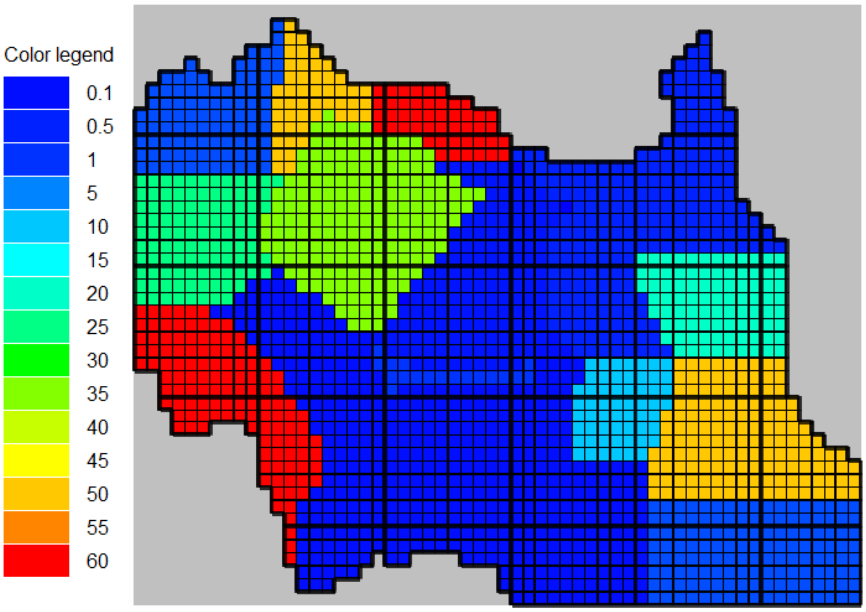

Figure 3-13 The horizontal hydraulic conductivity map for the upper unconfined aquifer [m·day^{-1}].

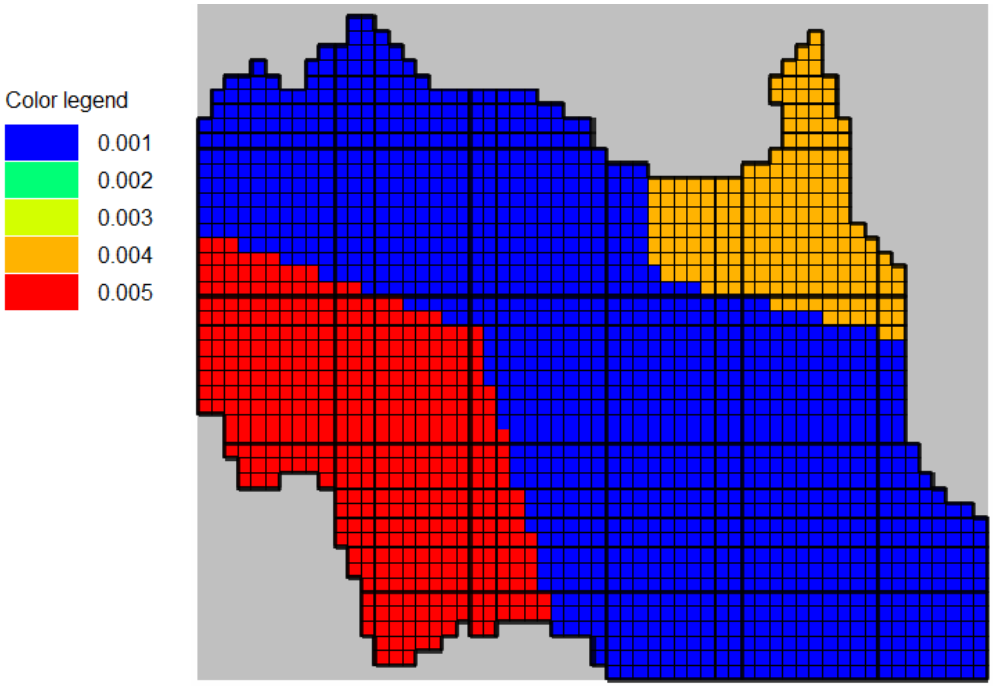

Figure 3-14 The horizontal hydraulic conductivity map for the middle aquitard layer [m·day^{-1}].

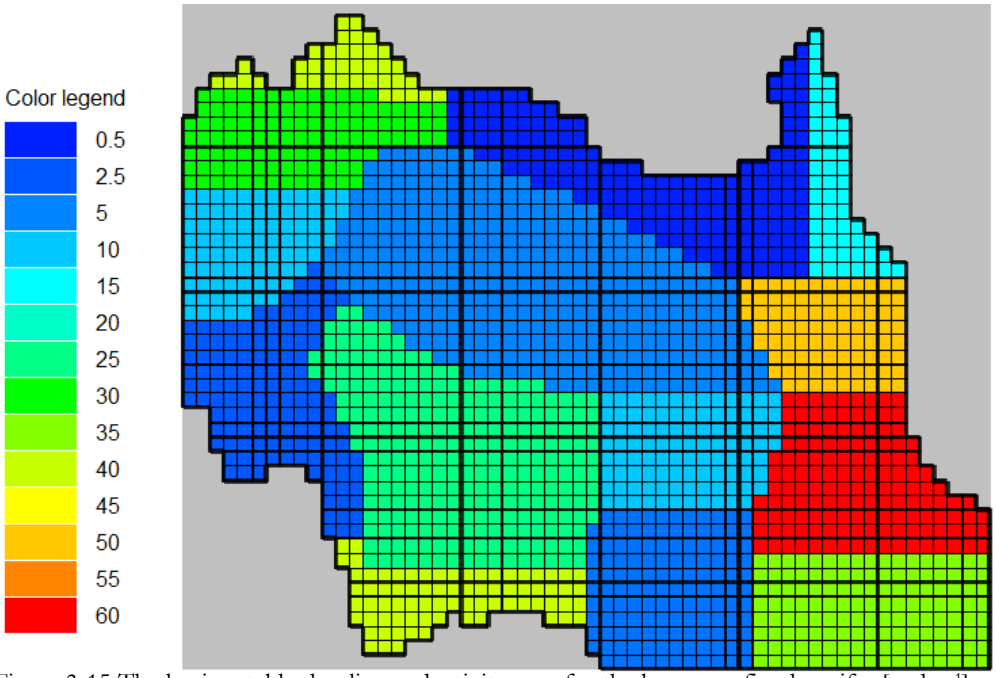

Figure 3-15 The horizontal hydraulic conductivity map for the lower confined aquifer [m·day^{-1}].

According to calibration results, the middle aquitard layer has relatively low horizontal hydraulic conductivity values 0.004 and 0.005 m/day in the upper north-eastern and lower south-western parts of the study area, respectively, and even lower, 0.001 m/day, along the MPR valley.

Figure 3-15 shows calibrated K_h distribution of the lower confined aquifer. The blue areas have quite low horizontal hydraulic conductivity values ranging from 0.5 to 15 m/day and the remaining zones have horizontal hydraulic conductivity ranging from 20 to 60 m/day.

3.2.3. Recharge and groundwater evapotranspiration

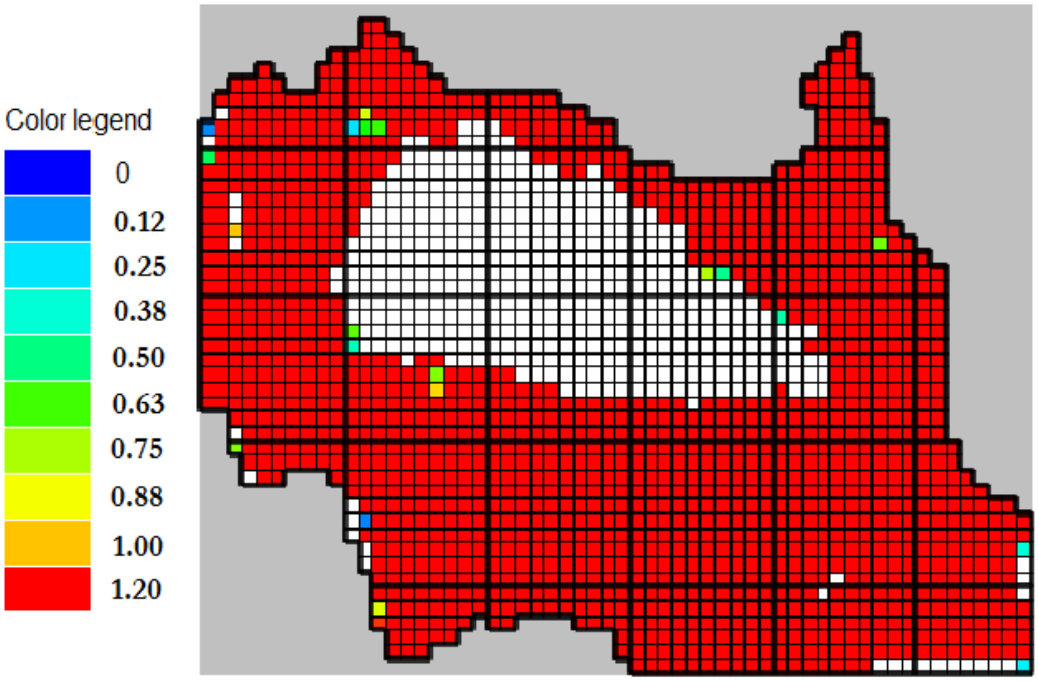

Figure 3-16 Groundwater total recharge map [mm.day-[1]].

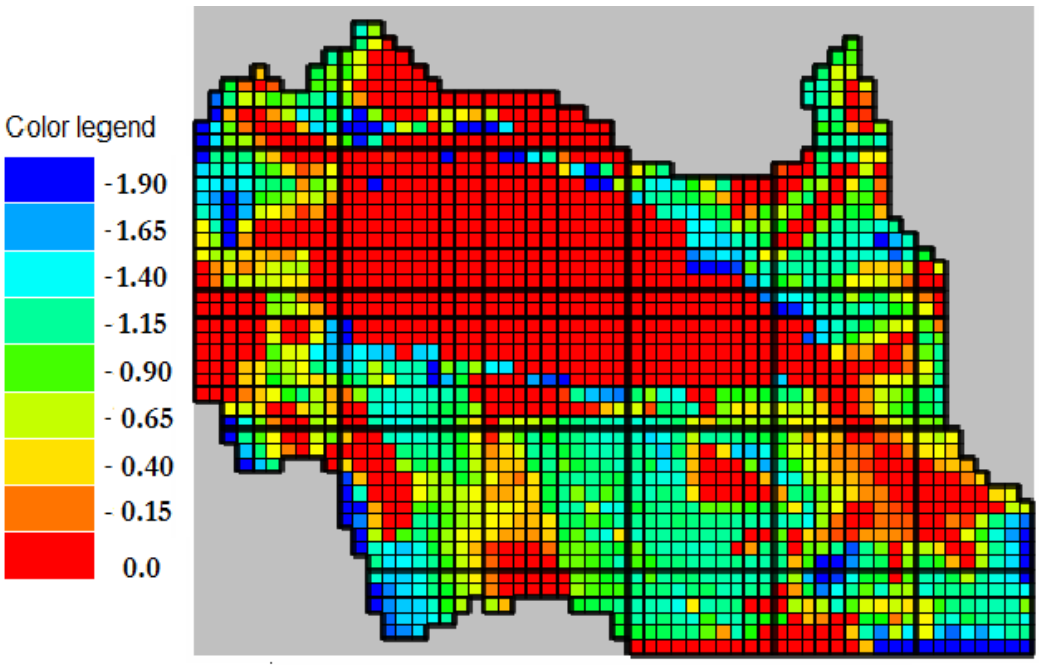

Figure 3-17 Groundwater evapotranspiration map [mm.day-[1]].

Figure 3-16 shows the total groundwater recharge which is equal to the net infiltration rate minus the evapotranspiration demand in this case. For steady state simulation, the applied infiltration rate is set equal to groundwater recharge, and ET demand is removed from the infiltration rate and groundwater above the extinction depth (Niswonger et al., 2006). The UZF package was assigned only to the land not to the lake cells. Figure 3-16 shows quite uniform recharge rate value (1.2 mm.day-[1]) for most of the cells except for a small number of cells that have lower recharge values. This might be because the soil is fully

saturated in those cells due to the existence of deep streams, general head boundary, or groundwater table near the land surface. The applied infiltration rate for these saturated cells was routed to the lake as a surface runoff with total amount of 3116 m^3/day.

Figure 3-17 shows the groundwater evapotranspiration map calculated by the UZF Package. The value of the groundwater evapotranspiration is ranging from 0.0 to -1.9 $mm.day^{-1}$, the negative sign indicates that water is subtracted from groundwater budget. It is clear from the figure that the groundwater evapotranspiration values for the lake area and below most of the streams are equal to zero; this is because the ET demand for these cells was satisfied from surface water only (lake or streams) and there is no more water extracted from groundwater by evapotranspiration. The net groundwater recharge value which is equal to the total recharge minus the groundwater evapotranspiration can be calculated by adding the total recharge and the groundwater evapotranspiration maps together.

3.2.4. Groundwater budget

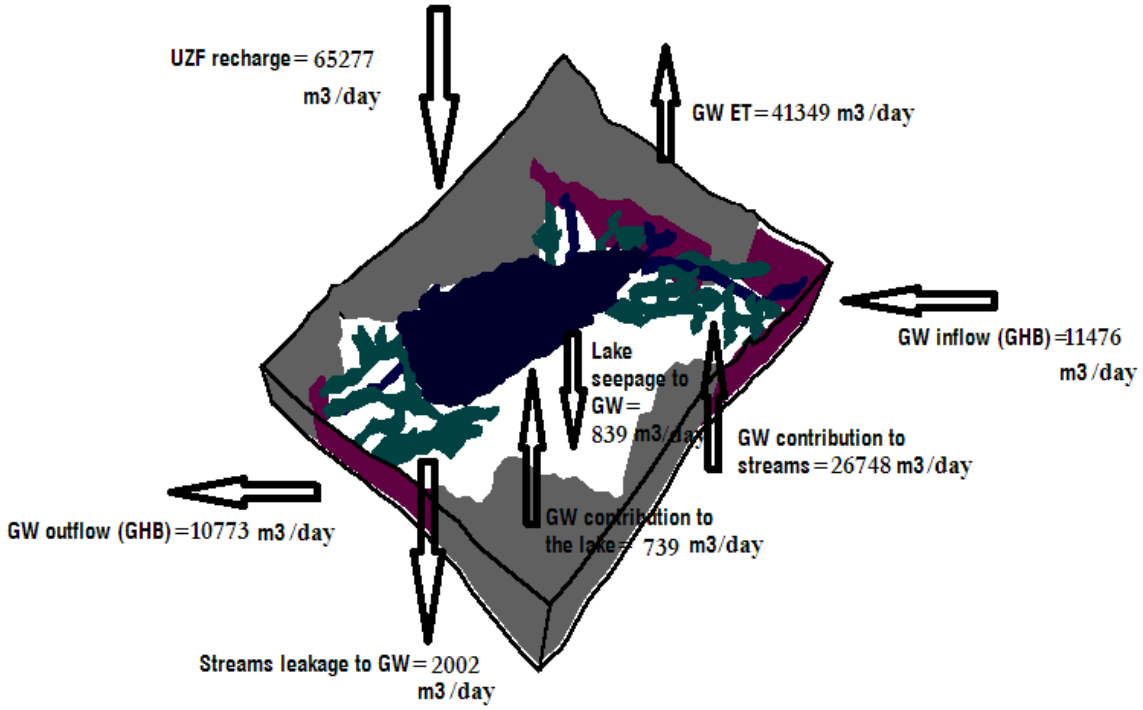

Figure 3-18 Groundwater budget schematic diagram.

The groundwater budget of the model in Table2 shows the total daily inflows and outflows from the study area. The shown fluxes should balance or be within the acceptable error or discrepancy limits. The lake seepage in and out of the aquifer is quite low compared to the other components, this might be due to and equilibrium state between the lake and the aquifers. The final discrepancy value between the inflows and the outflows was equal to 0.02 % and is within the acceptable limits (less than or equal to 1 %). Figure 3-18 is a schematic diagram showing all the components of the groundwater budget.

Table 2: The groundwater budget.

IN		[m^3/day]	OUT		[m^3/day]
STORAGE	=	0	STORAGE	=	0
CONSTANT HEAD	=	0	CONSTANT HEAD	=	0
HEAD DEP BOUNDS	=	11476	HEAD DEP BOUNDS	=	10773
STREAM LEAKAGE	=	2002	STREAM LEAKAGE	=	26748
LAKE SEEPAGE	=	839	LAKE SEEPAGE	=	739
UZF RECHARGE	=	65277	UZF RECHARGE	=	0
GW ET	=	0	GW ET	=	41349
TOTAL IN	=	79594	TOTAL OUT	=	79609
		IN - OUT	=	-15	
		PERCENT DISCREPANCY	=	-0.02 %	

3.2.5. Lake budget

Table 3 shows the total inflows and outflows from the lake. Figure 3-19 is a schematic diagram of all the lake water balance components. The final simulated lake stage is 173.77 m a.m.s.l which is equal to the average lake water level during the whole study period. The final discrepancy value between the total inflows and outflows are within the acceptable limits.

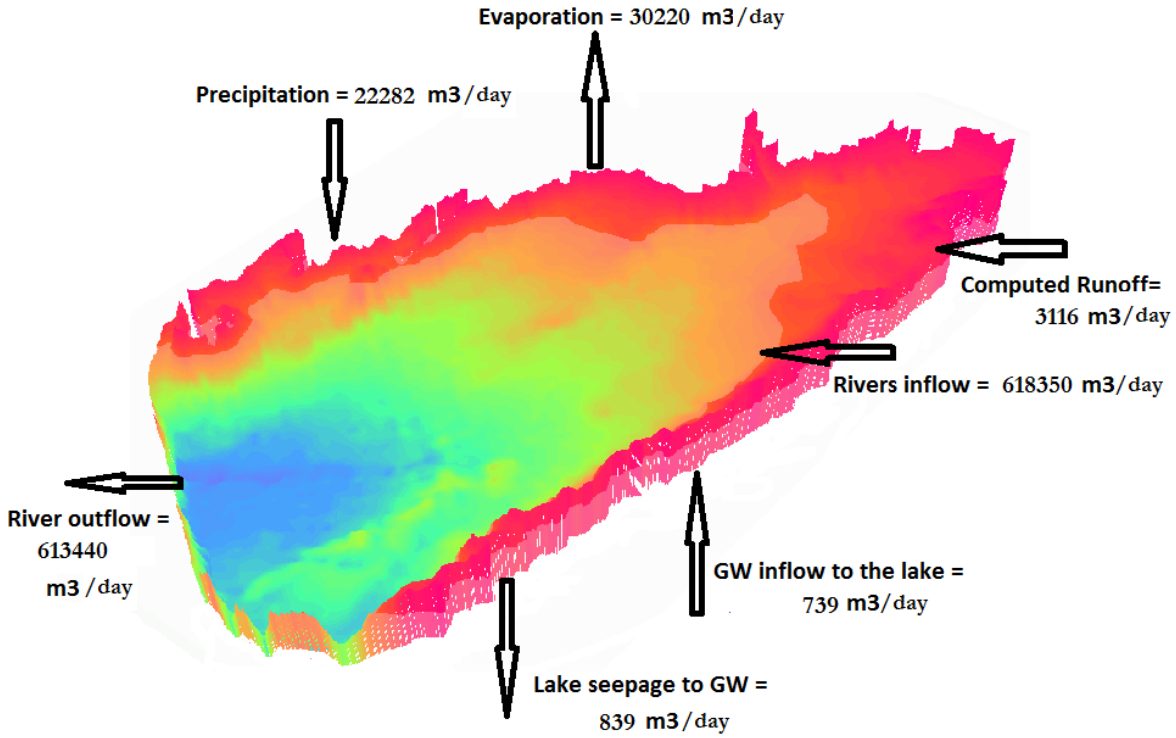

Figure 3-19 Lake water budget schematic diagram.

Table 3: The Lake water budget.

IN		[m^3/day]	OUT		[m^3/day]
Precipitation	=	22282			
Computed Runoff [UZF]	=	3116	Evaporation	=	30220
Surface Water Inflow	=	618350	Surface Water Outflow	=	613440
Ground Water Inflow	=	739	Ground Water outflow	=	839
TOTAL IN	=	644487	TOTAL OUT	=	644499
IN - OUT			=	-12.0	
PERCENT DISCREPANCY			=	0.00	

3.2.6. Lake seepage

Figure 3-20 shows the distribution of lake seepage at the bottom of the lake where positive values indicate seepage from lake to groundwater and negative values indicate seepage from groundwater to the lake. Within the eastern and the middle part of the lake, where the lake is relatively shallow, seepage from groundwater to the lake is dominant. Whilst, within the western part of the lake, where the lake is relatively deep, seepage occurs from lake to groundwater, with high seepage values next to the earthen dam and the lake outlet. The figure also shows the zero contour line separating the two seepage zones.

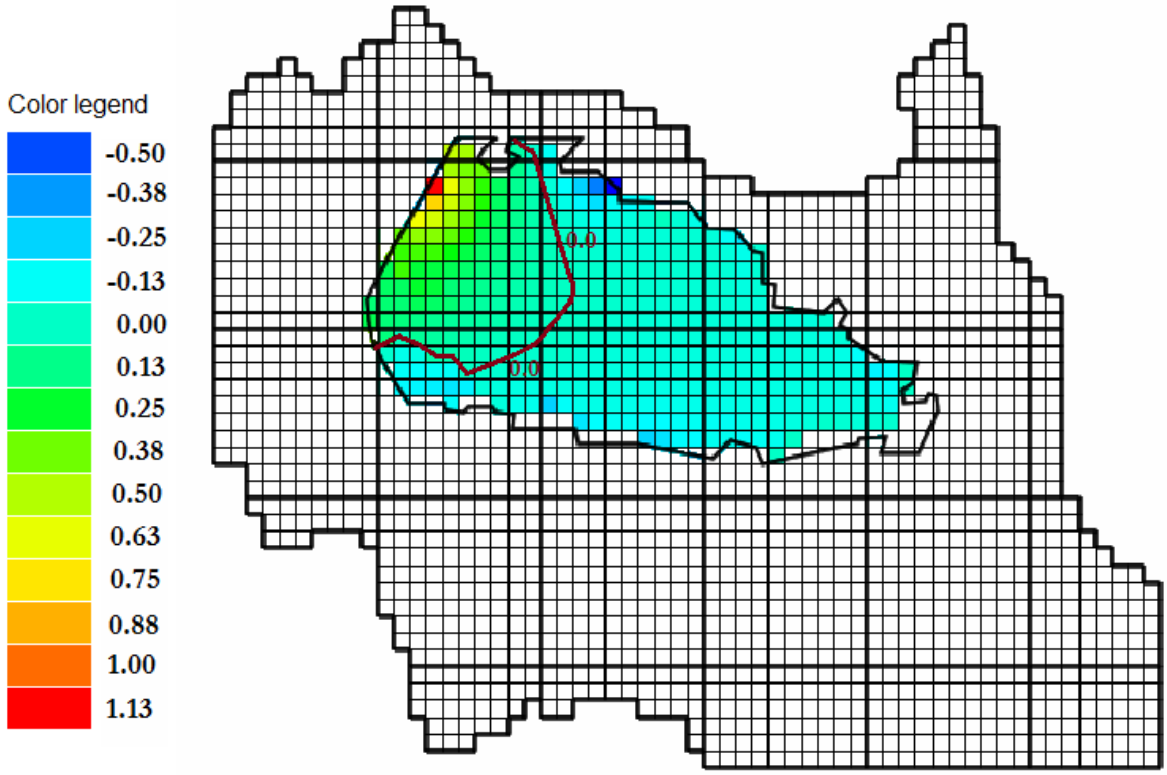

Figure 3-20 Distribution of lake seepage [mm.day^{-1}] and zero contour line.

3.2.7. Dam simulation

The HFB (Horizontal Flow Barrier) Package was used to simulate the earthen dam downstream of Turawa Lake in both steady state and transient state models. During the steady state simulation the horizontal flow barrier thickness was set equal to 10.0 meters and the barrier hydraulic conductivity to 10^{-7} m/day.

3.2.8. SFR Package

In the steady state model, all the river and drain bed thickness were set equal to 1.0 meter, Manning coefficient for all the streams was equal to 0.035, and the hydraulic conductivity for all stream beds were equal to 0.08 m/day.

3.2.9. Layer budget

In order to calculate the groundwater budget for each layer; each single layer was assigned as a separate zone: zone1=layer1 corresponding with shallow unconfined aquifer, zone2=layer2 coresponding with aquitard and zone3=layer3 corresponding with second, deeper confined aquifer. The final water budget for each layer is shown in Tables 4, 5, and 6, respectively. There are small differences between some values in these tables and the corresponding values shown in Table 2 calculated by MODFLOW; this might be

because the ZONBUDGET software uses only the cell-by-cell flow data file to do its own calculations which might be slightly different from the iterative calculations done by MODFLOW.

Table 4: Upper layer groundwater budget.

	IN	[m^3/day]		OUT	[m^3/day]
CONSTANT HEAD	=	0	CONSTANT HEAD	=	0
HEAD DEP BOUNDS	=	4949	HEAD DEP BOUNDS	=	4245
STREAM LEAKAGE	=	2002	STREAM LEAKAGE	=	26633
LAKE SEEPAGE	=	890	LAKE SEEPAGE	=	951
UZF RECHARGE	=	65258	UZF RECHARGE	=	0
GW ET	=	0	GW ET	=	41283
Layer 2 to 1	=	4180	Layer 1 to 2	=	4339
TOTAL IN	=	77279	TOTAL OUT	=	77451
		IN - OUT	=	-172	
		PERCENT DISCREPANCY	=	-0.22	

Table 5: Middle layer groundwater budget.

	IN	[m^3/day]		OUT	[m^3/day]
CONSTANT HEAD	=	0	CONSTANT HEAD	=	0
HEAD DEP BOUNDS	=	41	HEAD DEP BOUNDS	=	136
STREAM LEAKAGE	=	0	STREAM LEAKAGE	=	116
LAKE SEEPAGE	=	0	LAKE SEEPAGE	=	0
UZF RECHARGE	=	0	UZF RECHARGE	=	0
GW ET	=	20	GW ET	=	66
Layer 1 to 2	=	4339	Layer 2 to 1	=	4180
Layer 3 to 2	=	4346	Layer 2 to 3	=	4250
TOTAL IN	=	8746	TOTAL OUT	=	8748
		IN - OUT	=	-2.0	
		PERCENT DISCREPANCY	=	-0.02	

Table 6: Lower layer groundwater budget.

	IN	[m^3/day]		OUT	[m^3/day]
CONSTANT HEAD	=	0	CONSTANT HEAD	=	0
HEAD DEP BOUNDS	=	6486	HEAD DEP BOUNDS	=	6392
STREAM LEAKAGE	=	0	STREAM LEAKAGE	=	0
LAKE SEEPAGE	=	0	LAKE SEEPAGE	=	0
UZF RECHARGE	=	0	UZF RECHARGE	=	0
GW ET	=	0	GW ET	=	0
Layer 2 to 3	=	4250	Layer 3 to 2	=	4346
TOTAL IN	=	10736	TOTAL OUT	=	10738
		IN - OUT	=	-2.0	
		PERCENT DISCREPANCY	=	-0.02	

3.2.10. Sensitivity analysis results

3.2.10.1. Sensitivity of model parameters

Figures 3-21 to 3-23 and the corresponding tables (Tables 7 to 9) show the effect of changing the K_h of the upper unconfined aquifer, lake bed leakance, and the hydraulic conductivity of stream beds on the

error value between the observed and the simulated groundwater heads. Figure 3-24 and Table 10 show the effect of changing lake bed leakance on the simulated lake stage. From the figures, it can be deducted that the model groundwater heads show quite high sensitivity to the horizontal hydraulic conductivity Kh, while, the streams bed hydraulic conductivity and the lake bed leakance seem to be rather non-sensitive. Figure 3-24 shows that the simulated lake stage may be affected only by lower values of lake bed leakance.

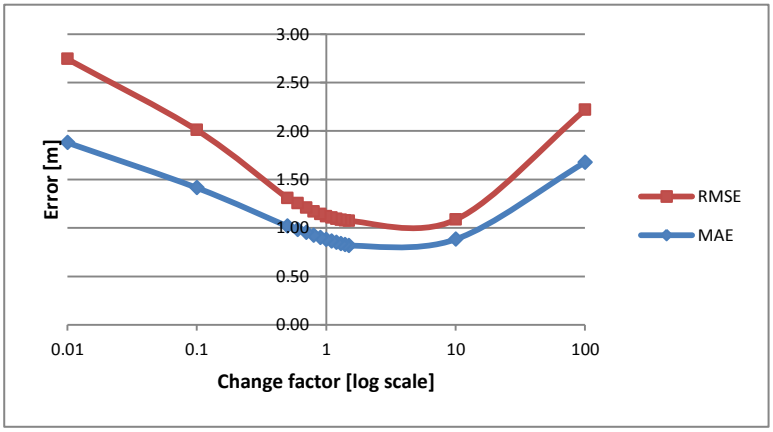

Figure 3-21 Effect of changing K_h on the piezometric heads.

Table 7

Factor	ME	MAE	RMSE
100	1.15	1.68	2.22
10	0.29	0.88	1.08
1.5	-0.13	0.82	1.07
1.4	-0.14	0.83	1.08
1.3	-0.16	0.84	1.08
1.2	-0.18	0.85	1.09
1.1	-0.20	0.86	1.10
1	**-0.23**	**0.88**	**1.12**
0.9	-0.26	0.90	1.14
0.8	-0.29	0.92	1.17
0.7	-0.33	0.95	1.21
0.6	-0.37	0.98	1.25
0.5	-0.42	1.02	1.31
0.1	-0.98	1.41	2.01
0.01	-1.22	1.88	2.74

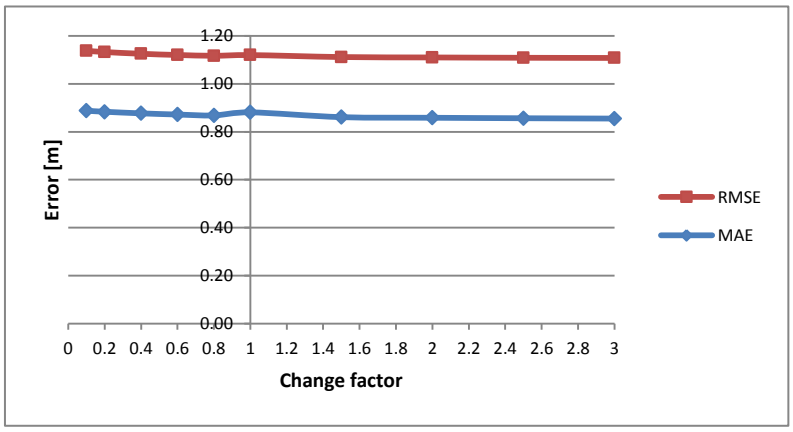

Figure 3-22 Effect of changing lake bed leakance on the piezometric heads.

Table 8

Factor	AE	MAE	RMSE
0.1	-0.24	0.89	1.14
0.2	-0.23	0.88	1.13
0.4	-0.23	0.88	1.13
0.6	-0.22	0.87	1.12
0.8	-0.22	0.87	1.12
1	**-0.23**	**0.88**	**1.12**
1.5	-0.21	0.86	1.11
2	-0.21	0.86	1.11
2.5	-0.20	0.86	1.11
3	-0.20	0.86	1.11

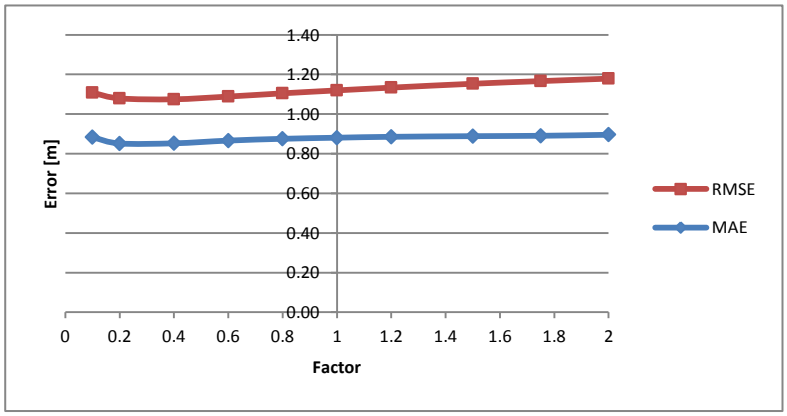

Figure 3-23 Effect of changing streams bed hydraulic conductivity on the piezometric heads.

Table 9

RMSE	MAE	AE	Factor
1.11	0.88	-0.52	0.1
1.08	0.85	-0.45	0.2
1.07	0.85	-0.36	0.4
1.09	0.87	-0.30	0.6
1.10	0.88	-0.26	0.8
1.12	**0.88**	**-0.23**	**1**
1.13	0.89	-0.20	1.2
1.15	0.89	-0.18	1.5
1.17	0.89	-0.16	1.75
1.18	0.90	-0.14	2

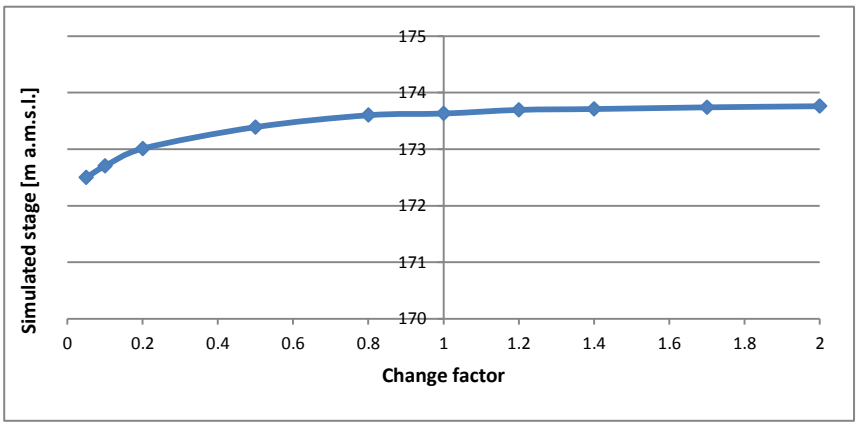

Figure 3-24 Effect of changing lake bed leakance on the simulated lake stage.

Table 10

Change factor	simulated lake level
0.05	172.5
0.1	172.7
0.2	173.01
0.5	173.39
0.8	173.6
1	**173.77**
1.2	173.695
1.4	173.71
1.7	173.74
2	173.76

3.2.10.2. Sensitivity of hydrologic stresses

Figure 3-25 and it corresponding table (Table11) show the effect on changing river inflows on the simulated groundwater heads. Moreover, Figures 3-26 to 3-28 and the corresponding tables (Table 12 to 14) show the effect of changing river inflows, lake evaporation, and lake precipitation on the simulated lake stage. From the figures, it is clear that river inflows show very high sensitivity to the simulated groundwater head and lake stage. Figure 3-25 and 3-26 show error values and simulated lake stages up to 160 m and 500 m a.m.s.l. respectively, as multiplying the inflow values by a factor equal to 1.5 causes the groundwater heads to rise more than 500 meters in some piezometers especially these piezometers next to the lake. The left part of the figures seems to be horizontal as reducing the inflow to the lake by a certain factor causes the lake to dry out and the piezometric heads would be controlled by the other assigned boundary conditions. The lake evaporation and precipitation show relatively lower sensitivity; approximately with the same magnitude but with an inverse effect.

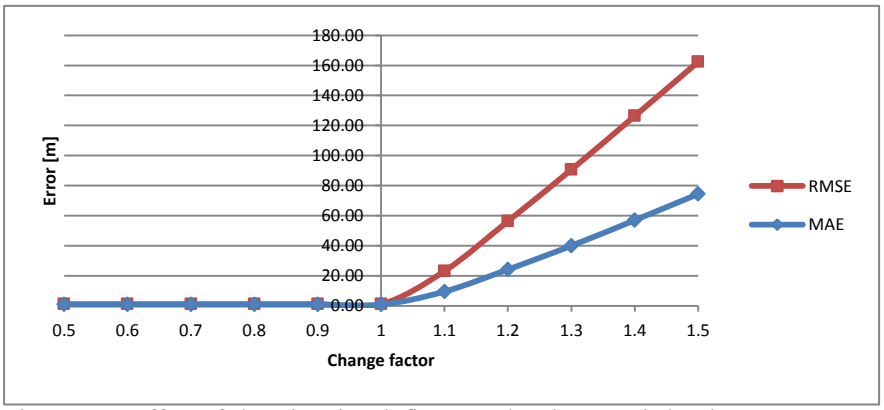

Figure 3-25 Effect of changing river inflows on the piezometric heads.

Table 11

Factor	AE	MAE	RMSE
1.5	-74.13	74.39	162.30
1.4	-56.69	56.98	126.31
1.3	-39.66	39.98	90.61
1.2	-23.87	24.21	56.35
1.1	-9.09	9.52	23.12
1	**-0.23**	**0.88**	**1.12**
0.9	-0.18	0.85	1.10
0.8	-0.18	0.85	1.10
0.7	-0.18	0.85	1.10
0.6	-0.18	0.85	1.10
0.5	-0.18	0.85	1.10

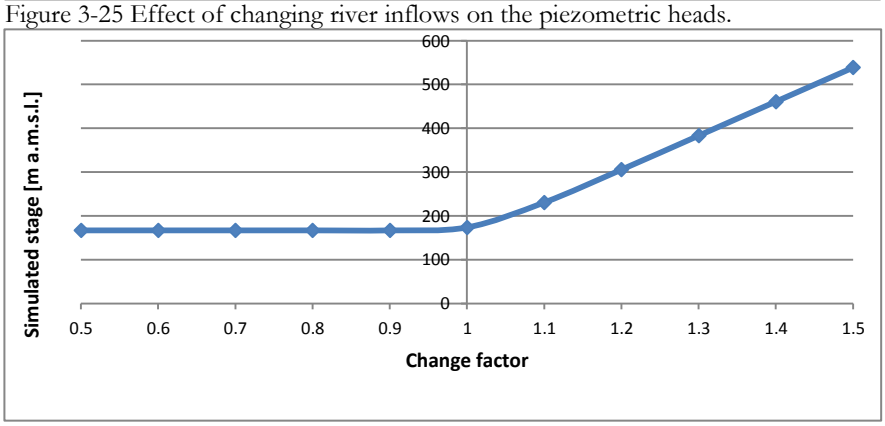

Figure 3-26 Effect of changing rivers inflow on the simulated lake stage.

Table 12

change factor	simulated stage
0.5	166.85
0.6	166.85
0.7	166.85
0.8	166.85
0.9	166.85
1	**173.77**
1.1	230.5
1.2	305.47
1.3	383.07
1.4	460.83
1.5	538.38

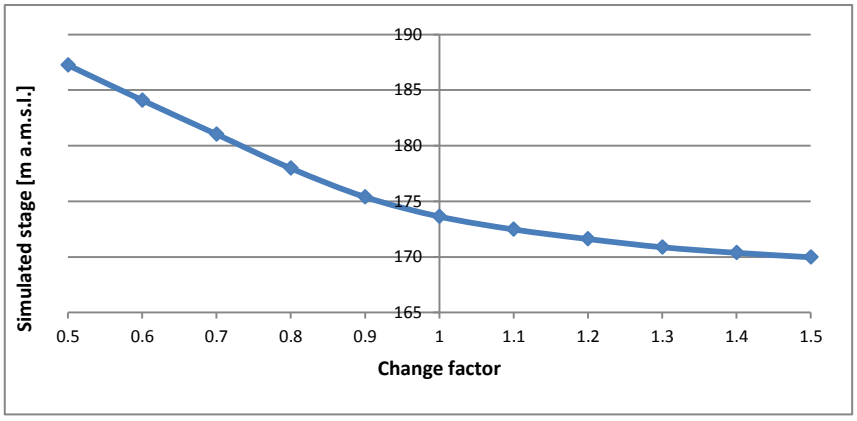

Figure 3-27 Effect of changing lake evaporation on the simulated lake stage.

Table 13

change factor	simulated stage
0.5	187.25
0.6	184.09
0.7	181.03
0.8	177.97
0.9	175.39
1	**173.77**
1.1	172.47
1.2	171.61
1.3	170.87
1.4	170.37
1.5	169.97

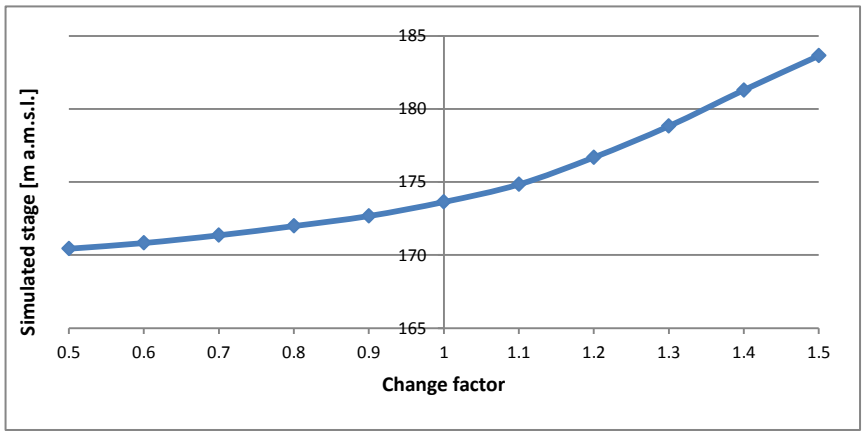

Figure 3-28 Effect of changing lake precipitation on the simulated lake stage.

Table 14

change factor	simulated stage
0.5	170.43
0.6	170.82
0.7	171.35
0.8	171.98
0.9	172.67
1	**173.77**
1.1	174.83
1.2	176.68
1.3	178.82
1.4	181.29
1.5	183.64

3.2.11. Comparing results with previous work

Gurwin (2008) constructed two steady state models for the high and the low lake water levels. Table 15 shows the errors between the simulated and observed groundwater heads, horizontal hydraulic conductivity ranges for each layer, and the different water balance components obtained from the steady state model and Gurwin's models. Comparing the steady state model results with the average results for the two cases done by Gurwin (2008); the final mean error, mean absolute error, and the root mean square error between the observed and the calculated heads in this study are equal to -0.49, 0.89, and 1.16 m respectively, but in the study done by Gurwin (2008) they were found to be 0.10, 0.72, and 0.96 m, respectively, however, the calibration process in this study was done manually and in Gurwin's study it was done automatically. In this study, the horizontal hydraulic conductivity of the upper unconfined aquifer was ranging from 0.1 to 60 m/day, for the middle aquitard layer it has a range between 0.001 and 0.005 m/day, and for the lower confined aquifer it is ranging from 0.5 to 60 m/day. In Gurwin's study, the horizontal hydraulic conductivity of the upper unconfined aquifer was ranging from 0.2 to 27 m/day, for the middle aquitard layer it has a fixed value equal to 10^{-7} m/sec or 0.009 m/day, and for the lower confined aquifer it is ranging from 5 to 60 m/day. The net recharge calculated from the UZF Package was found to be 23928 m^3/day, while in Gurwin's study it was equal to 25962 m^3/day which is quite similar to the calculated value from the UZF Package. In this study the stream leakage to groundwater was found to be 2002 m^3/day, the groundwater contribution to streams was equal to 26748 m^3/day, the lake seepage to groundwater was equal to 839 m^3/day, and the groundwater contribution to the lake was 739 m^3/day. In Gurwin's study; the streams leakage to groundwater, the groundwater contribution to streams, the lake seepage to groundwater, and the groundwater contribution to the lake were equal to 4319, 70431, 8031, 2231 m^3/day respectively. The total amount of water inflow and outflow from the aquifer system in this

study were 79594 and 79609 m^3/day with discrepancy value equal to -0.02 %, while these values in Gurwin's model were equal to 111401, 111396, and 0.01 % respectively.

In general there is quite good match for the hydraulic conductivity values, error criteria, and the net recharge between the two studies. The final streams-groundwater interaction, lake-groundwater interaction, and the total amount of inflow and outflow from the models may differ due to the different boundaries, lake and streams simulation approaches used in the two studies and also due to the change in the modelled area.

Table 15 Comparison between the steady state model and average of Gurwin's models.

	Error between observed & calculated GW heads			K_h of upper layer	K_h of middle layer	K_h of lower layer	net GW recharge	streams leakage to GW	GW to streams	lake seepage to GW	GW to the lake	total inflow	total outflow	budget discrepancy
	ME	MAE	RMSE											
	[m]			[m/day]				[m^3/day]						
Gurwin Models average	0.10	0.72	0.96	0.2 to 27	0.009	5 to 60	25962	4319	70431	8031	2231	111401	111396	0.01 %
This study model	-0.49	0.89	1.16	0.1 to 60	0.001 to 0.005	0.5 to 60	23928	2002	26748	839	739	79594	79609	-0.02 %

3.3. Transient state model results

The calibration process of the transient model, which was done manually, was the most challenging objective of this study due to the complexity of that task and the long time needed for each model run which might last for more than half an hour, and also because the model was double constrained, by the observed groundwater levels and lake stages. Changing any lake parameter usually affects the groundwater levels and vice versa.

Due to the surface water and groundwater contamination within the study area, there is no groundwater subtraction scenarios applied neither in reality nor in this study.

3.3.1. Calibration of heads

Transient model calibration using K_h values from the steady state model was not giving satisfactory head results so these values were subjected to some changes. Figure 1-2 shows the location of the 6 time series piezometers which were mainly used for the transient calibration process. The final head calibration results for these time series piezometers are shown in Figures 3-30 to 3-35. Figure 3-29 is a scatter plot of the observed and simulated heads for the time series piezometers during the four years simulation period. The points in the figure are distributed on both sides of the line and do not have any systematic deviation, also the correlation coefficient is very good. The mean error, mean absolute error, root mean square error for all the daily records of the time series piezometers were found to be equal -0.05, 0.28, and 0.36 m respectively.

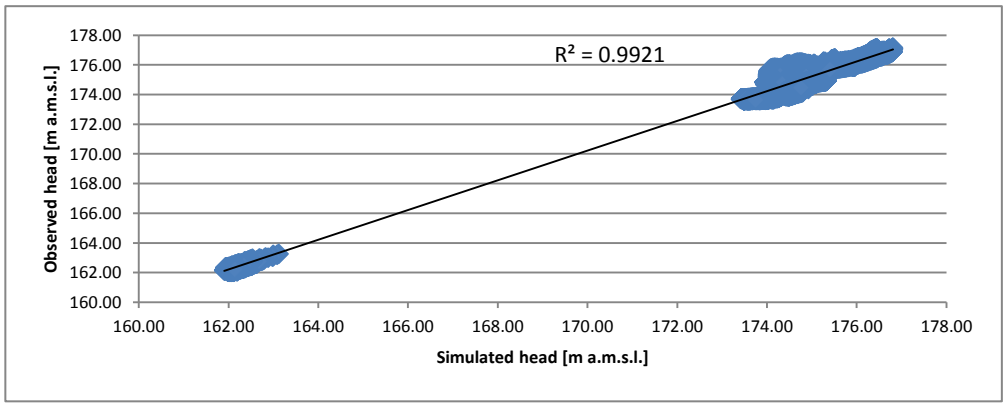

Figure 3-29 Scatter plot of the observed and simulated heads for the time series piezometers.

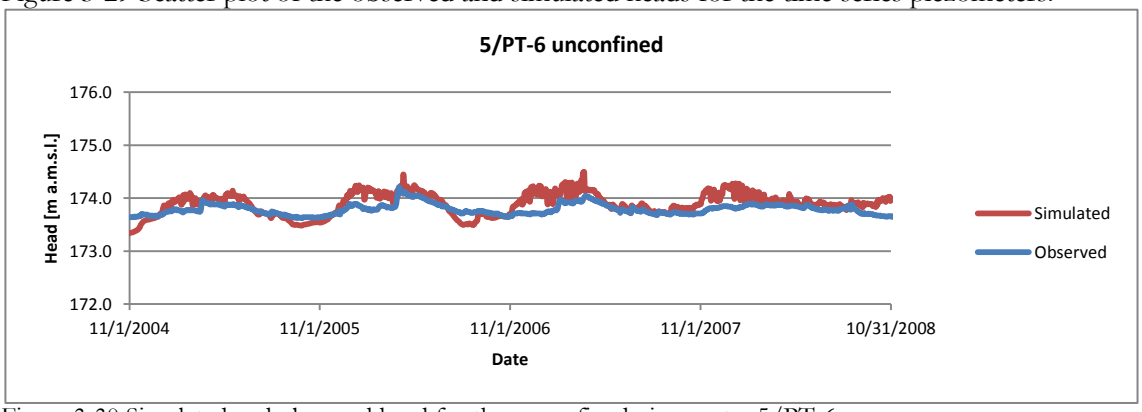

Figure 3-30 Simulated and observed head for the unconfined piezometer 5/PT-6.

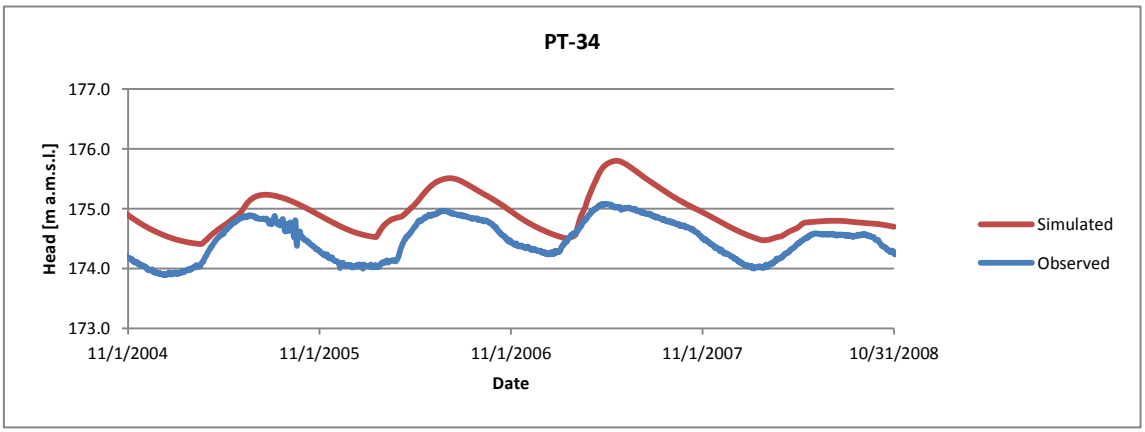

Figure 3-31 Simulated and observed head for piezometer PT-34.

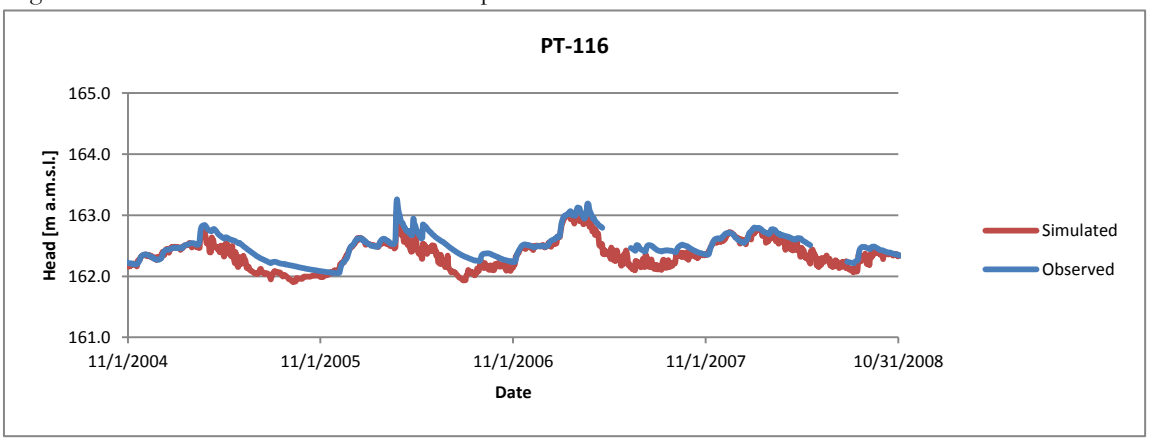

Figure 3-32 Simulated and observed head for piezometer PT-116.

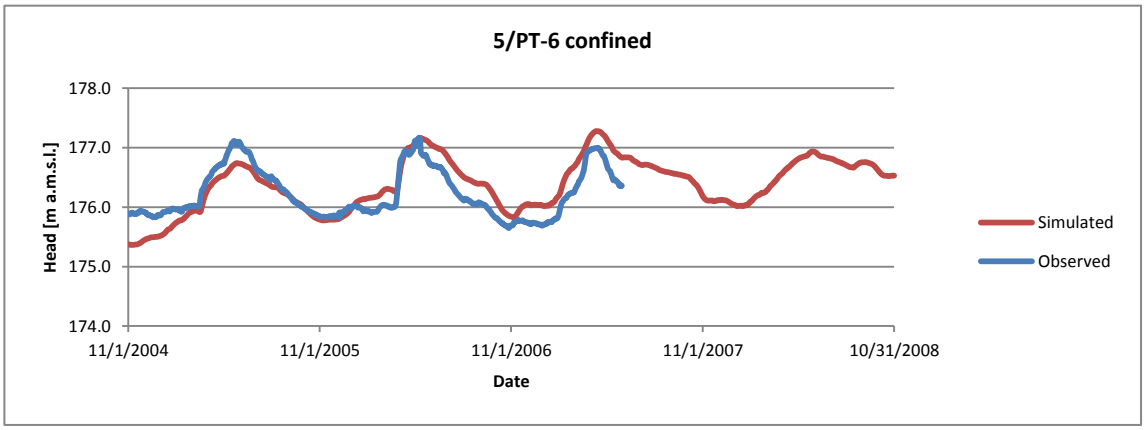

Figure 3-33 Simulated and observed head for the confined piezometer 5/PT-6.

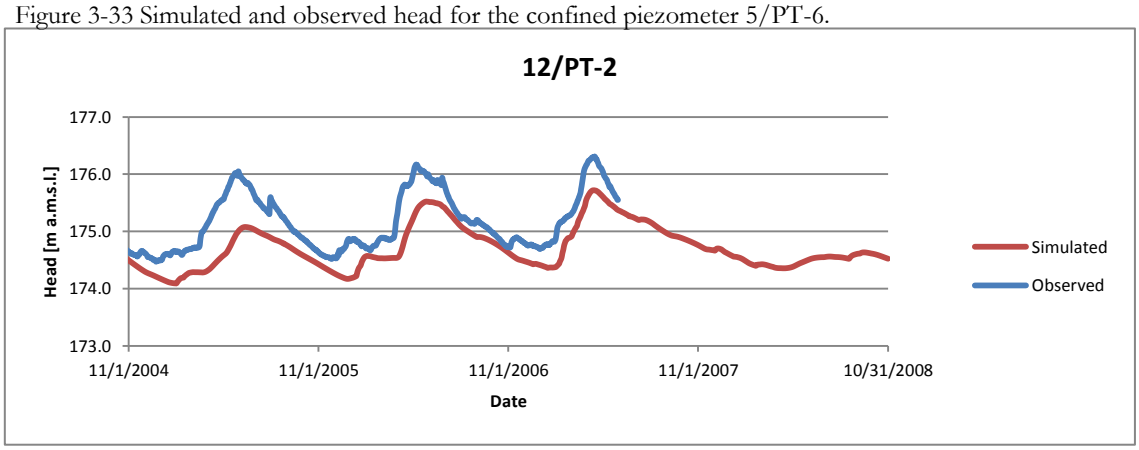

Figure 3-34 Simulated and observed head for piezometer 12/PT-2.

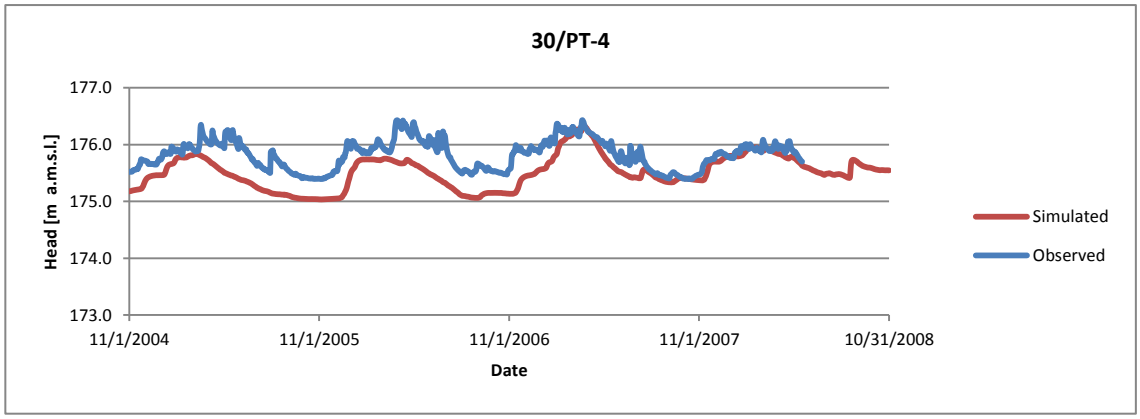

Figure 3-35 Simulated and observed head for piezometer 30/PT-4.

3.3.2. Hydraulic conductivities

After modifying the horizontal hydraulic conductivity values obtained from the steady state model, the final horizontal hydraulic conductivity values for the upper unconfined layer still have the same range from 0.1 m/day and 60 m/day but the middle K_h zones located under the lake, the north-eastern, and the south-western areas were modified [see Figure 3-36]. According to Figure 3-37, the only modification done to the middle aquitard layer was changing the horizontal hydraulic conductivity value of the south-western zone from 0.005 to 0.01 m/day. Figure 3-38 shows the modified K_h of the lower confined aquifer which was subjected to a lot of modification.

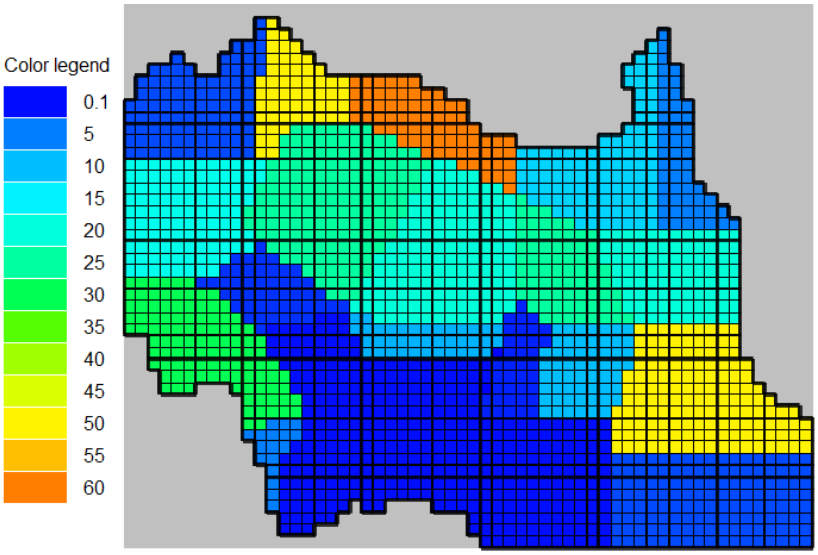

Figure 3-36 The horizontal hydraulic conductivity map for the upper unconfined aquifer [m·day^{-1}].

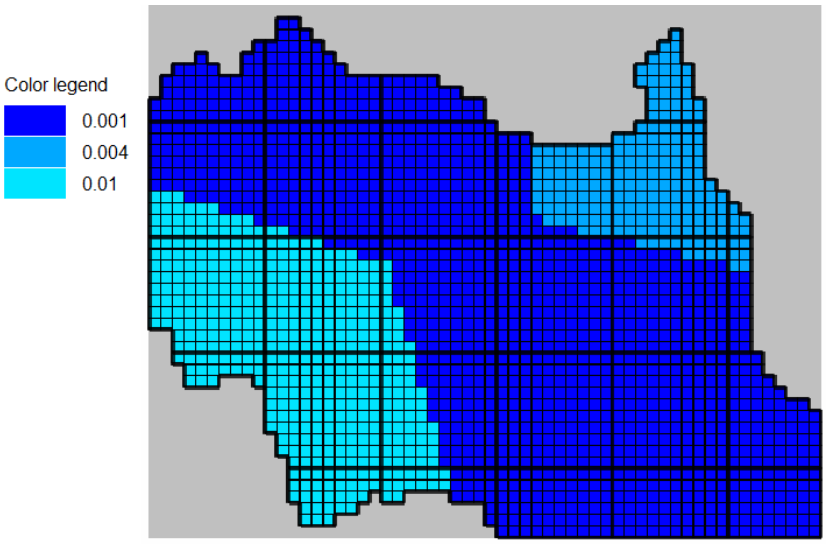

Figure 3-37 The horizontal hydraulic conductivity map for the middle aquitard layer [m·day^{-1}].

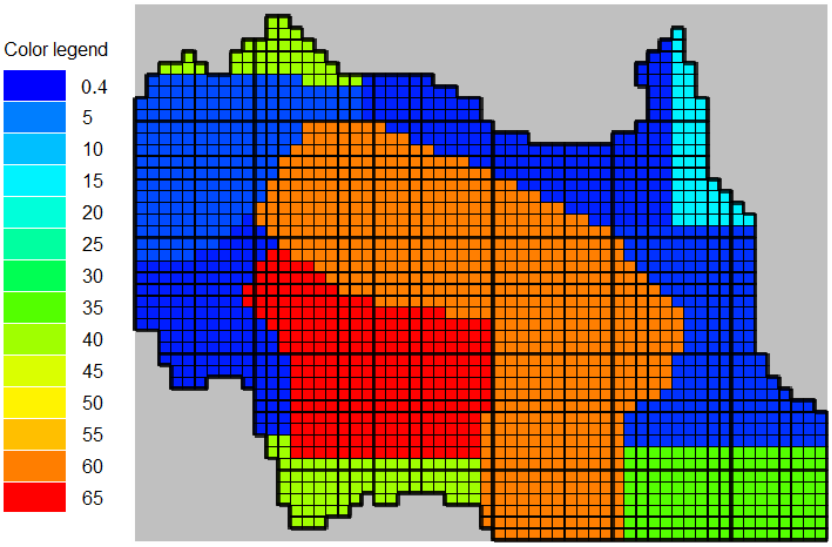

Figure 3-38 The horizontal hydraulic conductivity map for the lower confined aquifer [m·day^{-1}].

3.3.3. Specific yield and specific storage

The final calibrated values for the specific yield and specific storage are shown in Figures 3-39 and 3-40. Figure 3-39 shows the specific yield (S_y) values for the upper unconfined aquifer where the dominant value is equal to 0.15 expect one relatively high value near piezometer 5/PT-6 and equal to 0.2, and four relatively low values equal to 0.07, 0.10, 0.11 and 0.13 in the middle of the northern, middle of the southern, and north-western of the modelled area. Figure 3-40 shows the specific storage for the lower confined aquifer where the dominant specific storage (S_s) value is 0.00001 [m^{-1}] except near piezometer 5/PT-6 the value is 0.0001 [m^{-1}]. The specific storage value for the middle aquitard layer was assigned as spatially uniform and equal to 0. 00001[m^{-1}].

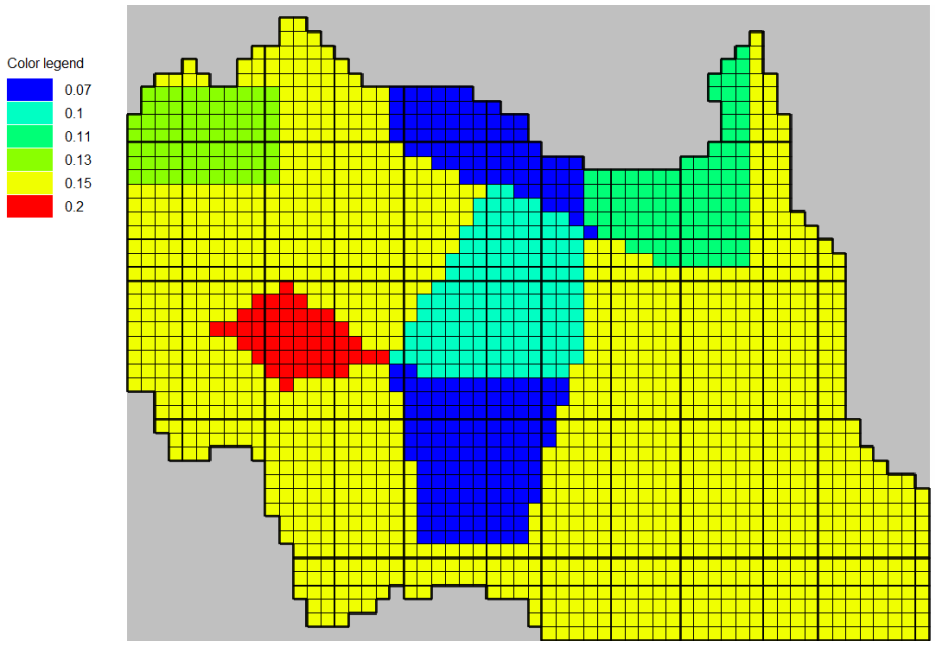

Figure 3-39 The specific yield (S_y) values for the upper unconfined aquifer.

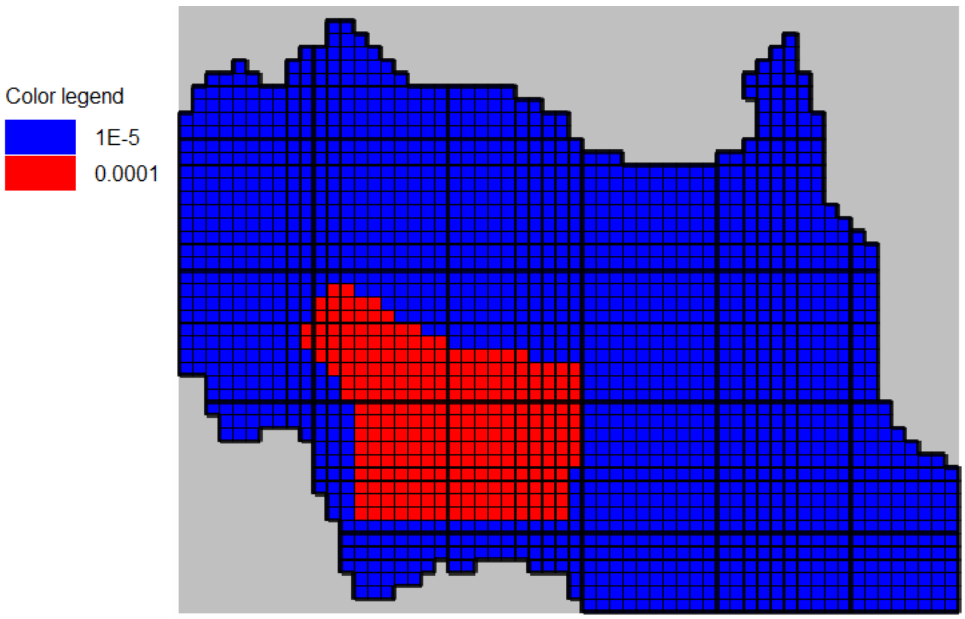

Figure 3-40 Specific storage (Ss) values for the lower confined aquifer [m^{-1}].

3.3.4. Recharge and groundwater evapotranspiration

Figure 3-41 shows the final calculated daily total recharge and groundwater evapotranspiration fluxes from the UZF Package, and the net groundwater recharge calculated by adding the groundwater evapotranspiration, with negative sign, to the total recharge. Figure 3-41 shows that the net groundwater recharge follows the total recharge curve for zero or low groundwater evapotranspiration values, and follows the groundwater evapotranspiration curve for high rates of groundwater evapotranspiration. Figure 3-42 shows the applied daily rainfall, potential evapotranspiration rates, and the calculated actual infiltration rates from UZF Package. The actual infiltration rates shown in that figure depend on the rainfall intensities, the vertical hydraulic conductivity of the soil, and the saturation degree of the unsaturated zone. The shown peaks for the actual infiltration rates in the figure correspond to high rainfall events. After routing the excess infiltration to the lake and subtracting the unsaturated zone storage from the net infiltration rates; the remaining water is further divided into groundwater net recharge, unsaturated zone evapotranspiration, and groundwater evapotranspiration.

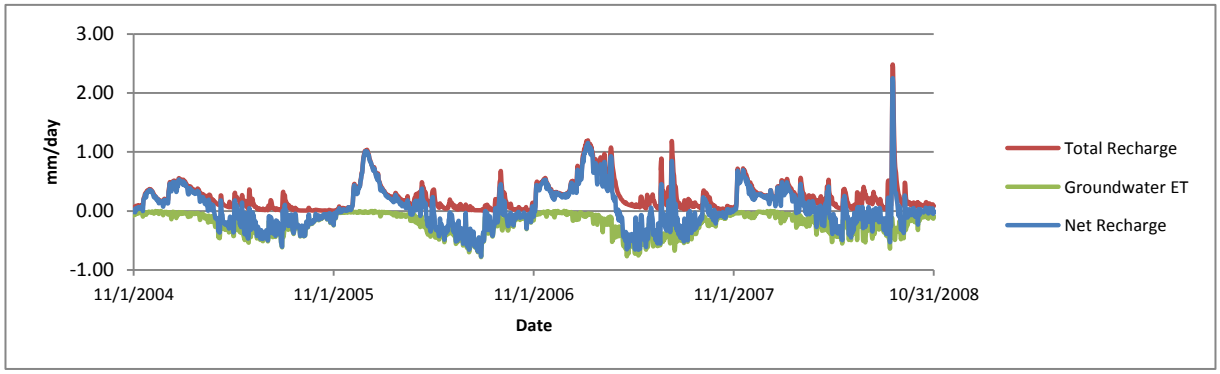

Figure 3-41 Daily total recharge, groundwater evapotranspiration, and net recharge rates from the UZF Package.

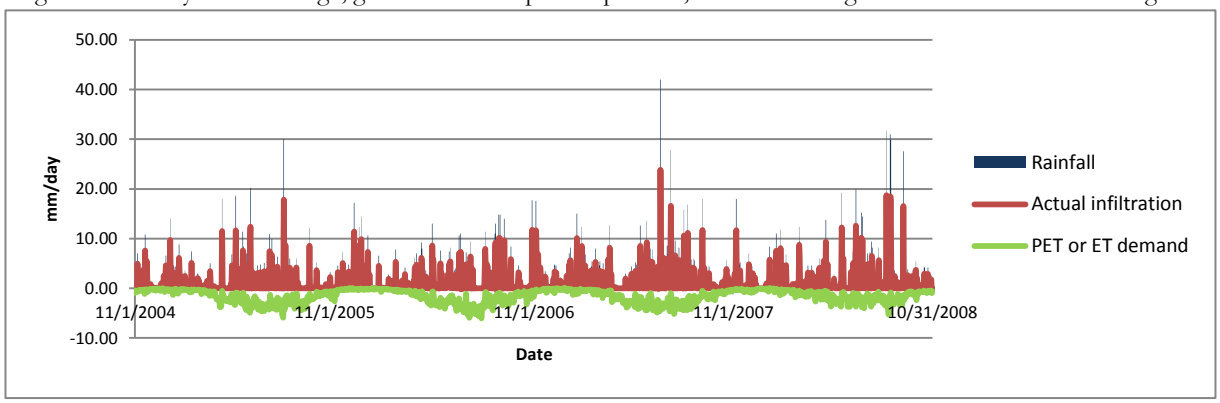

Figure 3-42 Applied daily rainfall and potential evapotranspiration, and actual infiltration rates from UZF Package.

One of the problems associated with the UZF Package in this study was the solver criteria; during this study the model stopped running many times with message "failed to meet solver convergence criteria" because of the UZF Package. According to Niswonger et al. (2011) the recommended values for the flux tolerance and the head tolerance, which might be considered as the most effective parameters for the solver criteria, are 500 (m^3/day) and 0.0001 (m), respectively . In this model, the use of the recommended solver criteria was not applicable. Consequently, after many attempts, these values were increased to be finally equal to ~200000 (m^3/day) and 0.015 (m) in order to be able to run the model, but using such values for the solver criteria caused the final discrepancy values of the groundwater budget to be higher than 1 % during some time steps. This problem was overcome as described in section 3.3.7.

3.3.5. Calibration of lake stages

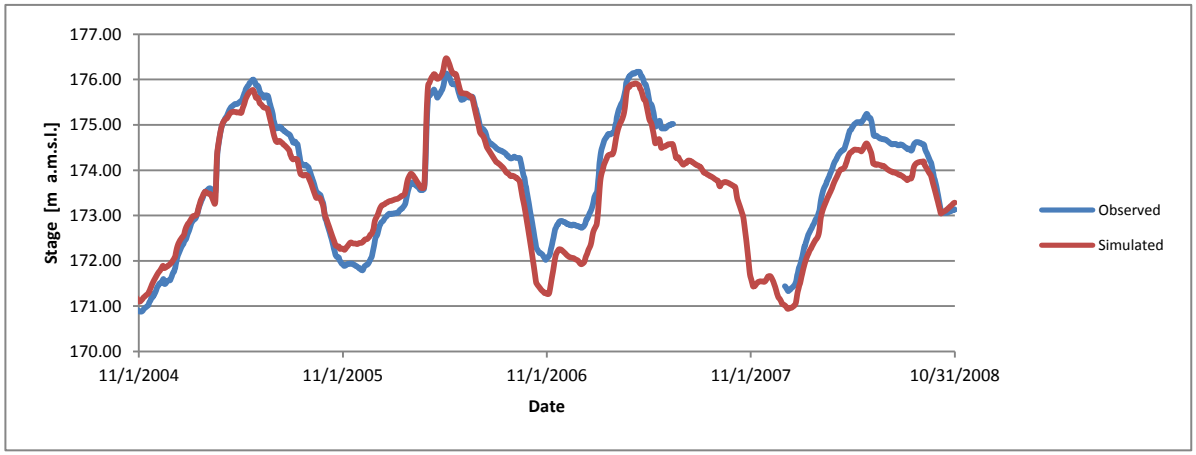

Figure 3-43 Time series plot of the observed and simulated daily lake stages (1st Nov. 2004 to 31st Oct. 2008).

Figure 3-43 shows the time series observed and simulated daily lake stages during the four years simulation period with one gap within the measured lake stages during the period from 16th June 2007 to 31st December 2007. The simulated lake levels have a good trend matching with the observed lake stages with a small error within some specific periods. This error might be because the observed daily lake stages and rivers discharges are instantaneous records not average records of the day. Also it might be due to some uncertainties within the used rivers inflow, which is considered as the most sensitive and quite uncertain stress input, as the multiplication factor used to estimate inflow to the lake from the gauged river discharges [according to section 2.5.5.] may be temporally changing. Nevertheless, the final mean error, mean absolute error, root mean square error between the observed and the simulated lake stages [calculated according to equations 2.28, 2.29 and 2.30] were low, i.e. 0.83, 0.32, and 0.39 m respectively. Also the scatter plot shown in Figure 3-44 confirms a good match between the observed and simulated daily lake stages with a squared correlation coefficient equal to 0.93.

During the calibration process of the transient model, using the lake bathymetric file shown in appendix 3 causes the lake solver not to converge, this might be because this bathymetric table is limited only to the minimum and maximum observed lake stages, and during the simulation the solver might need to try higher stages, i.e. lake surface area and volume above the maximum lake stage that the lake might have in reality. To solve this problem, the lake bathymetry option in ModelMuse software was assigned "automatically"; it means that the software was allowed to creat the lake bathymetry file base on the assigned topography for the lake cells in the model.

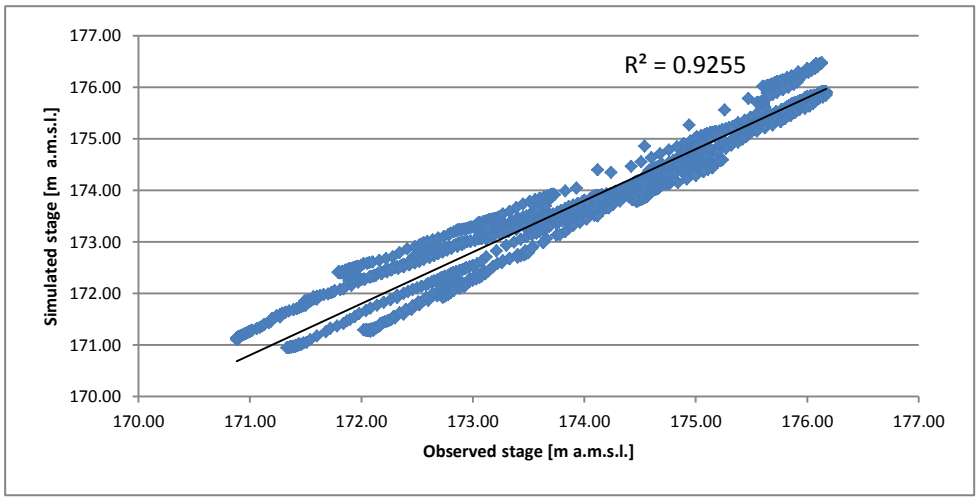

Figure 3-44 A scatter plot of the observed and calculated lake levels (1st Nov. 2004 to 31st Oct. 2008).

3.3.6. Lake water budget

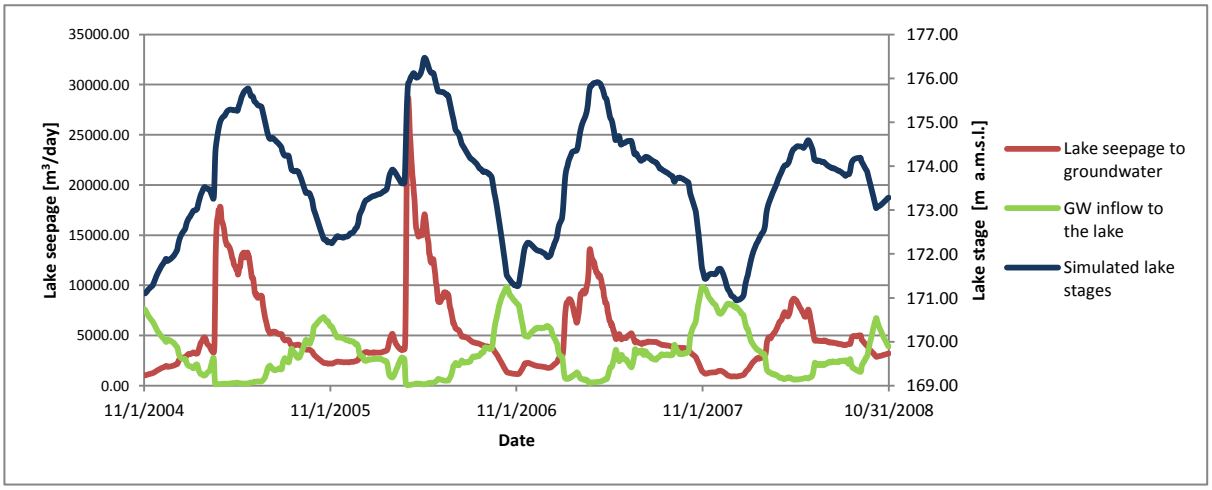

Figure 3-45 The daily groundwater inflow to and from the lake (1st Nov. 2004 to 31st Oct. 2008).

Figure 3-45 shows the daily volumetric seepage to and from the lake bed during the four year simulation period and the corresponding simulated daily lake stages. The figure shows that lake seepage to groundwater is dominant in general and specially during high and average lake stages. The groundwater contribution to the lake increases only in short periods when the lake stages are low. The average lake water balance during the four year simulation period is shown in Table 16.

Table 16 Daily average lake water balance during the four-year simulation period.

	IN	[m³/day]	OUT		[m³/day]
Precipitation	=	23446			
Computed Runoff	=	53935	Evaporation	=	34639
Surface Water Inflow	=	590363	Surface Water Outflow	=	613415
Ground Water Inflow	=	3204	Ground Water outflow	=	5129
Total in	=	670948	Total out	=	653183
Change in Volume	=	17749			
PERCENT DISCREPANCY	=		0.00		

3.3.7. Groundwater budget

MODFLOW-NWT with the Newtonian (NWT) solver was used to run the transient state model. Due to some problems associated with the solver conversion criteria when the UZF Package was active [see section 3.3.4], and in order to solve that problem, the residual control option was activated for the Newtonian (NWT) solver. As recommended by Niswonger et al. (2011), the residual control with MODFLOW-NWT can be used if the discrepancy values increases significantly. The residual control option reduces the head closure between iterations until the error decreases. The final solver head tolerance was adjusted to 0.005 meter and the flux tolerance was 3000 m³/day, the model complexity was set as specified, and all the remaining solver criteria were accepted by default. The absolute ground water discrepancy ranged from 1.35 % to -1.13 % for all stress periods, and the cumulative discrepancy value at the end of the four year simulation period was 0.03 % with an average discrepancy value equal to 0.0 %.

Table 17 Daily average groundwater balance during the four year simulation period.

	IN	[m^3/day]	OUT	[m^3/day]	
STORAGE	=	12098	STORAGE	=	14746
CONSTANT HEAD	=	0	CONSTANT HEAD	=	0
HEAD DEP BOUNDS	=	13508	HEAD DEP BOUNDS	=	3847
STREAM LEAKAGE	=	2276	STREAM LEAKAGE	=	13911
LAKE SEEPAGE	=	5129	LAKE SEEPAGE	=	3204
UZF RECHARGE	=	14420	UZF RECHARGE	=	0
GW ET	=	0	GW ET	=	11694
TOTAL IN	=	47431	TOTAL OUT	=	47401
		IN - OUT	= 30		
		PERCENT DISCREPANCY	= 0.0 %		

Table 17 shows the average groundwater budget during the four year simulation period. The results show that the aquifer system is supplied with water mainly by rainfall recharge, lateral groundwater inflow from the eastern side of the model and by lake seepage. The groundwater outflows from the aquifer system mainly to streams and by evapotranspiration.

3.3.8. Yearly variability of water fluxes

Table 18 shows the average yearly rainfall, evapotranspiration, lake evaporation, interception, infiltration rates, groundwater budget, lake water budget, and unsaturated zone budget for each year within the simulation period and also for the steady state simulation. The table includes the mean, standard deviation, minimum, and maximum for each flux within the four year simulation period.

Table 18:

Hydrologic year	Rainfall	PET	E_{lake}	interception	Infiltration	GW IN					GW OUT					Lake IN				Lake OUT			UZF		
						GHB inflow	streams leakage to GW	Lake seepage to GW	GW total Recharge from UZF	Storage	GHB outflow	GW to streams	GW to Lake	GW ET	Storage	Precipitation	Computed Runoff [UZF]	Surface Water Inflow	Ground Water Inflow	Evaporation	Surface Water Outflow	Ground Water outflow	Actual infiltration	Unsaturated zone ET	UZF storage change
	[mm/day]					[m^3/day]					[m^3/day]					[m^3/day]				[m^3/day]			[m^3/day]		
Steady state	1.6	1.6	2.17	0.44	1.16	11476	2002	839	65277	0	10773	26748	739	41349	0	22282	3116	618350	739	30220	613440	839	65277	0	0
1st Nov. 2004 - 31st Oct. 2005	1.32	1.71	2.33	0.36	0.96	14013	2267	5725	9819	11219	3752	13422	2741	10804	12305	19786	70744	539370	2741	37797	555205	5725	53527	47394	-3658
1st Nov. 2005 - 31st Oct. 2006	1.51	1.68	2.30	0.41	1.10	14084	2389	6041	11877	11714	3681	13208	3050	11500	14639	23000	25992	679726	3050	37586	717973	6041	61970	46481	3652
1st Nov. 2006 - 31st Oct. 2007	1.88	1.68	2.30	0.51	1.37	13309	2236	4865	20220	14170	3953	15006	3295	13974	18525	27649	52271	680384	3295	36855	710795	4865	75572	54126	1282
1st Nov. 2007 - 31st Oct. 2008	1.68	1.30	1.76	0.46	1.22	12628	2212	3889	15761	11292	4001	14006	3730	10501	13517	23347	66699	462322	3730	26339	470082	3890	67140	50233	1151
Mean	**1.60**	**1.59**	**2.17**	**0.44**	**1.16**	**13508**	**2276**	**5129**	**14420**	**12098**	**3847**	**13911**	**3204**	**11694**	**14746**	**23446**	**53935**	**590363**	**3204**	**34639**	**613415**	**5129**	**64554**	**49559**	**607**
Standard Deviation	0.21	0.17	0.24	0.06	0.15	592	68	836	3971	1210	134	697	362	1365	2332	2796	17529	93654	362	4808	105295	836	8006	2978	2656
Min	1.32	1.30	1.76	0.36	0.96	12628	2212	3889	9819	11219	3681	13208	2741	10501	12305	19786	25992	462322	2741	26339	470082	3890	53527	46481	-3658
Max	1.88	1.71	2.33	0.51	1.37	14084	2389	6041	20220	14170	4001	15006	3730	13974	18525	27649	70744	680384	3730	37797	717973	6041	75572	54126	3652

Comparing the steady state fluxes in Table 18 with the corresponding mean values from the four year transient simulation; there is a match for some fluxes such as streams leakage to groundwater, lake precipitation, surface water inflow and outflow from the lake, and lake evaporation. For the remaining fluxes there is mismatch which is due to the fundamental simplification of steady state model but additionally might be due to the oversimplification of the UZF Package in steady state. In steady state, the UZF Package neglects the water storage, evapotranspiration from the unsaturated zone and also the infiltration capacity of the soil. It simply assigns the input values for infiltration rates as total recharge to groundwater, and the ET demand is removed later from the assigned total recharge to give the groundwater net recharge. This approach may result in higher groundwater recharge and lower computed surface runoff values for the steady state model. Consequently, the calibrated steady state parameters, lake, surface water, and groundwater fluxes change from the average values obtained from the transient state model.

3.3.9. Sensitivity analysis results

3.3.9.1. Sensitivity of model parameters

Figures 3-46 to 3-53 and the corresponding tables (Table 19 to 26) show the effect of changing the horizontal hydraulic conductivity of the upper unconfined aquifer, specific yield, specific storage of the lower aquifer, and lake bed leakance on the error value between the observed and the simulated groundwater heads and between the observed and simulated daily lake levels. From the presented figures it can be deducted that groundwater heads are sensitive to the horizontal hydraulic conductivity and moderately only to lowering of specific yield while insensitive to enlarging of specific yield and to any changes of specific storage and lake bed leakance. The lake stage was quite insensitive to most of the parameters except of the horizontal hydraulic conductivity.

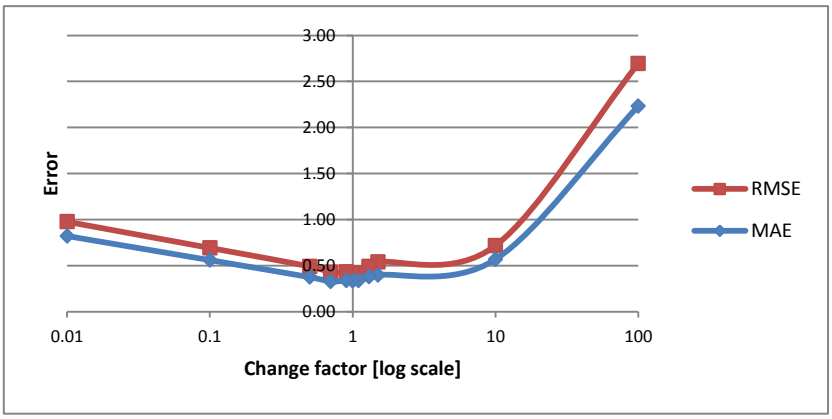

Figure 3-46 Effect of changing K_h on the piezometric heads.

Table 19

Factor	ME	MAE	RMSE
100	0.63	2.23	2.70
10	0.24	0.57	0.72
1.5	0.26	0.40	0.54
1.3	0.19	0.38	0.49
1.1	0.12	0.34	0.42
1	0.10	0.33	0.41
0.9	0.11	0.34	0.43
0.7	-0.05	0.33	0.43
0.5	-0.15	0.37	0.49
0.1	-0.21	0.56	0.69
0.01	-0.11	0.82	0.98

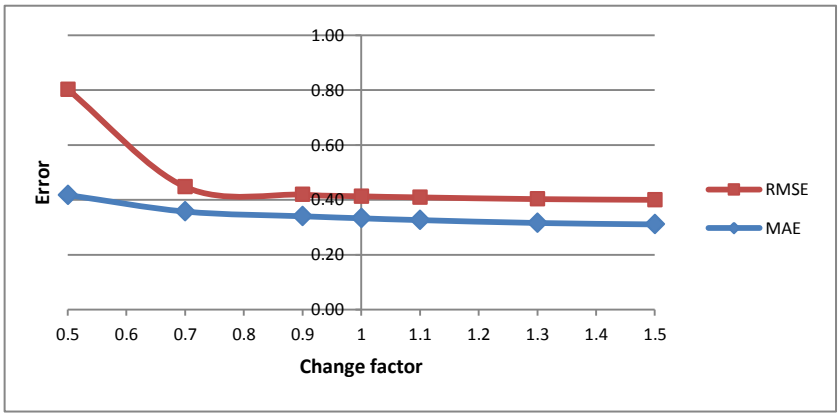

Figure 3-47 Effect of changing specific yield (Sy) on the piezometric heads.

Table 20

factor	ME	MAE	RMSE
0.5	0.10	0.42	0.80
0.7	0.11	0.36	0.45
0.9	0.11	0.34	0.42
1	**0.10**	**0.33**	**0.41**
1.1	0.10	0.33	0.41
1.3	0.08	0.32	0.40
1.5	0.06	0.31	0.40

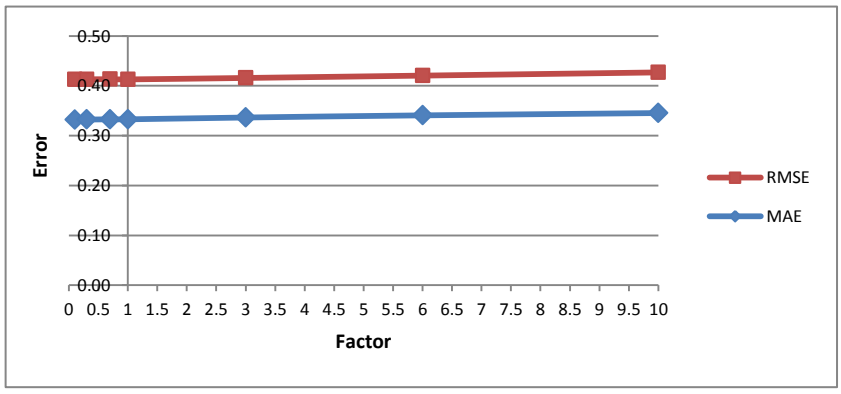

Figure 3-48 Effect of changing specific storage (Ss) on the piezometric heads.

Table 21

Factor	ME	MAE	RMSE
0.1	0.11	0.33	0.41
0.3	0.11	0.33	0.41
0.7	0.11	0.33	0.41
1	**0.10**	**0.33**	**0.41**
3	0.11	0.34	0.42
6	0.11	0.34	0.42
10	0.11	0.35	0.43

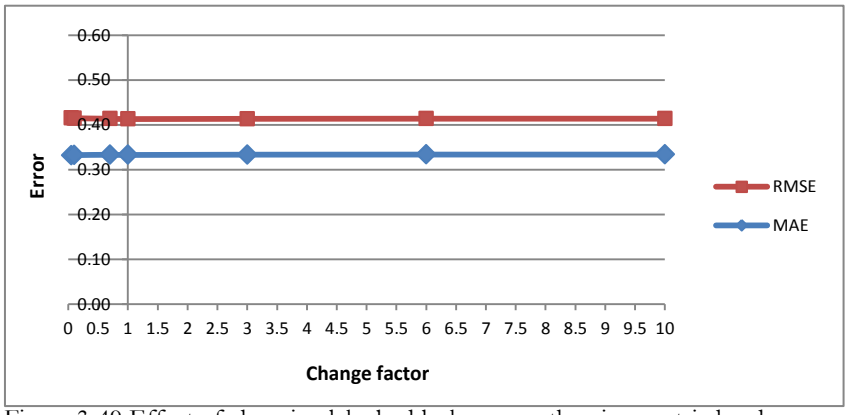

Figure 3-49 Effect of changing lake bed leakance on the piezometric heads

Table 22

Factor	ME	MAE	RMSE
0.05	0.10	0.33	0.42
0.1	0.11	0.33	0.41
0.7	0.11	0.33	0.41
1	**0.10**	**0.33**	**0.41**
3	0.11	0.33	0.41
6	0.11	0.33	0.41
10	0.11	0.33	0.41

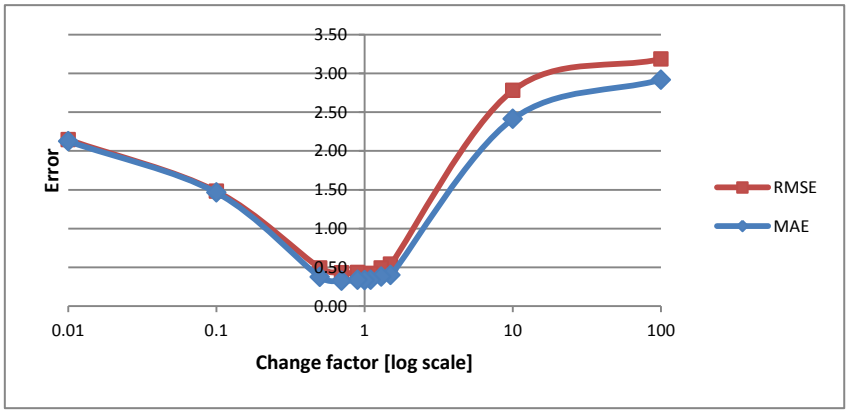

Figure 3-50 Effect of changing K_h on the simulated lake stages.

Table 23

Factor	ME	MAE	RMSE
100	2.92	2.92	3.18
10	2.41	2.41	2.78
1.5	0.26	0.40	0.54
1.3	0.19	0.38	0.49
1.1	0.12	0.34	0.42
1	0.10	0.33	0.41
0.9	0.11	0.34	0.43
0.7	-0.05	0.33	0.43
0.5	-0.15	0.37	0.49
0.1	-1.46	1.46	1.48
0.01	-2.12	2.12	2.15

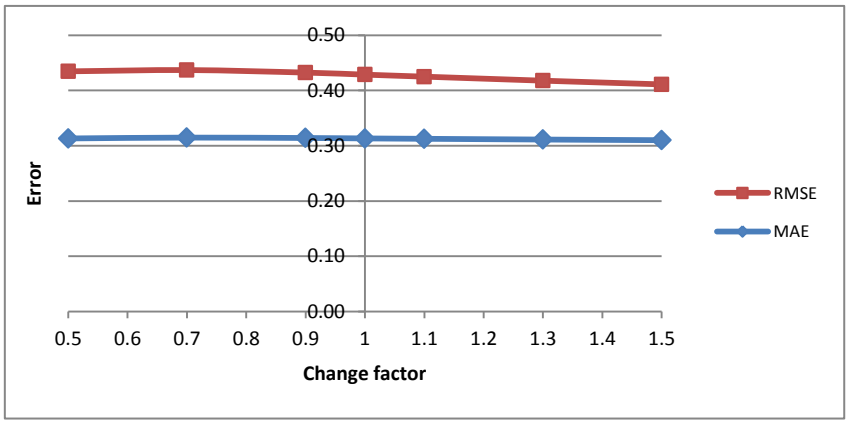

Figure 3-51 Effect of changing specific yield (S_y) on the simulated lake stages.

Table 24

Factor	ME	MAE	RMSE
1.5	0.19	0.31	0.41
1.3	0.21	0.31	0.42
1.1	0.23	0.31	0.43
1	**0.24**	**0.31**	**0.43**
0.9	0.25	0.31	0.43
0.7	0.26	0.31	0.44
0.5	0.27	0.31	0.43

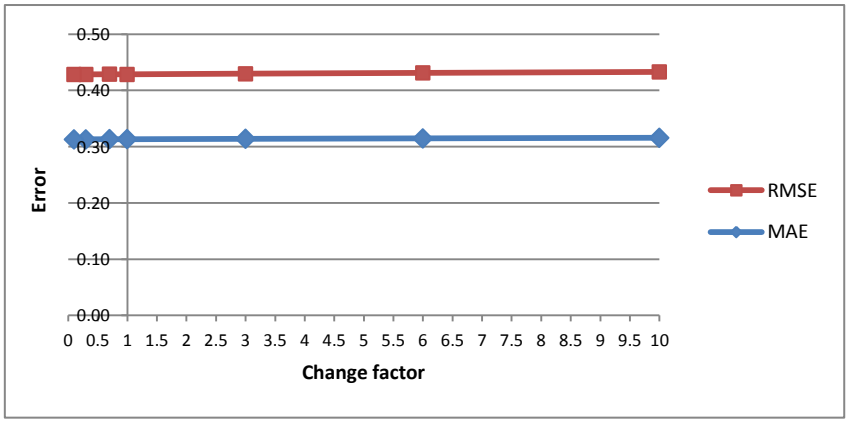

Figure 3-52 Effect of changing specific storage (S_s) on the simulated lake stages.

Table 25

Factor	ME	MAE	RMSE
10	0.25	0.32	0.43
6	0.24	0.31	0.43
3	0.24	0.31	0.43
1	**0.24**	**0.31**	**0.43**
0.7	0.24	0.31	0.43
0.3	0.24	0.31	0.43
0.1	0.24	0.31	0.43

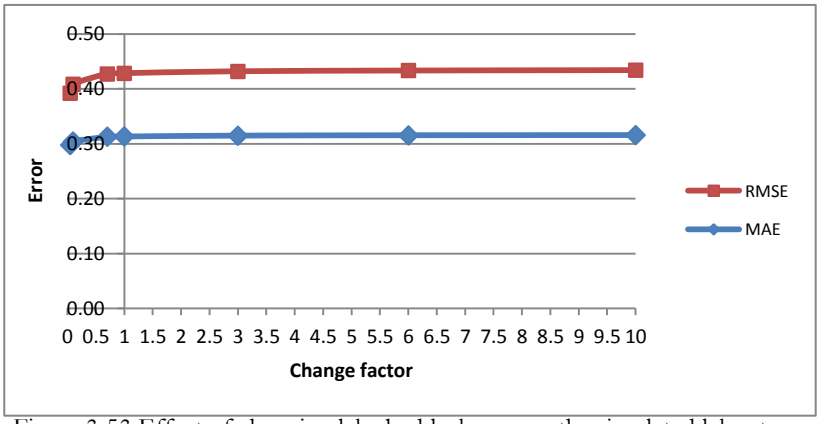

Figure 3-53 Effect of changing lake bed leakance on the simulated lake stages.

Table 26

Factor	ME	MAE	RMSE
10	0.25	0.32	0.43
6	0.25	0.32	0.43
3	0.24	0.31	0.43
1	**0.24**	**0.31**	**0.43**
0.7	0.24	0.31	0.43
0.1	0.21	0.30	0.41
0.05	0.18	0.30	0.39

3.3.9.2. Sensitivity of river inflows

Figures 3-54, 3-55 and the corresponding tables (Table 27 and 28) show the effect of changing the river inflows on the difference between the observed and the simulated groundwater heads and between the observed and simulated daily lake stages. The two figures show that the model is very sensitive to any changes in the river inflows, however, these changes have higher effect on the simulated lake stages than on the groundwater heads.

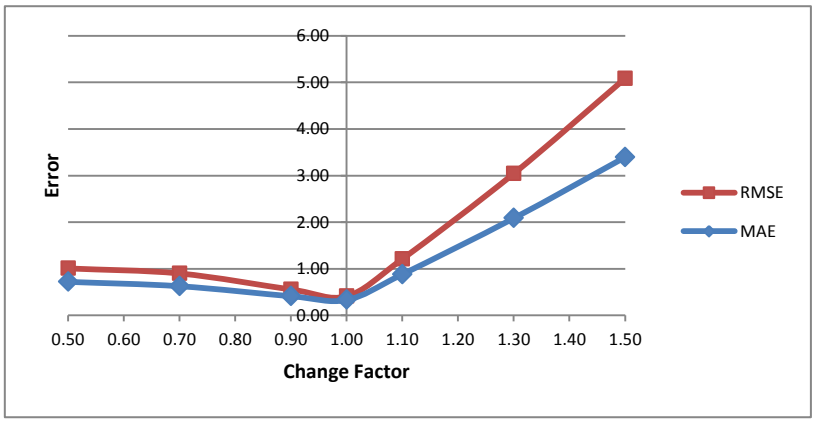

Figure 3-54 Effect of changing rivers' inflow on the piezometric head.

Table 27

Factor	ME	MAE	RMSE
1.50	-3.22	3.39	5.08
1.30	-1.91	2.08	3.04
1.10	-0.69	0.88	1.21
1.00	**0.10**	**0.33**	**0.41**
0.90	0.24	0.41	0.56
0.70	0.54	0.63	0.90
0.50	0.65	0.72	1.01

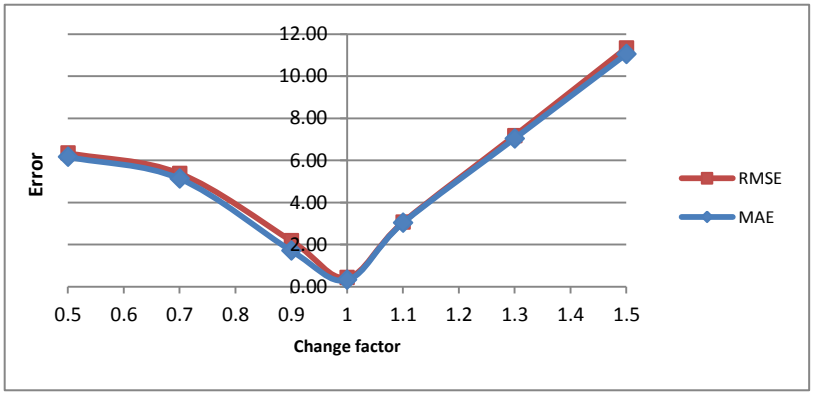

Figure 3-55 Effect of changing rivers' inflow on the simulated lake stages.

Table 28

Factor	ME	MAE	RMSE
1.5	-11.05	11.05	11.34
1.3	-7.03	7.03	7.17
1.1	-3.02	3.02	3.05
1	**0.24**	**0.31**	**0.43**
0.9	1.64	1.71	2.18
0.7	5.13	5.13	5.38
0.5	6.16	6.16	6.35

3.3.10. Spatial and temporal effect of the lake on groundwater

Figure 3-56 and 3-57 show the observed daily lake stages and the simulated groundwater heads in the two transects of piezometers shown in Figure 2-10. Both figures show that the lake has an impact on groundwater heads, but it is different between the two transects. The northern transect presented in Figure 3-56 extends 900 m to the watershed boundary assigned as no-flow boundary of this model and all piezometers of that transect are heavily affected by lake water fluctuation with strength of that impact only slightly declining towards the watershed boundary. The presented experiment also shows that there is a few days lag between the lake peaks or dips and the corresponding groundwater head responses. In order to check if there is effect of the lake on groundwater heads beyond these 900 meters, there is an option to extend the northern boundary of the model far away from the lake shore and to replace that no-flow boundary with a head dependent boundary (GHB). However, this interesting problem was not investigated yet due to the time constraint of this study.

Figure 3-57 shows southern transect groundwater response to the lake fluctuations. In contrast to the northern transect, the groundwater of the southern transect was much less affected by lake fluctuation. The lake impact extended only for 100-300 m distance from the lake shore line. This might be because the groundwater heads at this location is higher than the average lake stage, and there might be more groundwater seepage to the lake at this location. It could be also due to the lower K_h value near the southern transect compared to the relatively high northern K_h value. The reason of the increasing trend of the simulated hydraulic heads requires more research. In conclusion, the spatial and temporal effect of the lake on groundwater heads differ from one location to another depending on the groundwater heads with respect to the lake stages, and the existing boundary conditions surrounding each location. More concerted research of this type is needed around the lake perimeter to define extent and strength of the impact of lake fluctuation on groundwater. Where such impact reaches the model boundary then model boundary in such location need to be extended outward or simpler, replaced with GHB.

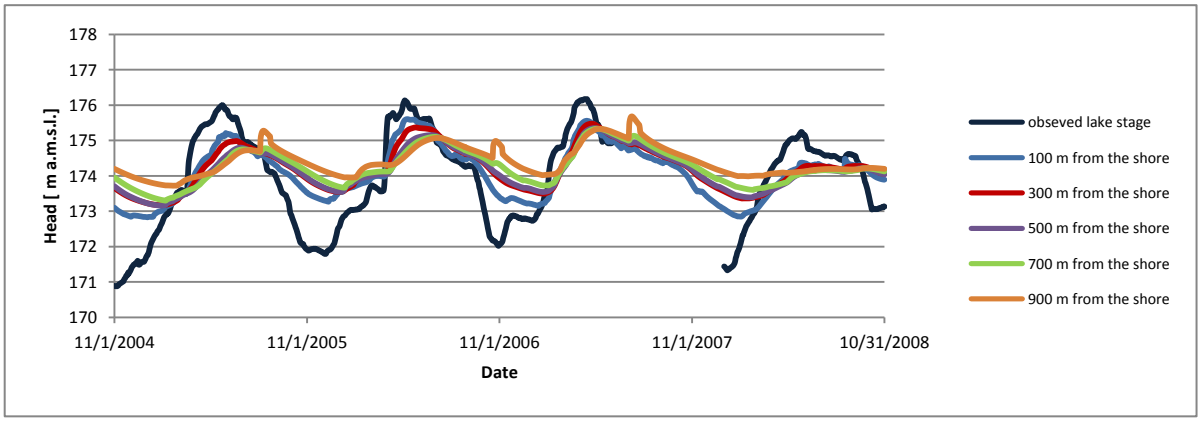

Figure 3-56 Spatial and temporal impact of the lake on groundwater heads [northern piezometric series].

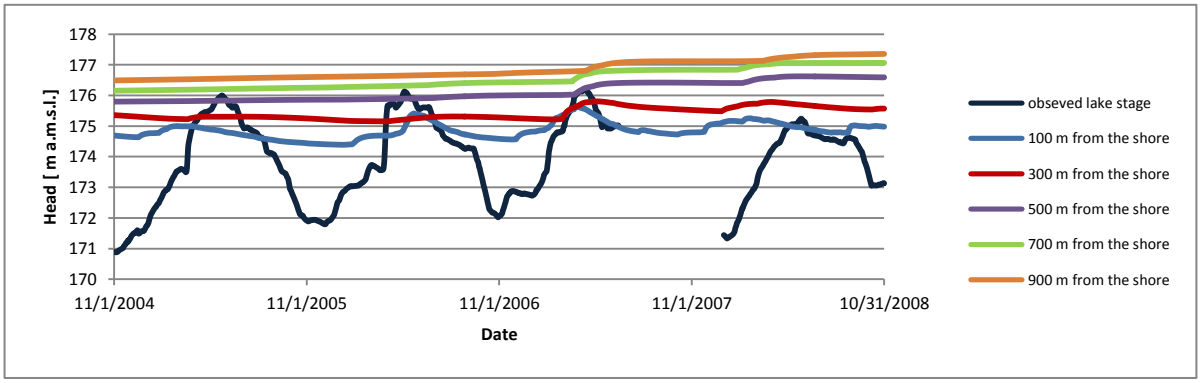

Figure 3-57 Spatial and temporal impact of the lake on groundwater heads [southern piezometric series].

4. CONCLUSION AND RECOMMENDATIONS

4.1. Conclusion

In order to achieve the main objective of this study, i.e. to evaluate the lake groundwater interaction, a steady state and transient state 3D models were built and calibrated manually. The steady state model matched exactly the observed lake level, and the simulated aquifer heads matched the observed heads with a squared correlation coefficient [R^2] equal to 0.96. The transient model covered four years simulation period (from 1st Nov. 2004 to 31st Oct. 2008). The modelled daily lake stages matched the observed daily lake stages within the simulation period with a squared correlation coefficient [R^2] equal to 0.93, and the match between the observed and simulated time series of aquifer heads was with a squared correlation coefficient [R^2] equal to 0.99.

The four years, daily average lake water balance was extracted from the Lake Package (LAK7) output file. During the four years simulation period, the average simulated lake stage and volume were found to be 173.60 m a.m.s.l. and 52 mln m^3, respectively. The surface water inflow and outflows to and from the lake were the major components of the lake water balance and represented 96 and 94% of the total lake inflow and outflow, respectively. The precipitation and groundwater inflow to the lake representrd 3.5 and 0.5% of the total amount of the lake inflow respectively, whereas lake evaporation and lake seepage to groundwater, 5 and 0.8% of the total lake outflow. The four years long lake water balance indicated that the lake is in equilibrium with the groundwater system.

The long term groundwater budget during the four years simulation period is represented by inflows and outflows to and from the modelled aquifer system [Table 17]. The major inflow components to the groundwater system are the total recharge and lateral inflow representing 30 and 29% of the total inflow to the aquifer system while the lake seepage and stream leakages to groundwater represent 11 and 5% of the total inflow to the aquifer system. The main groundwater outflows from the aquifer system are seepage to streams and groundwater evapotranspiration representing 29 and 25% of the total outflow from the aquifer system. The groundwater outflow to the lake represents only 7% of the total groundwater outflow. The final groundwater balance cumulative discrepancy value was 0.03%, indicating that the aquifers system was gaining water either from the lake, the unsaturated zone, streams or from the surrounding area.

The steady state model results showed that the lake seepage to groundwater is slightly higher than groundwater inflow to the lake. The four years transient state simulation showed that the lake seepage to groundwater was dominant during high and average lake water levels, and vice versa during low lake water levels. It showed also that the amount of groundwater seepage to and from the lake was approximately one order of magnitude higher than these values obtained from the steady state model. The transient state model results are more realistic than steady state results due to the larger reduction of number of model degrees of freedom during transient model calibration than in steady state calibration (Lubczynski & Gurwin, 2005) and also due to the oversimplification of the UZF Package and the consequences of that for the steady state model.

The sensitivity analysis of the steady state model was carried out by observing the effect of changing the horizontal hydraulic conductivity of the upper unconfined aquifer, lake bed leakance, the hydraulic conductivity of stream beds, and river inflows on the difference between the observed and the simulated groundwater heads. This analysis showed that the model was most sensitive to the horizontal hydraulic conductivity [Kh], while the stream bed hydraulic conductivity and the lake bed leakance were insensitive.

Another type of sensitivity analysis tested the effect of changing the lake bed leakance, lake evaporation, lake precipitation, and rivers inflow upon the difference between measured and simulated lake stages. That analysis showed that the model was sensitive to hydraulic conductivity changes and to low values of lake bed leakance only. Finally, the changes of the river inflows showed very high influence upon the simulated lake stages and groundwater heads. The lake evaporation and precipitation showed relatively lower impact on the simulated lake stages. The sensitivity analysis of the transient model was carried in similar way as in the steady state. Similarly, it showed that the heads and lake stages were mainly sensitive to changes in horizontal hydraulic conductivity, less sensitive to the changes of specific yield while other parameters were insensitive. Also similarly to steady state model solution, the transient solution was highly sensitive to changes in river inflows.

The influence of the lake fluctuations on groundwater heads was found to be spatio-temporally dependent. The regime of that dependence differed from one location to another and was dependent on the groundwater heads with respect to the lake stages as well as on the type of boundary conditions and their distance from the lake. The seepage from the lake to groundwater was mainly in the western deep part of the lake near the earthen dam, while in the middle and in the eastern part of the lake the seepage had opposite direction, representing groundwater inflow to the lake.

4.2. Recommendations

The calibrated transient model simulation was done for four years, with relatively coarse grid, due to some constrains related to the available computer power. Using more powerful computers may allow refining the model grid and achieving better calibration results.

This work can be extended to study the groundwater contamination due to the surface water contamination from the contaminated sediment at the lake bottom.

The spatial extent of the influence of lake fluctuations should be investigated and where necessary the model boundary should either be moved away of the lake or eventually the existing no-flow boundary should be replaced by GHB.

The current version of ModelMuse (version 2.19.1.0 released on May 13, 2013) contains a lot of bugs related to Lake Package, SFR Package, defining the parameters, using MODFLOW-NWT, and ZONEBUDGET. It is better for any future work to be done with a newer version of ModelMuse.

ModelMuse requires a lot of memory within any computer especially when the Unsaturated Zone Flow (UZF) Package is active. Building a model with fine grid requires a very advanced computer; using standard computer with fine grid models may cause the model not to converge or to converge only after several hours.

LIST OF REFERENCES

Allen, R. G., Pereira, L. S., Raes, D., & Smith, M. (1998). *Crop evapotranspiration - Guidelines for computing crop water requirements - FAO Irrigation and drainage paper 56*.

Anderson, M. P., Hunt, R. J., Krohelski, J. T., & Chung, K. (2002). Using High Hydraulic Conductivity Nodes to Simulate Seepage Lakes. *Ground Water, 40*(2), 117-122. doi: 10.1111/j.1745-6584.2002.tb02496.x

Anderson, M. P., & Woessner, W. W. (1991). *Applied Groundwater Modeling: Simulation of Flow and Advective Transport*: Academic Press.

Banta, E. R. (2011). ModelMate-A Graphical User Interface for Model Analysis. *U.S. Geological Survey Techniques and Methods, book 6, chap. E4, 31 p.*

Cheng, X., & Anderson, M. P. (1993). Numerical Simulation of Ground-Water Interaction with Lakes Allowing for Fluctuating Lake Levels. *Ground Water, 31*(6), 929-933. doi: 10.1111/j.1745-6584.1993.tb00866.x

Deme, G. (2011). *Partitioning subsurface water fluxes using coupled hydrus - modflow model : case study of La Mata catchment, Spain.* University of Twente Faculty of Geo-Information and Earth Observation (ITC), Enschede. Retrieved from http://www.itc.nl/library/papers_2011/msc/wrem/deme.pdf

Fenske, J. P., Leake, S. A., & Prudic, D. E. (1996). Documentation of a computer program (RES1) to simulate leakage from reservoirs using the modular finite-difference ground-water flow model (MODFLOW). *U.S. Geological Survey Open-File Report 96-364, 51 p.*

Furman, A. (2008). Modeling coupled surface-subsurface flow processes: A review. *Vadose Zone Journal, 7*(2), 741-756. doi: 10.2136/vzj2007.0065

Govaerts, Y. (2013). *Albedo influence on the climate*. Lecture notes. Govaerts Consulting.

Gunduz, O., & Aral, M. M. (2005). River networks and groundwater flow: a simultaneous solution of a coupled system. *Journal of Hydrology, 301*(1–4), 216-234. doi: http://dx.doi.org/10.1016/j.jhydrol.2004.06.034

Gurwin, J. (2008). *Numerical model of groundwater–surface water interaction in vicinity of the Turawa Lake, SW Poland.* Unpublished research paper. Faculty of Earth Science and Environmental Management. Wrocław University.

Gurwin, J., Kryza, H., Kryza, J., Kurowski, L., Jędrysek, M., Raczyński, P., Solecki, A., & Szynkiewicz, A. (2004). "Ocena stanu ekologicznego Jeziora Turawskiego w celu opracowania działań na rzecz jego poprawy" (Environmental assessment of the Turawa Lake for its ecological improvement). *Geological Institute of the Wroclaw University.*

Harbaugh, A. W. (1990). A Computer Program for Calculating Subregional Water Budgets Using Results from the U.S. Geological Survey Modular Three-dimensional Finite-difference Ground-water Flow Model. *U.S. Geological Survey Open-File Report 90-392, 46 p.*

Harbaugh, A. W. (2005). MODFLOW-2005, the U.S. Geological Survey modular ground-water model - the Ground-Water Flow Process: U.S. Geological Survey Techniques and Methods, 6-A16, variously p. Retrieved from http://pubs.usgs.gov/tm/2005/tm6A16/PDF.htm

Hsieh, P. A., & Freckleton, J. R. (1993). Documentation of a computer program to simulate horizontal-flow barriers using the U.S. Geological Survey's modular three-dimensional finite-difference ground-water flow model: U.S. Geological Survey Open-File Report 92-477, 32 p.

Hunt, R. (2003). Ground Water-Lake Interaction Modeling Using the LAK3 Package for MODFLOW 2000. *Ground Water, 41*(2), 114-118. doi: 10.1111/j.1745-6584.2003.tb02575.x

Kidmose, J., Engesgaard, P., Nilsson, B., Laier, T., & Looms, M. C. (2011). Spatial Distribution of Seepage at a Flow-Through Lake: Lake Hampen, Western Denmark. *Vadose Zone Journal, 10*(1), 110-124. doi: 10.2136/vzj2010.0017

Lee, T. M. (1996). Hydrogeologic Controls on the Groundwater Interactions with an Acidic Lake in Karst Terrain, Lake Barco, Florida. *Water Resources Research, 32*(4), 831-844. doi: 10.1029/96wr00162

Lubczynski, M., & Gurwin, J. (2005). Integration of various data sources for transient groundwater modeling with spatio-temporally variable fluxes—Sardon study case, Spain. *Journal of Hydrology, 306*(1–4), 71-96. doi: http://dx.doi.org/10.1016/j.jhydrol.2004.08.038

McDonald, M. G., & Harbaugh, A. W. (1988). A Modular Three-Dimensional Finite-Difference Ground-Water Flow Model *Techniques of Water-Resources Investigations*: U.S. Geological Survey.

McMahon, T. A., Peel, M. C., Lowe, L., Srikanthan, R., & McVicar, T. R. (2013). Estimating actual, potential, reference crop and pan evaporation using standard meteorological data: a pragmatic synthesis. *Hydrol. Earth Syst. Sci., 17*(4), 1331-1363. doi: 10.5194/hess-17-1331-2013

Merritt, M. L., & Konikow, L. F. (2000). Documentation of a computer program to simulate lake-aquifer interaction using the MODFLOW ground water flow model and the MOC3D solute-transport model. pp.146. Retrieved from USGS website: http://pubs.er.usgs.gov/publication/wri004167

Niswonger, R. G., Panday, S., & Ibaraki, M. (2011). MODFLOW-NWT, A Newton Formulation for MODFLOW-2005. *U.S. Geological Survey Techniques and Methods 6-A37, 44 p.*

Niswonger, R. G., Prudic, D. E., & Regan, R. S. (2006). Documentation of the Unsaturated-Zone Flow (UZF1) Package for Modeling Unsaturated Flow Between the Land Surface and the Water Table with MODFLOW-2005. *U.S. Geological Techniques and Methods Book 6, Chapter A19, 62 P.*

Prudic, D. E., Konikow, L. F., & Banta, E. R. (2004). A new Stream Flow-Routing (SFR1) Package to simulate stream-aquifer interaction with MODFLOW-2000. *U.S. Geological Survey Open-File Report 2004-1042, 95 p.*

Reta, G. L. (2011). *Groundwater and lake water balance of lake Naivasha using 3 - D transient groundwater model.* University of Twente Faculty of Geo-Information and Earth Observation (ITC), Enschede. Retrieved from http://www.itc.nl/library/papers_2011/msc/wrem/reta.pdf

Rientjes, T. H. M. (2012). *Modelling in hydrology*. Department of water resources, Faculty of geo-information science and earth observation (ITC), University of Twente.

Shakya, D. R. (2001). *Spatial and temporal groundwater modeling integrated with remote sensing and GIS : hard rock experimental catchment, Sardon, Spain.* ITC, Enschede.

Simeonov, V., Wolska, L., Kuczyńska, A., Gurwin, J., Tsakovski, S., Protasowicki, M., & Namieśnik, J. (2007). Sediment-quality assessment by intelligent data analysis. *TrAC Trends in Analytical Chemistry, 26*(4), 323-331. doi: http://dx.doi.org/10.1016/j.trac.2006.12.004

Sophocleous, M. (2002). Interactions between groundwater and surface water: the state of the science. *Hydrogeology Journal, 10*(2), 348-348. doi: 10.1007/s10040-002-0204-x

Wang, D., Wang, G., & Anagnostou, E. N. (2007). Evaluation of canopy interception schemes in land surface models. *Journal of Hydrology, 347*(3–4), 308-318. doi: http://dx.doi.org/10.1016/j.jhydrol.2007.09.041

Wang, Y. L., Wang, X., Zheng, Q. Y., Li, C. H., & Guo, X. J. (2012). A Comparative Study on Hourly Real Evapotranspiration and Potential Evapotranspiration during Different Vegetation Growth Stages in the Zoige Wetland. *Procedia Environmental Sciences, 13*(0), 1585-1594. doi: http://dx.doi.org/10.1016/j.proenv.2012.01.150

Winston, R. B. (2009). ModelMuse-A graphical user interface for MODFLOW–2005 and PHAST: *U.S. Geological Survey Techniques and Methods 6–A29* (pp. 52).

Yihdego, Y., & Becht, R. (2013). Simulation of lake–aquifer interaction at Lake Naivasha, Kenya using a three-dimensional flow model with the high conductivity technique and a DEM with bathymetry. *Journal of Hydrology, 503*(0), 111-122. doi: http://dx.doi.org/10.1016/j.jhydrol.2013.08.034

Yimam, Y. T. (2010). *Groundwater– Surface Water Interaction Modeling of the Grote-Nete Catchment using GSFLOW*. Universiteit Gent & Vrije Universiteit Brussel, Brussel. Retrieved from http://phylares.vub.ac.be/Thesissen/2010%20Yohannes%20Tadesse%20Yimam.pdf

Appendix 1:

borehole number	X	Y	borehole depth [m]	surface ELEV. [AMSL]	stabilized water level [AMSL]	hydraulic conductivity [m/hr]	pumping rate [m^3/h]	depression [m]	depression extent [m]	transmissivity [m^2/d]	depth to filter top [m]	depth to filter bottom [m]
1	434284.32	312685.01	75.5	164.0	163.8						29	72
2	443902.16	312943.84	16.2	180.3	179.8		2.5	6.3			8.2	12.2
3	437060.77	313484.77	69.0	197.0	167.0						50	52
4	436325.08	314296.62	30.0	182.3	173.1	0.792	15.0	1.5	68.0	190.08	23	28
5	440644.01	314585.62	29.0	185.2	177.4	0.378	12.0	2.3	70.0	104.33	23	27
6	440645.06	314678.26	34.0	174.8	176.1	0.515	72.0	8.7	312.0	252.05	17	27
7	440645.06	314678.26	30.0	174.7	175.7	0.340	56.0	10.0	221.0	138.80	16	26
8	433805.81	315192.59	26.0	171.8	169.5						24	25
9	442476.81	315368.12	38.5	175.0	176.1	0.211	30.0	8.4	184.0	83.40	29.3	34.5
10	442476.81	315368.12	41.0	175.8	176.4	1.202	77.0	4.7	262.0	461.72	21	35
11	439047.62	315623.09	30.0	177.9	175.9	1.735	17.4	2.5	105.0	187.40	16	20.5
12	436442.64	315901.13	17.5	180.3	175.8	0.180	5.0	1.7	36.0	44.06	12.5	15.5
13	436443.01	315932.00	14.0	180.1	175.6	0.108	2.0	1.5	24.0	19.44	10.5	12.5
14	436403.80	315932.48	23.3	179.3	175.4	0.490	5.4	0.6	168.0	225.61	18	22
15	437307.61	316076.00	27.0	181.2	175.2	0.763	25.2	2.0	370.0	333.37	20	24.5
16	438641.26	316091.08	27.0	179.7	175.8	0.454	40.0	7.0	210.0	125.19	17	24
17	437739.33	316101.73	26.0	180.7	174.7	932.400	15.0	1.8	150.0	380419.20	17	23
18	438190.66	316127.26	24.0	177.2	173.2		15.2	3.0	125.0		20	22.5
19	437936.87	316222.91	11.0	179.0	175.4	0.432	6.0	2.6	80.0	76.72	8	10
20	437093.78	316232.98	26.0	181.1	175.1	0.792	5.4	0.4	266.0	370.66	18	24
21	437625.37	316411.92	25.0	175.4	173.6	0.450	35.0	3.9	117.0	207.36	17	21
22	435237.26	316749.75	22.0	176.5	174.3						19	20
23	439281.69	318893.97	27.0	179.4	175.2	1.249	48.0	6.0	331.0	299.81	18	24
24	434776.79	319133.50	50.0	170.0	166.0		15.9	5.0			5.5	21.5
25	439188.02	319265.65	29.2	181.2	174.9	0.360	13.0	2.9	87.0	101.09	22.9	27.9
26	442853.34	319316.98	15.5	179.0	176.5		9.0	8.0			10.5	13.5
27	438680.35	319426.00	28.5	181.3	176.6	0.216	16.0	6.9	160.0	54.43	20.5	25.5
28	438406.03	319429.22	27.0	179.2	171.3	0.396	15.0	2.5	60.0	123.55	20	24
29	439095.08	319450.10	25.5	180.5	175.0	1.156	10.8	3.8	204.0	77.66	22.8	24.8
30	439719.94	319506.56	29.0	180.4	173.2	0.792	8.0	1.1	49.0	133.06	22	27
31	437937.22	319558.30	28.5	181.2	175.2	0.472	60.0	7.9	320.0	192.41	20.5	26.5
32	436781.17	319572.14	18.8	177.9	175.4	0.138	5.5	2.3	52.0	53.61	12	17
33	437898.40	319589.64	24.0	179.0	177.3		6.0	3.0			19	22.5
34	434351.88	319632.96	25.0	165.0	182.0						9	19
35	434195.91	319696.68	15.0	164.1	162.3						13	14
36	435471.41	319835.21	27.0	205.0	198.2	0.576	16.0	2.4	91.0	138.24	19	24
37	444779.84	319883.05	43.0	187.0	183.8	0.518	48.0	9.0	410.0	292.38	33	39
38	444779.84	319883.05	43.0	185.9	183.1	0.684	48.0	4.0	168.0	300.41	30	38
39	440665.37	319928.11	51.0	179.8	179.0	0.400	82.0	8.0	369.0	273.33	19	32
40	435738.64	320851.07	13.0	188.9	188.0	0.360	12.0	4.7	140.0	67.39	6	9.5
41	435915.33	320879.79	20.5	176.3	172.3	1.339	54.0	5.0	301.0	417.83	10.5	17.5
42	435641.46	320914.04	13.0	190.0	189.0	0.328	9.1	3.5	98.0	62.90	6	9
43	435740.54	321005.47	20.0	175.8	172.8	1.076	40.5	4.9	256.0	201.50	12	17
44	435819.28	321035.39	21.0	175.6	171.9	1.260	40.5	5.0	301.0	211.68	11	17
45	443970.84	321188.73	54.0	194.4	189.6	0.316	61.0	7.0	202.0	257.63	42	51

Appendix 2:

borehole number	X [m]	Y [m]	surface elevation [AMSL]	depth to initial WT [m]	depth to 1st layer bottom [m]	depth to 2nd layer bottom [m]	depth to 3rd layer bottom [m]
1	443970.84	321188.73	195.00	4.40	13.00	18.00	52.00
2	444779.84	319883.05	185.70	1.30	5.00	11.50	39.00
3	442853.34	319316.98	182.21	2.50	8.50	9.50	13.50
4	440665.37	319928.11	179.66	4.50	11.00	14.00	33.00
5	439281.69	318893.97	177.23	4.20	6.20	14.00	24.00
6	439095.08	319450.10	182.10	5.50	11.00	22.00	24.80
7	438680.35	319426.00	180.20	6.50	8.00	15.00	25.50
8	438406.03	319429.22	180.20	6.50	8.00	14.00	29.00
9	437937.22	319558.30	179.40	6.00	7.00	11.00	27.00
10	435471.41	319835.21	166.88	6.00	10.00	14.00	24.00
11	439719.94	319506.56	179.60	6.00	8.00	20.00	27.00
12	439188.02	319265.65	178.95	9.40	11.00	16.20	27.90
13	435915.33	320879.79	176.00	0.50	1.30	4.50	17.50
14	435738.64	320851.07	175.00	0.90	8.00	8.80	9.50
15	435740.54	321005.47	175.00	2.50	3.80	9.20	17.00
16	434776.79	319133.50	165.28	4.00	8.50	19.50	21.50
17	434351.88	319632.96	163.86	3.00	17.00	20.00	22.00
18	435237.26	316749.75	170.84	3.20	8.50	15.50	21.00
19	436325.08	314296.62	181.66	9.00	16.00	18.00	28.00
20	437307.61	316076.00	183.04	6.00	7.00	15.00	25.20
21	437093.78	316232.98	180.00	6.00	7.00	16.00	25.50
22	436403.80	315932.48	179.56	3.90	5.50	14.70	23.10
23	438190.66	316127.26	176.68	4.00	8.00	19.50	22.50
24	438641.26	316091.08	175.17	7.40	11.40	12.60	24.10
25	439047.62	315623.09	179.67	5.00	6.50	16.00	20.50
26	440645.06	314678.26	184.94	3.00	11.00	13.00	31.00
27	440644.01	314585.62	185.00	10.40	12.90	15.70	27.20
28	442476.81	315368.12	176.44	3.00	4.00	19.50	36.00
29	437060.77	313484.77	194.87	14.00	26.00	34.00	62.00
30	434284.32	312685.01	165.42	28.60	35.00	36.20	72.80

Appendix 3:

Stage [m]	Volume [m3]	Surface area [m2]
166.00	0.00	0.00
166.08	2500.00	2500.00
166.16	5000.00	5000.00
166.24	8000.00	10000.00
166.32	10000.00	15000.00
166.40	12000.00	20000.00
166.48	15000.00	25000.00
166.56	17000.00	30000.00

166.64	20000.00	35000.00
166.72	22000.00	40000.00
166.80	25000.00	60000.00
166.88	30000.00	80000.00
166.96	35000.00	100000.00
167.04	40000.00	120000.00
167.12	50000.00	150000.00
167.20	55000.00	180000.00
167.28	60000.00	211699.04
167.36	65000.00	295232.21
167.44	70000.00	385627.59
167.52	75000.00	482631.08
167.60	80000.00	585992.43
167.68	93449.74	695465.20
167.76	156182.36	810806.81
167.84	228165.98	931778.49
167.92	309806.05	1058145.32
168.00	401496.00	1189676.20
168.08	503617.27	1326143.87
168.16	616539.29	1467324.90
168.24	740619.46	1612999.70
168.32	876203.21	1762952.51
168.40	1023623.94	1916971.39
168.48	1183203.03	2074848.25
168.56	1355249.87	2236378.82
168.64	1540061.84	2401362.69
168.72	1737924.32	2569603.25
168.80	1949110.66	2740907.73
168.88	2173882.21	2915087.21
168.96	2412488.34	3091956.59
169.04	2665166.37	3271334.61
169.12	2932141.63	3453043.83
169.20	3213627.46	3636910.65
169.28	3509825.15	3822765.31
169.36	3820924.04	4010441.89
169.44	4147101.40	4199778.27
169.52	4488522.54	4390616.19
169.60	4845340.74	4582801.22
169.68	5217697.27	4776182.77
169.76	5605721.40	4970614.05
169.84	6009530.40	5165952.15
169.92	6429229.52	5362057.95
170.00	6864912.00	5558796.20
170.08	7316659.08	5756035.45
170.16	7784539.99	5953648.11
170.24	8268611.94	6151510.41
170.32	8768920.16	6349502.40
170.40	9285497.86	6547508.00
170.48	9818366.22	6745414.93
170.56	10367534.43	6943114.75
170.64	10932999.69	7140502.86

170.72	11514747.16	7337478.49
170.80	12112750.02	7533944.71
170.88	12726969.41	7729808.41
170.96	13357354.50	7924980.32
171.04	14003842.42	8119375.00
171.12	14666358.31	8312910.84
171.20	15344815.30	8505510.09
171.28	16039114.50	8697098.79
171.36	16749145.04	8887606.84
171.44	17474784.00	9076967.97
171.52	18215896.50	9265119.75
171.60	18972335.62	9452003.55
171.68	19743942.43	9637564.62
171.76	20530546.01	9821752.01
171.84	21331963.43	10004518.61
171.92	22147999.75	10185821.16
172.00	22978448.00	10365620.20
172.08	23823089.24	10543880.13
172.16	24681692.49	10720569.19
172.24	25554014.79	10895659.41
172.32	26439801.15	11069126.71
172.40	27338784.58	11240950.79
172.48	28250686.08	11411115.22
172.56	29175214.64	11579607.40
172.64	30112067.27	11746418.53
172.72	31060928.92	11911543.69
172.80	32021472.58	12074981.75
172.88	32993359.20	12236735.45
172.96	33976237.74	12396811.34
173.04	34969745.15	12555219.80
173.12	35973506.38	12711975.07
173.20	36987134.34	12867095.19
173.28	38010229.96	13020602.05
173.36	39042382.16	13172521.38
173.44	40083167.86	13322882.72
173.52	41132151.94	13471719.48
173.60	42188887.30	13619068.86
173.68	43252914.82	13764971.92
173.76	44323763.39	13909473.55
173.84	45400949.87	14052622.46
173.92	46483979.12	14194471.22
174.00	47572344.00	14335076.20
174.08	48665525.35	14474497.63
174.16	49762992.01	14612799.55
174.24	50864200.80	14750049.85
174.32	51968596.56	14886320.26
174.40	53075612.10	15021686.32
174.48	54184668.21	15156227.41
174.56	55295173.71	15290026.76
174.64	56406525.37	15423171.40
174.72	57518107.99	15555752.24

174.80	58629294.34	15687863.98
174.88	59739445.18	15819605.17
174.96	60847909.28	15951078.20
175.04	61954023.38	16082389.29
175.12	63057112.24	16213648.47
175.20	64156488.58	16344969.63
175.28	65251453.13	16476470.49
175.36	66341294.62	16608272.60
175.44	67425289.76	16740501.34
175.52	68502703.24	16873285.91
175.60	69572787.78	17006759.38
175.68	70634784.05	17141058.61
175.76	71687920.74	17276324.33
175.84	72731414.52	17412701.07
175.92	73764470.05	17550337.23
176.00	74786280.00	17689385.00
176.08	75796025.01	17830000.44
176.16	76792873.73	17972343.43
176.24	77775982.79	18116577.67
176.32	78744496.81	18262870.71
176.40	79697548.42	18411393.94
176.48	80634258.22	18562322.56
176.56	81553734.81	18715835.61
176.64	82455074.80	18872115.97
176.72	83337362.77	19031350.36
176.80	84199671.30	19193729.31
176.88	85041060.95	19359447.21
176.96	85860580.30	19528702.26
177.04	86657265.89	19701696.50
177.12	87430142.29	19878635.81
177.20	88178222.02	20059729.90
177.28	88900505.61	20245192.31
177.36	89595981.60	20435240.42
177.44	90263626.50	20630095.43
177.52	90902404.82	20829982.38
177.60	91511269.06	21035130.16
177.68	92089159.70	21245771.46
177.76	92635005.25	21462142.82
177.84	93147722.17	21684484.62
177.92	93626214.93	21913041.07
178.00	94069376.00	22148060.20